UNIVERSITY OF CALIFORNIA
RIVERSIDE

Profiling Metabolic Transport Along the Segmentally Stratified Rat Colon

A Dissertation submitted in partial satisfaction
of the requirements for the degree of

Doctor of Philosophy

in

Chemistry

by

Meredith Michelle Dinges

September 2017

Dissertations Committee:
Dr. Cynthia K. Larive, Chairperson
Dr. Wenwan Zhong
Dr. Quan Cheng

The Dissertation of Meredith Michelle Dinges is approved:

Committee Chairperson

University of California, Riverside

Acknowledgements

This adventure through graduate school has been long and arduous. I would like to acknowledge the many people that have provided support and guidance throughout this process. First, I would like to thank my parents, Larry and Kathleen Dinges who provided both financial and emotional support throughout my education. They have been there for the emotional lows as well as continually cheering me on throughout the awards and accomplishments. I would not be where I am today without the opportunities they provided throughout my life.

I would also like to thank my husband, Zachary Holman, for making the choice to enter my life after I came to California. You have been my rock, and an everlasting source of support. You have listened to countless science lessons, instrument frustrations, and research complaints, none of which you probably understood, but pretended to flawlessly. I thank you for all of your help raising Aubrey and providing a safe and loving environment for her. The Holman family and extended relatives, took my daughter in as one of the family from the beginning. Thank you for all of the help and good times.

While my grandparents are no longer with us, they provided me with a model of hard work and perseverance. They lived in a time that is much different than now, and I believe they would be proud of the strong, educated woman I have become. They also provided me with Aunts and Uncles that have been extremely supportive throughout this journey. I would like to thank my Aunt and Uncle, Sylvia and Timothy Robinson who helped me in many extraordinary ways, and must know how much their help has truly meant to me and my family. My God-mother Cecelia and Uncle Willy have always

offered emotional support and motivation. My Uncle Willy will always have a place in my heart. I cannot wait to one day meet him again with one of his great big bear hugs.

The amazing people I have had a chance to work with have not only had an impact on my research, but have made me a better person. This includes my professors at Drury University, especially Dr. Albert Korir. The time and effort you took into mentoring me as a chemist is something I treasure dearly. I also want to thank my co-workers in the Larive lab, including Andrew Green, Corey Griffith, Melissa Morgan, Caroline Mathon, Kemal Solakyildirim, Consuelo Beecher, and Gregory Barding Jr. Special thanks also goes out to all visiting scholars who have come through this lab. You have all been a wonderful source of inspiration. I want to specifically thank Luzineide (Luzi) Tinoco and her husband, Alvicler (Calvin) Magalhaes who helped tremendously with the NMR and provided wonderful memories including those on my wedding cruise.

Thank you to all of my undergraduate students who put a smile on my face almost every day. This includes a wonderful undergraduate researcher in the lab named Pauline Carrington who helped with the IC data and sample prep. It was these interactions with students that helped propel me into an education career path.

I also want to thank Professor Christian Lytle, who provided me with endless samples, and insight into the physiology of my project. With great joy I would like to thank Professor Cynthia Larive, who opened her lab to me with open arms. I have learned so much from you, and I continually hope to make you proud.

Lastly, I must thank my daughter, Aubrey. No one has made me more proud, happy, frustrated, or crazy. You are amazing. Thank you for this wild ride together.

Dedication

This dissertation is dedicated to the one who has been with me since day one of my college adventure. She traveled many miles by my side, and is the main source of motivation that kept me going. I would do it all over again for you, my bright, beautiful, blue-eyed baby girl, Aubrey Lynn Fairchild.

ABSTRACT OF THE DISSERTATION

Profiling Metabolic Transport Along the Segmentally Stratified Rat Colon

by

Meredith Michelle Dinges

Doctor of Philosophy, Graduate Program in Chemistry
University of California, Riverside, September 2017
Dr. Cynthia K. Larive, Chairperson

The colon has long been considered as a waste-packing organ, but has been gaining importance with the discovery of the complex gut microbiome which is located primarily in the colon. The gut microbiome is comprised of more than 800 species of bacteria that help harvest energy, synthesize vitamins, and shape the immune system. Disturbances in the gut microbiome have been implicated in many diseases including allergies, autism, colorectal cancer, Crohn's disease, diabetes, and obesity, making it critically important for human health. While the focus of most researchers has been solely on the bacterial component of the gut, little is understood about the mechanism of metabolic communication between the gut microbiome and its human host.

In this work, nuclear magnetic resonance, ion chromatography, and gas chromatography-mass spectrometry are used to identify and quantify major metabolites in extracts of fecal material isolated from the rat ileum, cecum, proximal, mid, and distal colon.

These metabolites include short chain fatty acids that are the preferred energy source for colonocyte, amino acids, polyamines, bile acids, choline metabolites, phenolic compounds, and inorganic ions. This study provides information on the luminal metabolome, its stratification along the colon, and the assortment of metabolites available for absorptive transporters within each segment.

Metabolic profiling of along different segments of the colon provides knowledge about the metabolites available in the stool for transport across the epithelial tissue into the bloodstream or for further transformation by the gut microbiome. In this work, use of the Ussing chamber provides evidence of the transport behavior of metabolites including short-chain fatty acids, amino acids, vitamins, and choline derivatives across excised colonic epithelial tissue. These *in vitro* experiments utilize two chambers separated by epithelial tissue representing both the lumen and serosal sides of the colon. ^{1}H-NMR analysis of these chambers has shown that over a dozen metabolites including SCFAs, amino acids, and choline derivatives are involved in transport.

Table of Contents

LIST OF FIGURES

LIST OF TABLES

CHAPTER ONE

Introduction

The research presented in this dissertation focuses on metabolic profiling of the rat colon to reveal differences in the abundance of individual metabolites over the length of the large intestine. The overarching goal of this work is to increase our understanding of the function of the colon by gaining knowledge of how segmental stratification affects the localized concentration of metabolites. Emphasis is placed on the development of optimized methods for the analysis of a wide range of compounds, providing a global view of the metabolites present and afforded access to the epithelium for transport or further metabolism. Most studies focus on the analysis of voided stool, missing the dynamic changes in the luminal metabolome as stool travels through the large intestine. The luminal metabolome potentially holds a wealth of knowledge related to colon health and disease. Gaining an understanding of how segmental stratification affects the overall function of the large intestine can potentially aid in the development of new treatments for diseases like irritable bowel syndrome (IBS) and colitis. Beyond short chain fatty acids, little is known about the transport of metabolites across the intestinal epithelium into the bloodstream.

Current methods for the investigation of metabolite transport require the use of labeled compounds or lack the ability to monitor the simultaneous transport of many metabolites. The analytical approach employed in this work uses ^{1}H nuclear resonance spectroscopy (NMR) to monitor transported metabolites without the use of labeled compounds, and NMR, gas chromatography – mass spectrometry (GC-MS) and ion chromatography (IC) to measure changes in the metabolites present in stool as it passes through the intestine.

The goals of this research are to map the transport and transformation of metabolites along the segments of the rat colon and investigate metabolite transport across the epithelium through the following objectives:

Objective 1: Develop analytical methods optimized for the study of colonic metabolite signatures with the ability to quantify segmental differences, as well as provide insight into the transport activities of the epithelial tissue. (Chapter 2)

Objective 2: Profile the composition of stool as it travels along the length of the colon using metabolic fingerprinting to better understand colonic function and segmental stratification. (Chapter 3)

Objective 3: Identify and quantify metabolites involved in transport across the colonic epithelium and measure their rate of transport using the Ussing chamber coupled with ^{1}H NMR analysis. (Chapter 4)

This chapter presents an overview of the analytical strategies involving metabolomics and metabolic profiling used to accomplish these objectives and the biological context in which the results of these measurements are interpreted.

1.1 Metabolomics

Metabolomics is a comprehensive study of small molecule (<1500 da) metabolites with an aim to identify and quantify all metabolites within a biological sample.[1] Metabolomics is an emerging and dynamic field and is still a relatively young branch of "omics" science.[2] The term "omics" comes from the Latin voice *-omne* meaning "everything, or whole", and applies to many aspects of biology including genomics, transcriptomics, and proteomics, which are considered to be upstream from metabolomics[3] (Figure 1.1) The primarily goal of most metabolomics studies is to gain a global understanding of a biological system. This approach is particularly useful in functional genomic studies in which metabolism is thought to be perturbed. In these cases, metabolomics provides a snapshot of the metabolic dynamics in response to pathophysiological stimuli and/or genetic modification.[4, 5]

The metabolome holds a wealth of knowledge, but is highly complex. The exhaustive analysis of all metabolites in a biological sample is hindered by the large variability (molecular weight, solubility, polarity, etc.) among metabolites.[6]

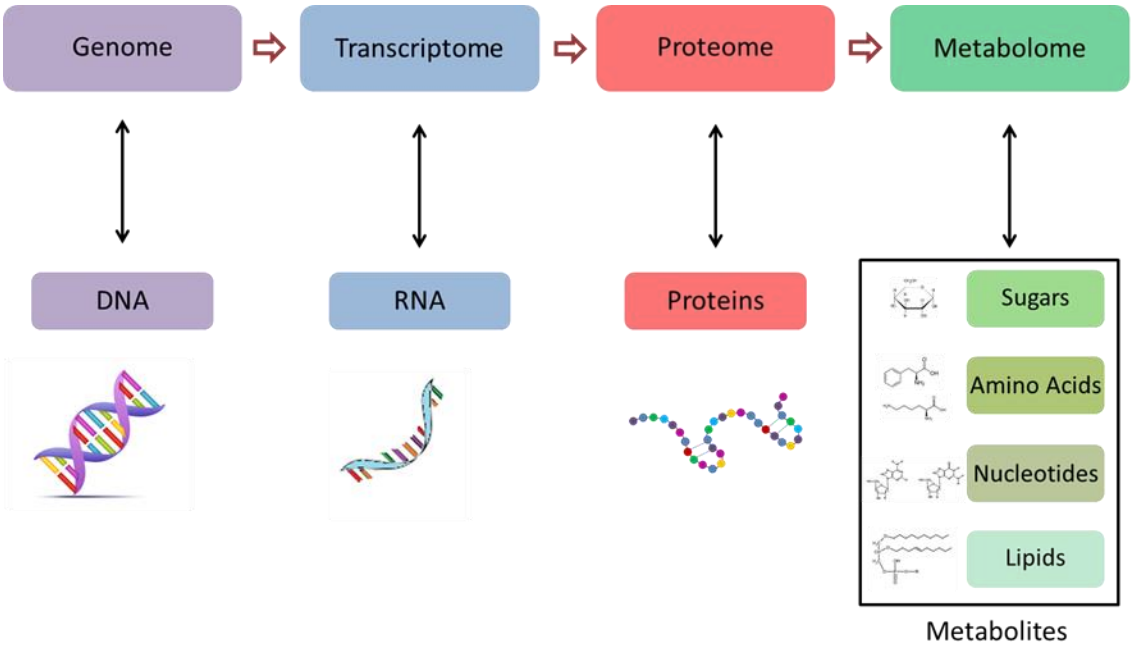

Figure 1.1. Levels of organization of "omics" are depicted from left to right. Changes in the genome would be detectable downstream through the transcriptome, proteome, and metabolome. Studies of the metabolome can be used to detect upstream disturbances.

There is still no known method able to simultaneously analyze all metabolites. In fact, metabolomics studies still struggle to cover even a fraction of the metabolome, with most published metabolomics studies identifying or categorizing fewer than 100 hundred compounds7, equaling less than 1% of the known human metabolome.8-10

Current metabolomics studies can be classified as 3 types including (1) targeted metabolomics: quantitative analysis of a specific class or limited number of known metabolites, (2) metabolic profiling: untargeted method analyzing a large group of metabolites including those whose identity is unknown, and (3) metabolic fingerprinting: rapid, untargeted evaluation of "fingerprints" for the purpose of discrimination, in which identification in not required.[11, 12] Another related term, "metabonomics" was coined by Nicholson *et al.* to define studies of change in metabolic activities in response to genetic modifications or patho-physiological stimuli.[13] There is a large degree of overlap between the working definitions of metabolomics and metabonomics, and they are often used synonymously.[14] For the purposes of this dissertation, the term metabolomics is used to encompass both definitions.

Targeted metabolomics focuses on identifying and quantifying specific metabolites, for example, substrates of an enzyme, direct products of a protein, a class of related compounds, or members of a particular pathway. Often, targeted analyses are driven by a hypothesis derived from previously obtained untargeted data.[15] In targeted metabolomics, the substrates and their chemical properties are known, permitting sample preparation methods to be tailored to the compounds of interest, reducing matrix effects and unwanted interferences.

Untargeted analysis provides a global view of the metabolites present in a sample whether the goal is metabolic profiling or fingerprinting. The difference between these two approaches lies with the data analysis steps.

1.1.1 Metabolic fingerprinting

With metabolic fingerprinting time is not spent identifying the sample components before analysis. The analytical data is often binned immediately following acquisition, uploaded into a statistical program to determine variance, and then only the resonances (or bins) contributing to the variance are investigated further. Metabolic fingerprinting has proven applicable to studies involving biomarker discovery[16] and those aimed towards using it as a diagnostic tool.[17, 18] Metabolic fingerprinting does not fit well within the scope of this projects which aims to study the composition of the luminal metabolome and the effect of segmental stratification, thus results described herein are categorized as metabolic profiling.

1.1.2 Metabolic profiling

Metabolic profiling is an untargeted approach with the goal of studying the complete metabolite composition and concentration of a sample that represents a single snapshot of time.[19, 20] This method allows for the comprehensive study of metabolites and may provide a global view of their role in health and disease,[21, 22] effect of exposure to a drug or toxicant,[23, 24] or the metabolic impact of a genetic alteration.[25-27]

Unfortunately, with current available analytical techniques it is not possible to profile all metabolites present in a biological matrix, making it preferable to use multiple complementary chemical analysis techniques including ^{1}H NMR and mass spectrometry (MS), more specifically GC-MS, liquid chromatography - mass spectrometry (LC-MS), or capillary electrophoresis - mass spectrometry (CE-MS) to maximize the coverage of the metabolome. The goal of these methods is to produce rapid, robust, and reproducible results confirming the identity and quantity of metabolites.[4]

Studies involving the measurement and interpretation of metabolite profiles from biological samples, such as urine or serum, have provided evidence of change induced by external stimuli (disease or drug treatment) and broadened our knowledge of biological variance among sub-populations.[28] While these studies most commonly involve a "control/dosed" model, the experiments detailed in this dissertation focus on the use of metabolic profiling to identify and quantify stool metabolites, referred to as the luminal metabolome.

1.2 Analytical methodology for metabolomics and metabolic profiling

Several types of analytical methods are employed in metabolomic analyses including NMR,[29, 30] GC-MS,[31, 32] LC-MS,[33, 34] CE-MS,[35, 36] and IC.[37] Each of these methods offers their own set of advantages and disadvantages summarized in Table 1.1, and consideration of each method should be made prior to any metabolomics study.

Table 1.1. Comparison of analytical instruments often used in metabolomics studies highlighting several advantages and disadvantages of each platform including NMR, GC-MS, LC-MS, CE-MS, and IC.

ANALYTICAL METHOD	ADVANTAGES	DISADVANTAGES
NMR	• Non-destructive • Highly reproducible, robust • Provides structural information • Ability to analyze tissue (HRMAS NMR)	• Lower sensitivity • No separation to increase resolution • High operational cost/low affordability
GC-MS	• High sensitivity • Extensive libraries of compounds available • Separation reduces component overlap • Retention index improves robustness	• Derivatization required • Chromatographic drift • Molecular ion may not be detected, high degree of fragmentation can hinder assignments of unknowns
LC-MS	• Superior for most targeted analyses • Separation reduces component overlap • High sensitivity • Molecular ion usually detected	• Need for different methods to analyze multiple classes of compounds • Ion-suppression/matrix effects can impact quantitation • Compounds not ionized equivalently
CE-MS	• Low sample consumption • High sensitivity • Enhanced resolution over other separation methods • Reduced matrix effects, improving quantification	• Highly sensitive to pH and temperature variations • Ion-suppression due to salt concentration • Poor separation of large or neutral compounds
IC	• High sensitivity • Reproducible • Detects inorganic ions	• Difficult to determine unknown compounds without mass or structural information • Can only detect ions

Analytical methods vary greatly depending on the class of compounds and the goals of the experiment. Often multiple methods are used in a metabolomics study due to the complementary nature of these methods and the analytes they are able to detect.

1.2.1 NMR spectroscopy

NMR has been widely used in metabolomics research[38-43] and has several advantages over other methods including: (1) it is robust and highly reproducible, (2) requires minimal sample preparation, (3) is non-destructive, allowing for preservation of the sample for further analysis, and (4) is able to detect multiple metabolites simultaneous.[44] NMR is well-suited for metabolite fingerprinting providing a simultaneous and comprehensive analysis of a wide variety of compounds. NMR metabolic profiling has been widely used in the field of plant science[45-47], as well as human health studies focusing on cancer[20, 48-50] and diagnostic testing using biological fluids[51] including urine,[52] plasma,[53] serum,[43, 54] and tissue[55]. NMR based metabolomics experiments provide a clear profile of the small molecules present at a given time-point. These metabolic profiles can be compared using statistical techniques to provide new insights into biological function.

Metabolomics aims to not only identify the metabolites present in a sample, but to quantify changes in metabolite concentrations in response to a stress or change. NMR experiments are able to quantify species on either a relative or absolute basis.

A major advantage of NMR is that it provides a uniform response for each nucleus, therefore a single internal standard can be used to quantify all the metabolites detected in the spectrum. As a result, NMR measurements are less impacted by matrix effects than LC-MS or CE-MS. For quantitative measurements it is necessary for an NMR resonance to have a signal-to-noise (S/N) ratio of at least 10:1, while it is suggested to have a ratio of 100:1 for accurate absolute quantitation.[56] Signal averaging is often used in NMR measurements to achieve better S/N, with the gain proportional to the square-root of the number of coadded scans which significantly increases the time of the experiment. There are other options available for increasing S/N, including the use of a higher field magnet, or the addition of a cryoprobe, both of which come with a significant cost.[57]

1.2.2 GC-MS

Complementary to NMR analysis, GC-MS offers better sensitivity enabling the quantification of less abundant metabolites.[58] Metabolomics samples are complicated mixtures of many small compounds, and a separation is often essential for the analysis of low abundant species whose presence may be obscured by more abundant metabolites. GC-MS offers a robust and reproducible gas chromatographic separation coupled with the sensitivity of MS analysis, making it a useful tool in the field of metabolomics and metabolic profiling.[59] The robustness of GC-MS comes in part from the use of retention indices (RI) that minimize discrepancies within the chromatographic separation, as well as the widely available libraries of MS fragmentation patterns, both aiding in the ability to identify compounds within a sample.[9, 60]

GC-MS separations use a temperature gradient (or ramp) with compounds separated based on volatility. Non-volatile metabolites such as amino acids and cyclic sugars must undergo derivatization prior to injection.[61] This chemistry involves silylation,[62] which can complicate the analysis. Derivatization by-products are common, and the reaction may be incomplete so that compounds are not fully silylated prior to analysis.[63] Some molecules rearrange during derivatization, for example arginine rearranges to form ornithine yielding unreliable concentrations for both species.[64]

The most common ionization method for GC-MS is electron impact (EI).[65] In EI, gas phase analytes collide with fast electrons emitted by a filament in the source. This impact ionizes the molecule and breaks it apart into fragments. Typically in MS measurements, the molecular ion provides the molecular weight of the analyte, while the fragment ions provide structural information. In EI, often no molecular ion is produced leaving only fragment ions for identification of the analyte and making the use of spectral libraries necessary for the identification of compounds.

After the compounds are ionized and fragmented, they are sent to a mass analyzer. In GC-MS, there are 2 common types of mass analyzers, the quadrupole and time of flight (TOF).[66] The quadrupole is a scanning mass analyzer that used the stability of ion trajectories within oscillating electric fields produced by 4 poles to separate ions according to the mass-to-charge ratio (m/z).[67] Because of the way the quadrupole functions, it is often referred to as a mass filter.

The quadrupole is able to perform both qualitative and quantitative analyses at a lower cost that the TOF. When coupled with a separation, the quadrupole is hindered by its slower scan rate that impacts the acquisition rate and can lead to spectral bias (skewing).

The TOF is a non-scanning mass analyzer in which pulses of ions are emitted from the source and accelerated so that each ion has equal kinetic energy before entering a field free drift region called a flight tube. Since kinetic energy is equal to $\frac{1}{2}mv^2$, where m is mass and v is velocity, the lower the mass of the ion consequently the greater the velocity and shorter its flight time in the flight tube. This gives TOF enhanced mass resolution and dynamic range in addition to the faster acquisition rate.[68, 69]

Because of the complexity of biological samples, introduction of a multidimensional separation can help resolve overlapping peaks and reduce matrix interferences. GC-GC-MS instruments use two different columns in tandem prior to the mass analyzer. The addition of a second column, often with a different stationary phase, can greatly increase resolution of the chromatographic separation.[70-72]

Another technique, tandem MS introduces a second (or more) mass analyzer, often as a combination of a quadrupole to with TOF (qTOF)[73] or 3 quadrupoles in tandem (QQQ)[74]. This arrangement can help reduce matrix interferences and allows for selected reaction monitoring (SRM) that is beneficial in targeted metabolomics when the specific masses are known. This type of instrument is more commonly used in conjunction with HPLC separations.[75, 76]

1.2.3 LC-MS

LC-MS is well-suited for proteomics studies and targeted metabolomics analysis due to its high sensitivity, especially as compared to NMR analysis,[15] but this method can be less useful for metabolic profiling experiments. Metabolomics methods aim for increased coverage of metabolites, and it is important to note that no single method exists that can cover the full metabolome. In order to cover a wide range of metabolites, minimal pretreatment such as solvent-protein precipitation and dilution are used.[79, 80] Lack of clean-up to remove interfering matrix compounds can negatively affect the selectivity and dynamic range of MS measurements.[78]

Direct infusion MS most commonly used with electrospray ionization (ESI), and can be adapted to detect a wide range of metabolites by being run in both positive and negative mode. Direct infusion can introduce samples via an LC system or by a syringe, and often uses a high-resolution mass spectrometer such as TOF, orbital ion trap, or Fourier transform ion cyclotron resonance (FTICR) for rapid fingerprinting analysis.[78, 81] The benefit of LC-MS compared to direct infusion MS is the benefit of the added chromatographic separation that allows the detection of isomers, reduces ion-suppression effects, and can often separate compounds according to their chemical properties.

LC-MS is well suited for targeted metabolomics studies,[82-84] but since the sample preparation, solvents, columns, and methods vary greatly depending on the classes of compounds being investigated, it is hard to obtain a global metabolomics view within a sample set. The two most common LC separation methods are reversed phase liquid chromatography (RPLC) and hydrophilic interaction chromatography (HILIC).[85]

RPLC methods are used for the separation of polar and medium-polarity metabolites. Separation of highly polar metabolites requires the use of an ion-pair reagent. While ion-pairing has shown positive results on the separation of polar metabolites, there are numerous pitfalls of this method including reduced sensitivity, ion suppression and system contamination.[86]

HILIC is considered an orthogonal method to RPLC, separating small polar compounds using a polar stationary phase without the use of an ion-pair reagent.[87] HILIC has been widely adopted as a separation technique due to the many stationary phases available for optimal separation. However, this same "advantage" is a disadvantage in metabolic profiling, with prior knowledge of the metabolites present in the sample necessary for selection of the proper column. Another drawback noted by *Heaton et al.* is the reliance on acetonitrile. In recent history, there have been periods of shortages of this solvent that can make it hard to obtain, or at least drive the cost of mobile phase up drastically.[88]

Both RPLC and HILIC can be used in conjunction with many different types of mass spectrometers, all offering their own set of advantages and disadvantages. This includes single stage instruments such as TOF and orbital ion trap, as well as tandem or "hybrid" instruments such as QTOF and quadrupole/orbital ion trap that are often used for metabolomics studies.[78] As previously discussed with GC-MS, TOF analyzers offer enhanced mass resolution and fast acquisition times. The orbital ion trap was first described in 2000,[89] and combines many features of FTICR and TOF, providing increased dynamic range in comparison to the TOF.[90]

While the TOF has been a gold standard in the field of metabolomics, high resolving power hybrid instruments such as the linear trap quadrupole (LTQ)-Orbitrap are rapidly gaining popularity in the field of metabolomics. However, a study by *Rousu et al*. reports that in their hands the TOF MS outperformed the LTQ-Orbitrap, which failed to identify as many metabolites, and produced false negatives.[91]

Similarly to GC-MS, LC-MS provides excellent sensitivity as well as information about compound mass, aiding in the identification of metabolites. However, compared with GC-MS, which takes advantage of large libraries of metabolites that match identification based on retention indices (RI) and fragmentation patterns, LC-MS metabolite libraries are much more limited. Retention time variability and the much greater array of chromatographic columns and separation conditions used in LC-MS further limits the current utilization of libraries for component identification. This complicates the identification of peaks, and for unknowns, it may be necessary to analyze standards to confirm identity. Often, uncommon metabolites of interest are not commercially available and can very expensive, or complicated to synthesize.

For quantitative analyses using LC-MS, the most accurate method is isotope dilution mass spectrometry (IDMS) in which the analyte is quantified relative to a stable isotope labeled standard of known concentration.[77] Since the labeled standard and unlabeled analyte elute simultaneously, any matrix effects that impact the ionization of the analyte similarly affect the standard.

Drawbacks to the IDMS approach include the limited availability of isotope labeled metabolites, and the challenges associated with adapting it to an untargeted method. Because an isotope labeled metabolite is necessary for quantification, it must be purchased prior to analysis, and therefore already identified as a target analyte. Because of the cost of labeled metabolites, in practice quantification is performed by using only one isotopically labeled internal standard per metabolite class. This has many drawbacks, but is still considered more reliable than the calibration curve methods, and is accurate enough for case/control comparisons.[78]

While there has been significant progress in the development of LC-MS methods for metabolomics, the work herein aims at comparing non-targeted metabolic profiles and thus opted for NMR and GC-MS because of their superior robustness, and wide range of metabolites detectable in a single experiment.

1.2.4 CE-MS

Many charged metabolites are poorly retained by RPLC columns making CE a potentially attractive alternative. CE differs from both LC and GC separations because resolution does not rely on interactions with a stationary phase. Instead analytes are separated electrophoretically based on their size-to-charge ratio in a silica capillary filled with a buffered solution.[3, 92]

Advantages of CE as a separation technique include low sample consumption and enhanced resolution in comparison to chromatographic methods.[93] Disadvantages include instability of migration times and adsorption of components to the capillary surface, a common problem encountered with complex biological samples.

The most common methods of detection in CE separations are UV and fluorescence.[94, 95] The drawbacks of these detection methods are their inability to provide structural or mass information to aid in determination and confirmation of metabolites present in complex samples. For this reason, CE coupled with a mass analyzer (CE-MS) is an ideal combination. CE-MS is still relatively new, with systems only becoming available for purchase from Agilent within the past couple years. As a result there are fewer well-established and validated methods available for metabolomics compared with GC-MS.

In the CE separation it is essential that the electrolyte contains ions to carry the charge of the applied voltage that connects the anode to the cathode. This electrolyte solution is composed of a weak acid and base that can keep the solution buffered over a narrow pH range. Typical CE buffers contain boric, phosphoric, or citric acids, which have low volatility and are incompatible with MS instruments.

A key feature of CE is the low sample consumption in the nanoliter range, making it essential that the mass spectrometer have high sensitivity necessary to obtain reducible results. Even with these drawbacks CE-MS is becoming a popular instrument in the field of metabolomics.[36, 96-98] For example, *Matsumoto et al.* recently reported the detection and identification of 179 metabolites in the luminal metabolome using a CE-MS equipped with a TOF mass analyzer compared to only 10-60 metabolites identified in previous studies using NMR and LC-MS.[99] The metabolites were identified by aligning similar m/z and migration times to that of standards.

Similar to LC-MS one drawback of metabolomics experiments using CE-MS lies in the identification step. There is currently no known public library of standards, making it necessary to run individual standards to create a system library which can be very time consuming. This can greatly reduce the ability to identify unknowns, especially when standards are not commercially available. One way to overcome this would be to use a hybrid mass spectrometer that provides structural information through fragmentation.

Although CE-MS is gaining popularity in the field of metabolomics, there are several reasons it was not used for the analyses within this dissertation. Limited availability of this instrumentation is a factor to consider, but also the lack of validated methods of analysis and metabolite libraries were also a determining factor. The aim of our experiments were to identify and profile as many metabolites as possible. The identify metabolites were unknown at the beginning of this research, leading us to choose NMR because it provides robust quantification and structural information to aid in identification, as well as GC-MS due to the availability of libraries for identification.

1.2.5 IC

IC is a well-established separation method often used in water analyses due to its robust, high throughput capabilities for measuring the concentrations of inorganic ions. In fact, IC has been approved in the USA for the compliance monitoring of common inorganic anions in drinking water since the 1980s.[100] One of the greatest advantages of IC is its sensitivity, allowing the detection of ions at levels of approximately 1 µg/L with minimal sample preparation. Even though IC was developed in 1975, it is still a popular technique with recent advances in the development of new stationary phases,[101-103] miniaturization,[104, 105] and hyphenated IC systems.[106-108]

IC differs from CE in that it utilizes a chromatographic separation employing a column filled with a stationary phase. The stationary phase carries a charge, allowing for a charge-based interaction with the analytes of interest carried through the column in the mobile phase. Analytes elute from the column based on charge, with monovalent ions eluted before divalent and so on due to the strength of interaction with the opposite charge of the stationary phase. When two analytes have similar charge, the size of the ion determines the elution time, with the ion of smaller surface area eluting first.

IC is not commonly used in the field of metabolomics because of the limited variety of metabolites that can be detected. Metabolomics data determined using IC is largely to inorganic ions and various weak acids. Inorganic ions play an important role in the function of the colon, making it a good fit for the analyses discussed in Chapter 3. However, to gain a global view of metabolites in solution other instrumental methods, such as NMR and GC-MS, must be employed in a complementary manner.

1.3 Statistical analysis of metabolomics and metabolic profiling data sets

Statistical analysis is an important component of metabolite profiling and metabolomics experiments. Statistical data treatments can help to correlate changes, and determine underlying factors contributing to change or variance among samples. They are also powerful visualization techniques that provide the ability to view univariate or complex multivariate distinctions between sample groups. Both univariate and multivariate analysis can be employed to extract relevant information from complex metabolomics data sets that aim to provide biological knowledge. While multivariate analysis has been most common in metabolomics studies, recently more publications are including both multivariate and univariate analysis such as t-tests and analysis of variance (ANOVA), especially for metabolite profiling.[109]

1.3.1 Univariate statistical methods

Univariate analysis is the simplest form of statistical analysis. As "uni" means one, univariate statistical treatments examine one variable at a time. Univariate analysis is popular in biostatistical methods, and is used to follow changes in the levels of individual metabolites using peak areas or concentrations.[110] Univariate analysis assumes the metabolites operate individually and does not directly consider the causes or relationships between metabolites, though these can sometimes be inferred. Multivariate analysis often includes univariate analysis as a validation step to confirm the significance of the variance observed between groups of samples.[109, 111]

Examples of univariate analysis employed in metabolomic and metabolic profiling studies includes ANOVA, histograms, bar charts, box and whisker plots, volcano plots, and distribution tables. Each of these offer a unique way of displaying data, and the choice of which methods to implement relies greatly on the type of analysis and the nature of the data obtained from experimentation. Univariate analyses including box plots and heat maps are employed within this dissertation and are used to highlight changes in metabolite concentrations between sample groups.

Box plots in chapter 3 display results using blue boxes representative of 50% of the values, with 25% of the values both above and below the box. The center of the box is considered the mean, while the dark line within the box is the median value. The T-bars that extend from the boxes (inner fences) represent approximately 95% of the data, and points that are displayed outside of the inner fences are considered outliers. If the outlier is denoted with an asterisk, it is considered an extreme outlier. An extreme outlier is defined as case in which the value is more than three times the height of the box.

1.3.2 Multivariate statistical methods

Multivariate analysis is widely employed in metabolomics studies and examines correlations between sample groups using multiple variables. The most common multivariate statistic model used in metabolomics is principal component analysis (PCA). PCA is an unsupervised multivariate clustering method requiring no knowledge of the data set.

PCA acts to reduce dimensionality of the data while preserving the variance.[112, 113] PCA decomposes the data into score vectors and loading vectors. The directions of the loadings are placed for maximum variation spanned by each vector, with the first principal component (PC1) accounting for the most variance and subsequent components accounting for decreasing degrees of variance. Often, the most interesting results are found in the first few components, with the later components reflecting variance due to artifacts, less interesting metabolites, noise or drift.[114]

Most often, PCA results are observed as score plots (Figure 1.2), which are plots of score vectors, often color-coded, that help visualize multivariate differences between samples. Figure 1.2 is a PCA score plot obtained from a ^{1}H-NMR stool data set, highlighting the ability of multivariate analysis to separate groups of samples based on variance in the detected spectral variables. This plot correlates the score vectors for the two most significant principal components, PC1 and PC2, explaining 64.3% of the overall variance in the data set. The implications of this data are explained in detail in Chapter 3. The loadings plot (Figure 1.3) highlights the source of the variance observed in the score plot by displaying those variables (NMR resonances) that are responsible for the greatest variation in each principle component (dimension). As with any statistical method, PCA cannot distinguish natural variance within a treatment, such as biological variance, from the variance between sample groups arising from the treatment.

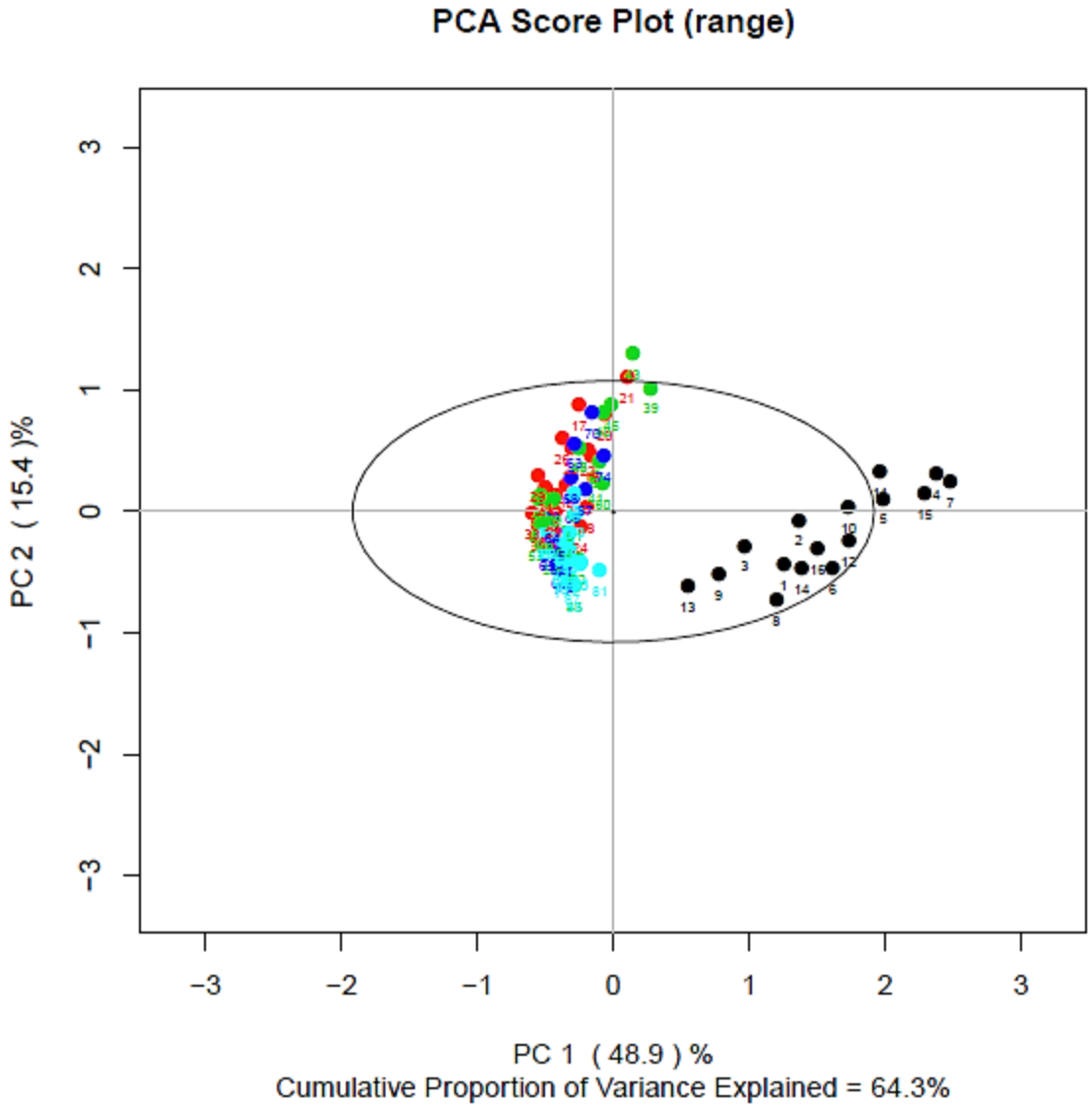

Figure 1.2. Multivariate analysis using a principal component analysis (PCA) model of stool samples obtained from multiple locations of the colon, including ileum (●), cecum (●), proximal (●), mid (●), and distal (●) colon. The largest proportion of variance is plotted as principle component 1 (PC 1) on the x-axis, and the second largest on the y-axis as principle component 2 (PC2). Together both PC1 and PC2 explain 64.3% of the variance between samples.

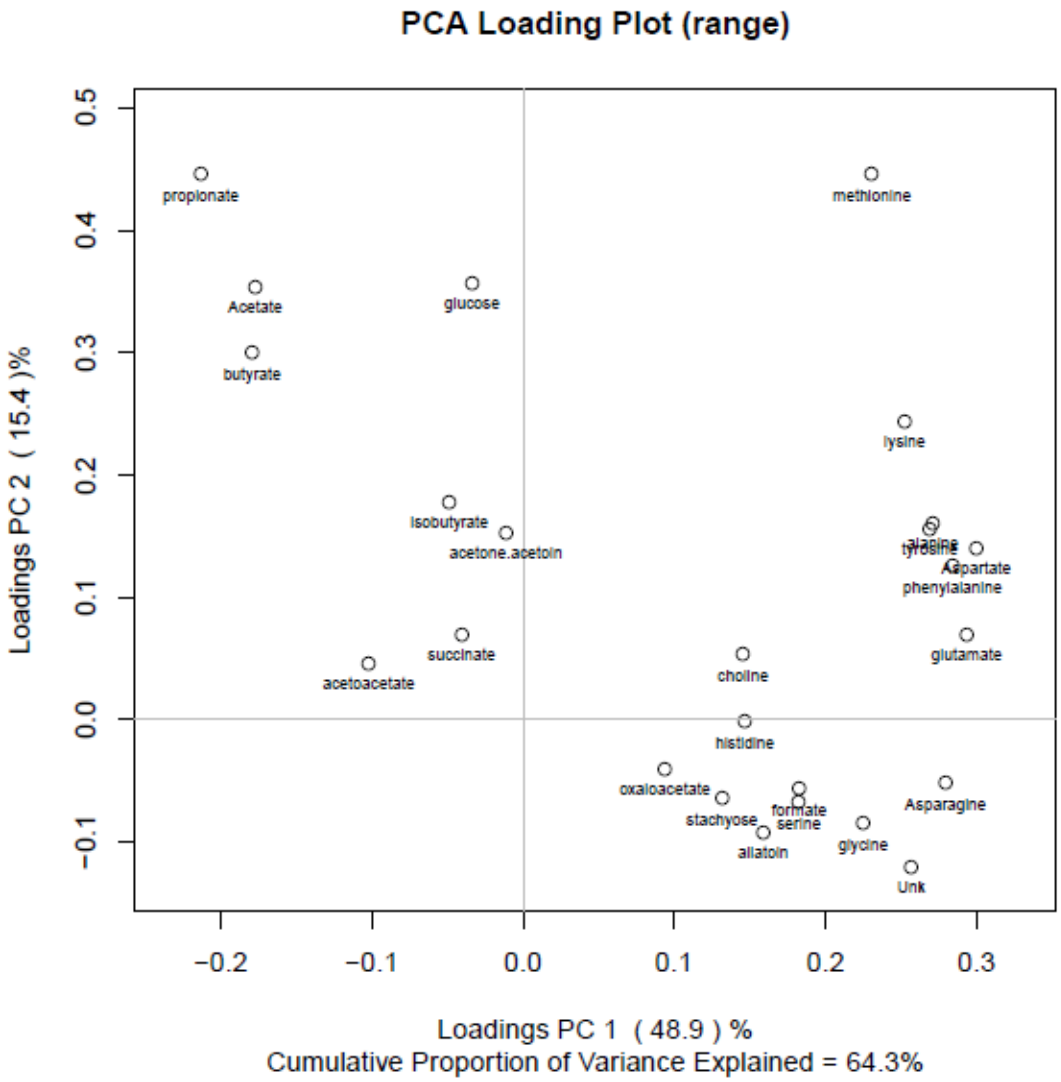

Figure 1.3. Corresponding loadings plot to the score plot of Figure 1.2, highlighting the variables, in this case metabolite ^{1}H NMR resonances, contributing to the variance in PC1 and PC2. Similar to the score plot, the x-axis represents the data for principal component 1 (PC 1) and the y-axis is principal component 2 (PC 2). The point of origin between these two axes is 0 variance. The further a point is from this origin the greater it contributes to the variance of the respective component.

When specific information is available about samples such as disease state, gender, age group, etc., partial least squares (PLS) analysis can provide a more interpretable decomposition by adding an explanatory variable such as time or dose, and maximizing variation between these explanatory variables.[114] PLS differs from PCA in that it is not a simple linear regression between response and independent variables, but is rather a bilinear model that projects predicted variables and observable variables into a new space. PLS-DA introduces discriminant analysis which is used when one variable is categorical, and maximization is done on the between-groups covariance.[115]

Both PCA and PLS-DA are used in the metabolic profiling experiments described in this dissertation. We found that the form of PLS-DA, Orthogonal Projections to Latent Structures Discriminant Analysis (OPLS-DA), which appears as a rotation of the original PLS-DA, has an advantage in interpretability leading to its increase in popularity amongst metabolomics practitioners.[116]

In this dissertation, statistical analyses were used to provide both univariate and multivariate comparisons of data sets and visualize the results obtained, as well as to highlight variance among metabolites between groups (e.g., samples taken from different locations in the colon). The section below describes the function of the colon and the role of its constituent microorganisms, providing a context for the biological implications of the scientific work described in the subsequent chapters of this dissertation.

1.4 Large intestine (colon)

The large intestine, often referred to as the colon, is located in the abdomen. The large intestine is the final stage of the digestive system or "gut", following the small intestine. It has been thought that the principal function of the colon is to conserve water and electrolytes secreted into the gut during digestion, and to excrete waste products left after digestion. Although long disregarded as a simple waste-packaging organ, the large intestine has recently been recognized as an astonishingly complex biochemical factory of vital importance to human health. The human colon harbors trillions of beneficial microbes of at least 160 species[35] that harvest energy, synthesize vitamins, metabolize toxins, and shape the immune system. The ability to profile metabolism and transport activity throughout the colon is imperative to understanding its overall function. This information also provides insights into the dysfunction of the colon in diseases such as IBD and colitis, and could potentially lead to new treatments for these disorders.

The colon can be thought of as comprised of distinct sections. Specifically for the rat colon, 5 sections are delineated as shown in Figure 1.4. First is the ileum, which is the end of the small intestine at the junction where it connects to the large intestine. The next section is the cecum, which is quite large in the rat, and acts as a fermenting chamber. The carbohydrate rich diet of the rat creates an essential need for this fermenting chamber as polysaccharides larger than disaccharides are not digested in prior sections of the digestive system. The rest of the colon is split into three segments in the order of: proximal, mid, and distal colon.

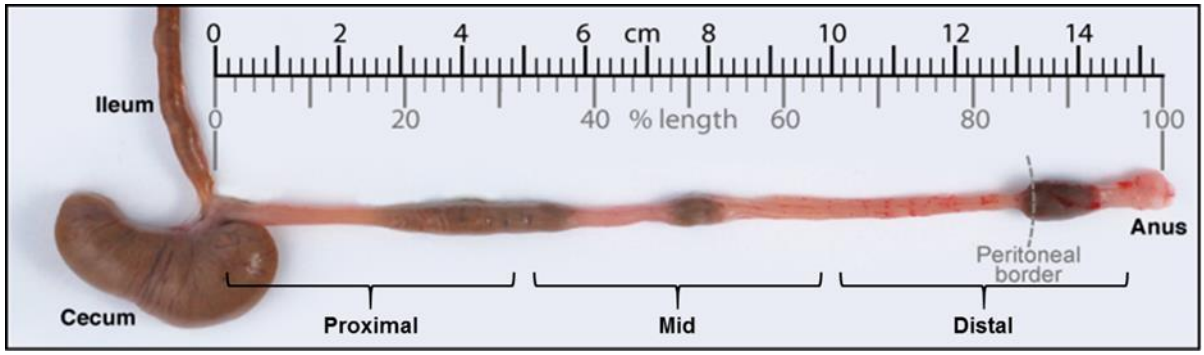

Figure 1.4. Example of a female rat colon removed before stool extraction. Segments of the colon are labeled including the ileum, cecum, and approximate locations of the proximal, mid, and distal colon.

1.4.1 Segmental stratification of the colon and its effect on the luminal metabolome

The term metabolome is defined as the entire metabolite collection within a body and is analogous to the genome and transcriptome terms already in common use.[117] Thus, the luminal metabolome refers to the collection of metabolites within the luminal contents of the colon, referred to as stool or feces, and is greatly defined by the gut microbiome housed within the colon. The gut microbiome contains an estimated 10-100 trillion organisms and is the largest collection of microbes found in the human body.[118, 119] In fact, the number of bacterial cells in the colon is 10 times greater than the total number of somatic and germ cells in the human body.[99]

This complex system of bacterial microbes is comprised of at least 160 different species, and is stratified along the length of the colon[120] with different species inhabiting different locations. The segmental stratification of the colon is often overlooked, but it is known that the community of bacterial species that inhabit the proximal colon is quite different than that found in the distal colon.[121] The questions of how these distinct microbial communities remain segmentally stratified in the face of continuous luminal transit, and what role they play in health, remain largely unanswered. However, it is believed the various microorganisms act in a symbiotic relationship, with some species in the proximal colon breaking down materials to provide an energy source for other species of bacteria located in the mid or distal colon, which further break down the stool contents.

This research aims to take a step forward in defining the functional segmentation of the rodent colon and the role of epithelial transport processes in creating luminal environments that impose biogeographical selection pressures on the microbial community assemblage by profiling the composition of the luminal metabolome in stool as it travels the length of the colon (Figure. 1.4). The luminal metabolome is complicated, and it is conceivable that the luminal metabolome could be considered to be comprised of several different metabolomes due to the segmental stratification present.

The segmental profile of fecal metabolites undoubtedly contains a wealth of information on the integrated functions of the epithelium and resident microbiome in health and disease. Previous studies of stool have been restricted to analysis of voided stool[44, 122], which has several limitations. Voided stool has moved through all compartments of the colon, and the information it carries is averaged both spatially and temporally, thus providing little information on the function of individual colon segments or their different microbial communities. In addition, fecal solutes may be lost through metabolism, absorption, or decomposition during colonic transit. Determining how fecal water is altered chemically and metabolically as it travels the length of the colon is expected to provide insight into transport processes and metabolism that add or remove solutes in each segment.

The metabolic profiling experiments presented in this dissertation provide snapshots of each segment of the colon to provide evidence of the consequences of segmental stratification of the luminal metabolome. Later chapters aim to use metabolic profiling techniques to identify the absorptive and secretory processes of the colon by identifying and quantifying metabolites transported across the epithelial tissue in an effort to better define healthy colon function.

1.5. References

1. Larive, C. K.; Barding, G. A.; Dinges, M. M., NMR Spectroscopy for Metabolomics and Metabolic Profiling. *Analytical Chemistry* **2015,** *87* (1), 133-146.

2. Bouatra, S.; Aziat, F.; Mandal, R.; Guo, A. C.; Wilson, M. R.; Knox, C.; Bjorndahl, T. C.; Krishnamurthy, R.; Saleem, F.; Liu, P.; Dame, Z. T.; Poelzer, J.; Huynh, J.; Yallou, F. S.; Psychogios, N.; Dong, E.; Bogumil, R.; Roehring, C.; Wishart, D. S., The Human Urine Metabolome. *Plos One* **2013,** *8* (9).

3. Mozzi, F., Metabolomics as a tool for the comprehensive understanding of fermented and functional foods with lactic acid bacteria. **2013,** *54* (1), 1152–1161.

4. Emwas, A.-H. M.; Salek, R. M.; Griffin, J. L.; Merzaban, J., NMR-based metabolomics in human disease diagnosis: applications, limitations, and recommendations. *Metabolomics* **2013,** *9* (5), 1048-1072.

5. Barding, G. A.; Beni, S.; Fukao, T.; Bailey-Serres, J.; Larive, C. K., Comparison of GC-MS and NMR for Metabolite Profiling of Rice Subjected to Submergence Stress. *Journal of Proteome Research* **2013,** *12* (2), 898-909.

6. Rochfort, S., Metabolomics reviewed: a new "omics" platform technology for systems biology and implications for natural products research. *J Nat Prod* **2005,** *68* (12), 1813-20.

7. Le Gall, G.; Noor, S. O.; Ridgway, K.; Scovell, L.; Jamieson, C.; Johnson, I. T.; Colquhoun, I. J.; Kemsley, E. K.; Narbad, A., Metabolomics of Fecal Extracts Detects Altered Metabolic Activity of Gut Microbiota in Ulcerative Colitis and Irritable Bowel Syndrome. *Journal of Proteome Research* **2011,** *10* (9), 4208-4218.

8. Bouatra, S.; Aziat, F.; Mandal, R.; Guo, A. C.; Wilson, M. R.; Knox, C.; Bjorndahl, T. C.; Krishnamurthy, R.; Saleem, F.; Liu, P.; Dame, Z. T.; Poelzer, J.; Huynh, J.; Yallou, F. S.; Psychogios, N.; Dong, E.; Bogumil, R.; Roehring, C.; Wishart, D. S., The Human Urine Metabolome. *Plos One 8* (9).

9. Wishart, D. S.; Jewison, T.; Guo, A. C.; Wilson, M.; Knox, C.; Liu, Y.; Djoumbou, Y.; Mandal, R.; Aziat, F.; Dong, E.; Bouatra, S.; Sinelnikov, I.; Arndt, D.; Xia, J.; Liu, P.; Yallou, F.; Bjorndahl, T.; Perez-Pineiro, R.; Eisner, R.; Allen, F.; Neveu, V.; Greiner, R.; Scalbert, A., HMDB 3.0--The Human Metabolome Database in 2013. *Nucleic Acids Res* **2013,** *41* (Database issue), D801-7.

10. Wishart, D. S.; Knox, C.; Guo, A. C.; Eisner, R.; Young, N.; Gautam, B.; Hau, D. D.; Psychogios, N.; Dong, E.; Bouatra, S.; Mandal, R.; Sinelnikov, I.; Xia, J.; Jia, L.; Cruz, J. A.; Lim, E.; Sobsey, C. A.; Shrivastava, S.; Huang, P.; Liu, P.; Fang, L.; Peng, J.; Fradette, R.; Cheng, D.; Tzur, D.; Clements, M.; Lewis, A.; De Souza, A.; Zuniga, A.; Dawe, M.; Xiong, Y.; Clive, D.; Greiner, R.; Nazyrova, A.; Shaykhutdinov, R.; Li, L.; Vogel, H. J.; Forsythe, I., HMDB: a knowledgebase for the human metabolome. *Nucleic Acids Res* **2009,** *37* (Database issue), D603-10.

11. Putri, S. P.; Yamamoto, S.; Tsugawa, H.; Fukusaki, E., Current metabolomics: technological advances. *J Biosci Bioeng* **2013,** *116* (1), 9-16.

12. Blekherman, G.; Laubenbacher, R.; Cortes, D. F.; Mendes, P.; Torti, F. M.; Akman, S.; Torti, S. V.; Shulaev, V., Bioinformatics tools for cancer metabolomics. *Metabolomics* **2011,** *7* (3), 329-343.

13. Nicholson, J. K.; Lindon, J. C.; Holmes, E., 'Metabonomics': understanding the metabolic responses of living systems to pathophysiological stimuli via multivariate statistical analysis of biological NMR spectroscopic data. *Xenobiotica* **1999,** *29* (11), 1181-1189.

14. Robertson, D. G., Metabonomics in toxicology: A review. *Toxicological Sciences* **2005,** *85* (2), 809-822.

15. Zhou, B.; Xiao, J. F.; Tuli, L.; Ressom, H. W., LC-MS-based metabolomics. *Molecular Biosystems* **2012,** *8* (2), 470-481.

16. de Santana, A. P.; Jacomasso, T.; Riter, D. S.; Barison, A.; Iacomini, M.; Winnischofer, S. M. B.; Sassaki, G. L., NMR metabolic fingerprints of murine melanocyte and melanoma cell lines: application to biomarker discovery. *Scientific Reports* **2017,** *7*.

17. Turano, P., Colorectal cancer: the potential of metabolic fingerprinting. *Expert Review of Gastroenterology & Hepatology* **2014,** *8* (8), 847-849.

18. Priolo, C.; Pyne, S.; Rose, J.; Regan, E. R.; Zadra, G.; Photopoulos, C.; Cacciatore, S.; Schultz, D.; Scaglia, N.; McDunn, J.; De Marzo, A. M.; Loda, M., AKT1 and MYC Induce Distinctive Metabolic Fingerprints in Human Prostate Cancer. *Cancer Research* **2014,** *74* (24), 7198-7204.

19. Dunn, W. B.; Broadhurst, D. I.; Atherton, H. J.; Goodacre, R.; Griffin, J. L., Systems level studies of mammalian metabolomes: the roles of mass spectrometry and nuclear magnetic resonance spectroscopy. *Chemical Society Reviews 40* (1), 387-426.

20. Griffin, J. L.; Shockcor, J. P., Metabolic profiles of cancer cells. *Nature Reviews Cancer* **2004,** *4* (7), 551-561.

21. Cui, L.; Hou, J.; Fang, J. L.; Lee, Y. H.; Costa, V. V.; Wong, L. H.; Chen, Q. F.; Ooi, E. E.; Tannenbaum, S. R.; Chen, J. Z.; Ong, C. N., Serum Metabolomics Investigation of Humanized Mouse Model of Dengue Virus Infection. *Journal of Virology* **2017,** *91* (14).

22. Lussu, M.; Noto, A.; Masili, A.; Rinaldi, A. C.; Dessi, A.; De Angelis, M.; De Giacomo, A.; Fanos, V.; Atzori, L.; Francavilla, R., The urinary H-1-NMR metabolomics profile of an italian autistic children population and their unaffected siblings. *Autism Research* **2017,** *10* (6), 1058-1066.

23. Mueller-Hennessen, M.; Sigl, J.; Fuhrmann, J. C.; Witt, H.; Reszka, R.; Schmitz, O.; Kastler, J.; Fischer, J. J.; Muller, O. J.; Giannitsis, E.; Weis, T.; Frey, N.; Katus, H. A., Metabolic profiles in heart failure due to non-ischemic cardiomyopathy at rest and under exercise. *Esc Heart Failure* **2017,** *4* (2), 178-189.

24. Kim, M.; Lee, S. H.; Lee, J. H., Global Metabolic Profiling of Plasma Shows that Three-Year Mild-Caloric Restriction Lessens an Age-Related Increase in Sphingomyelin and Reduces L-leucine and L-phenylalanine in Overweight and Obese Subjects. *Aging and Disease* **2017,** *7* (6), 721-733.

25. Zhang, X.; Xu, L.; Shen, J.; Cao, B.; Cheng, T.; Zhao, T.; Liu, X.; Zhang, H., Metabolic signatures of esophageal cancer: NMR-based metabolomics and UHPLC-based focused metabolomics of blood serum. *Biochimica Et Biophysica Acta-Molecular Basis of Disease* **2013,** *1832* (8), 1207-1216.

26. Zhang, A.; Sun, H.; Wang, P.; Han, Y.; Wang, X., Recent and potential developments of biofluid analyses in metabolomics. *J Proteomics* **2012,** *75* (4), 1079-88.

27. Ouyang, S. Q.; Beecher, C. N.; Wang, K.; Larive, C. K.; Borkovich, K. A., Metabolic Impacts of Using Nitrogen and Copper-Regulated Promoters to Regulate Gene Expression in Neurospora crassa. *G3-Genes Genomes Genetics* **2015,** *5* (9), 1899-1908.

28. Clarke, C. J.; Haselden, J. N., Metabolic Profiling as a Tool for Understanding Mechanisms of Toxicity. *Toxicologic Pathology* **2008,** *36* (1), 140-147.

29. Posma, J. M.; Garcia-Perez, I.; De Iorio, M.; Lindon, J. C.; Elliott, P.; Holmes, E.; Ebbels, T. M. D.; Nicholson, J. K., Subset Optimization by Reference Matching (STORM): An Optimized Statistical Approach for Recovery of Metabolic Biomarker Structural Information from H-1 NMR Spectra of Biofluids. *Analytical Chemistry* **2012,** *84* (24), 10694-10701.

30. Bradley, S. A.; Ouyang, A. L.; Purdie, J.; Smitka, T. A.; Wang, T. T.; Kaerner, A., Fermentanomics: Monitoring Mammalian Cell Cultures with NMR Spectroscopy. *Journal of the American Chemical Society* **2010,** *132* (28), 9531-9533.

31. Barding, G. A., Jr.; Salditos, R.; Larive, C. K., Quantitative NMR for bioanalysis and metabolomics. *Analytical and Bioanalytical Chemistry* **2012,** *404* (4), 1165-1179.

32. Warth, B.; Parich, A.; Bueschl, C.; Schoefbeck, D.; Neumann, N. K. N.; Kluger, B.; Schuster, K.; Krska, R.; Adam, G.; Lemmens, M.; Schuhmacher, R., GC-MS based targeted metabolic profiling identifies changes in the wheat metabolome following deoxynivalenol treatment. *Metabolomics* **2015,** *11* (3), 722-738.

33. Wikoff, W. R.; Anfora, A. T.; Liu, J.; Schultz, P. G.; Lesley, S. A.; Peters, E. C.; Siuzdak, G., Metabolomics analysis reveals large effects of gut microflora on mammalian blood metabolites. *Proceedings of the National Academy of Sciences of the United States of America* **2009,** *106* (10), 3698-3703.

34. Fardet, A.; Llorach, R.; Martin, J. F.; Besson, C.; Lyan, B.; Pujos-Guillot, E.; Scalbert, A., A liquid chromatography-quadrupole time-of-flight (LC-QTOF)-based metabolomic approach reveals new metabolic effects of catechin in rats fed high-fat diets. *Journal of Proteome Research* **2008,** *7* (6), 2388-2398.

35. Matsumoto, M.; Kibe, R.; Ooga, T.; Aiba, Y.; Kurihara, S.; Sawaki, E.; Koga, Y.; Benno, Y., Impact of Intestinal Microbiota on Intestinal Luminal Metabolome. *Scientific Reports, Published online: 25 January 2012; | doi:10.1038/srep00233* **2011**.

36. Zhang, W.; Hankemeier, T.; Ramautar, R., Next-generation capillary electrophoresis-mass spectrometry approaches in metabolomics. *Current Opinion in Biotechnology* **2017,** *43*, 1-7.

37. Sanchez, M. I. G.; McCullagh, J.; Guy, R. H.; Compton, R. G., Reverse Iontophoretic Extraction of Metabolites from Living Plants and their Identification by Ion-chromatography Coupled to High Resolution Mass Spectrometry. *Phytochemical Analysis* **2017,** *28* (3), 195-201.

38. Aranibar, N.; Reily, M. D., NMR Methods for Metabolomics of Mammalian Cell Culture Bioreactors. In *Animal Cell Biotechnology: Methods and Protocols, 3rd Edition*, pp 223-236.

39. Bingol, K.; Bruschweiler, R., Multidimensional Approaches to NMR-Based Metabolomics. *Analytical Chemistry 86* (1), 47-57.

40. DeFeo, E. M.; Wu, C. L.; McDougal, W. S.; Cheng, L. L., A decade in prostate cancer: from NMR to metabolomics. *Nature Reviews Urology 8* (6), 301-311.

41. Duarte, I. F.; Diaz, S. O.; Gil, A. M., NMR metabolomics of human blood and urine in disease research. *Journal of Pharmaceutical and Biomedical Analysis 93*, 17-26.

42. Heyman, H. M.; Meyer, J. J. M., NMR-based metabolomics as a quality control tool for herbal products. *South African Journal of Botany 82*, 21-32.

43. Sonkar, K.; Behari, A.; Kapoor, V. K.; Sinha, N., H-1 NMR metabolic profiling of human serum associated with benign and malignant gallstone diseases. *Metabolomics* **2013,** *9* (2), 515-528.

44. Bezabeh, T.; Somorjai, R. L.; Smith, I. C., MR metabolomics of fecal extracts: applications in the study of bowel diseases. *Magn Reson Chem* **2009,** *47 Suppl 1*, S54-61.

45. Colquhoun, I. J., Use of NMR for metabolic profiling in plant systems. *Journal of Pesticide Science* **2007,** *32* (3), 200-212.

46. Kaiser, K. A.; Barding, G. A.; Larive, C. K., A comparison of metabolite extraction strategies for H-1-NMR-based metabolic profiling using mature leaf tissue from the model plant Arabidopsis thaliana. *Magnetic Resonance in Chemistry* **2009,** *47*, S147-S156.

47. Krishnan, P.; Kruger, N. J.; Ratcliffe, R. G., Metabolite fingerprinting and profiling in plants using NMR. *Journal of Experimental Botany* **2005,** *56* (410), 255-265.

48. Wang, H. J.; Zhang, H. L.; Deng, P. C.; Liu, C. Q.; Li, D. D.; Jie, H.; Zhang, H.; Zhou, Z. G.; Zhao, Y. L., Tissue metabolic profiling of human gastric cancer assessed by H-1 NMR. *Bmc Cancer* **2016,** *16*.

49. Chan, E. C. Y.; Koh, P. K.; Mal, M.; Cheah, P. Y.; Eu, K. W.; Backshall, A.; Cavill, R.; Nicholson, J. K.; Keun, H. C., Metabolic Profiling of Human Colorectal Cancer Using High-Resolution Magic Angle Spinning Nuclear Magnetic Resonance (HR-MAS NMR) Spectroscopy and Gas Chromatography Mass Spectrometry (GC/MS). *Journal of Proteome Research* **2009,** *8* (1), 352-361.

50. Jain, M.; Nilsson, R.; Sharma, S.; Madhusudhan, N.; Kitami, T.; Souza, A. L.; Kafri, R.; Kirschner, M. W.; Clish, C. B.; Mootha, V. K., Metabolite Profiling Identifies a Key Role for Glycine in Rapid Cancer Cell Proliferation. *Science* **2012,** *336* (6084), 1040-1044.

51. Beckonert, O.; Keun, H. C.; Ebbels, T. M. D.; Bundy, J. G.; Holmes, E.; Lindon, J. C.; Nicholson, J. K., Metabolic profiling, metabolomic and metabonomic procedures for NMR spectroscopy of urine, plasma, serum and tissue extracts. *Nature Protocols* **2007,** *2* (11), 2692-2703.

52. Carrola, J.; Rocha, C. M.; Barros, A. S.; Gil, A. M.; Goodfellow, B. J.; Carreira, I. M.; Bernardo, J.; Gomes, A.; Sousa, V.; Carvalho, L.; Duarte, I. F., Metabolic Signatures of Lung Cancer in Biofluids: NMR-Based Metabonomics of Urine. *Journal of Proteome Research* **2011,** *10* (1), 221-230.

53. Rocha, C. M.; Carrola, J.; Barros, A. S.; Gil, A. M.; Goodfellow, B. J.; Carreira, I. M.; Bernardo, J.; Gomes, A.; Sousa, V.; Carvalho, L.; Duarte, I. F., Metabolic Signatures of Lung Cancer in Biofluids: NMR-Based Metabonomics of Blood Plasma. *Journal of Proteome Research* **2011,** *10* (9), 4314-4324.

54. Stolzenburg, S.; Lauridsen, M. B.; Toft, H.; Zalloua, P. A.; Baunsgaard, D., Improved quality of H-1 NMR spectroscopic data for enhanced metabolic profiling of low molecular weight metabolites in human serum. *Metabolomics* **2011,** *7* (2), 270-277.

55. Cacciatore, S.; Zadra, G.; Bango, C.; Penney, K. L.; Tyekucheva, S.; Yanes, O.; Loda, M., Metabolic Profiling in Formalin-Fixed and Paraffin-Embedded Prostate Cancer Tissues. *Molecular Cancer Research* **2017,** *15* (4), 439-447.

56. Malz, F., QUANTITATIVE NMR IN THE SOLUTION STATE NMR. *Nmr Spectroscopy in Pharmaceutical Analysis* **2008**, 43-62.

57. Webb, A., Increasing the Sensitivity of Magnetic Resonance Spectroscopy and Imaging. *Analytical Chemistry* **2012,** *84* (1), 9-16.

58. Weckwerth, W., Metabolomics in systems biology. *Annual Review of Plant Biology* **2003,** *54*, 669-689.

59. Shiomi, Y.; Nishiumi, S.; Ooi, M.; Hatano, N.; Shinohara, M.; Yoshie, T.; Kondo, Y.; Furumatsu, K.; Shiomi, H.; Kutsumi, H.; Azuma, T.; Yoshida, M., GCMS-based Metabolomic Study in Mice with Colitis Induced by Dextran Sulfate Sodium. *Inflammatory Bowel Diseases* **2011,** *17* (11), 2261-2274.

60. Kopka, J.; Schauer, N.; Krueger, S.; Birkemeyer, C.; Usadel, B.; Bergmuller, E.; Dormann, P.; Weckwerth, W.; Gibon, Y.; Stitt, M.; Willmitzer, L.; Fernie, A. R.; Steinhauser, D., GMD@CSB.DB: the Golm Metabolome Database. *Bioinformatics* **2005,** *21* (8), 1635-1638.

61. Fiehn, O.; Kopka, J.; Dormann, P.; Altmann, T.; Trethewey, R. N.; Willmitzer, L., Metabolite profiling for plant functional genomics. *Nature Biotechnology* **2000,** *18* (11), 1157-1161.

62. Khakimov, B.; Mongi, R. J.; Sorensen, K. M.; Ndabikunze, B. K.; Chove, B. E.; Engelsen, S. B., A comprehensive and comparative GC-MS metabolomics study of non-volatiles in Tanzanian grown mango, pineapple, jackfruit, baobab and tamarind fruits. *Food Chemistry* **2016,** *213*, 691-699.

63. Moros, G.; Chatziioannou, A. C.; Gika, H. G.; Raikos, N.; Theodoridis, G., Investigation of the derivatization conditions for GC-MS metabolomics of biological samples. *Bioanalysis* **2017,** *9* (1), 53-65.

64. Corso, G.; Esposito, M.; Gallo, M.; Dellorusso, A.; Antonio, M., TRANSFORMATION OF ARGININE INTO ORNITHINE DURING THE PREPARATION OF ITS TERT-BUTYLDIMETHYLSILYL DERIVATIVE FOR ANALYSIS BY GAS CHROMATOGRAPHY/MASS SPECTROMETRY. *Biological Mass Spectrometry* **1993,** *22* (12), 698-702.

65. Hao, C. Y.; Zhao, X. M.; Yang, P., GC-MS and HPLC-MS analysis of bioactive pharmaceuticals and personal-care products in environmental matrices. *Trac-Trends in Analytical Chemistry* **2007,** *26* (6), 569-580.

66. Kind, T.; Wohlgemuth, G.; Lee, D. Y.; Lu, Y.; Palazoglu, M.; Shahbaz, S.; Fiehn, O., FiehnLib: Mass Spectral and Retention Index Libraries for Metabolomics Based on Quadrupole and Time-of-Flight Gas Chromatography/Mass Spectrometry. *Analytical Chemistry* **2009,** *81* (24), 10038-10048.

67. Miller, P. E.; Denton, M. B., THE QUADRUPOLE MASS FILTER - BASIC OPERATING CONCEPTS. *Journal of Chemical Education* **1986,** *63* (7), 617-622.

68. Fiehn, O., Extending the breadth of metabolite profiling by gas chromatography coupled to mass spectrometry. *Trac-Trends in Analytical Chemistry* **2008,** *27* (3), 261-269.

69. Hoker, J.; Obersteiner, F.; Bonisch, H.; Engel, A., Comparison of GC/time-of-flight MS with GC/quadrupole MS for halocarbon trace gas analysis. *Atmospheric Measurement Techniques* **2015,** *8* (5), 2195-2206.

70. Welthagen, W.; Shellie, R. A.; Spranger, J.; Ristow, M.; Zimmermann, R.; Fiehn, O., Comprehensive two-dimensional gas chromatography-time-of-flight mass spectrometry (GC x GC-TOF) for high resolution metabolomics: biomarker discovery on spleen tissue extracts of obese NZO compared to lean C57BL/6 mice. *Metabolomics* **2005,** *1* (1), 65-73.

71. Ralston-Hooper, K.; Jannasch, A.; Adamec, J.; Sepulveda, M., The Use of Two-Dimensional Gas Chromatography-Time-of-Flight Mass Spectrometry (GC x GC-TOF-MS) for Metabolomic Analysis of Polar Metabolites. *Metabolic Profiling: Methods and Protocols* **2011,** *708*, 205-211.

72. Ly-Verdu, S.; Groger, T. M.; Arteaga-Salas, J. M.; Brandmaier, S.; Kahle, M.; Neschen, S.; de Angelis, M. H.; Zimmermann, R., Combining metabolomic non-targeted GCxGC-ToF-MS analysis and chemometric ASCA-based study of variances to assess dietary influence on type 2 diabetes development in a mouse model. *Analytical and Bioanalytical Chemistry* **2015,** *407* (1), 343-354.

73. Fan, R. J.; Zhang, F.; Wang, H. Y.; Zhang, L.; Zhang, J.; Zhang, Y.; Yu, C. T.; Guo, Y. L., Reliable screening of pesticide residues in maternal and umbilical cord sera by gas chromatography-quadrupole time of flight mass spectrometry. *Science China-Chemistry* **2014,** *57* (5), 669-677.

74. Tsikas, D., De novo synthesis of trideuteromethyl esters of amino acids for use in GC-MS and GC-tandem MS exemplified for ADMA in human plasma and urine: Standardization, validation, comparison and proof of evidence for their aptitude as internal standards. *Journal of Chromatography B-Analytical Technologies in the Biomedical and Life Sciences* **2009,** *877* (23), 2308-2320.

75. Portoles, T.; Sancho, J. V.; Hernandez, F.; Newton, A.; Hancock, P., Potential of atmospheric pressure chemical ionization source in GC-QTOF MS for pesticide residue analysis. *Journal of Mass Spectrometry* **2010,** *45* (8), 926-936.

76. Chace, D. H.; Kalas, T. A., A biochemical perspective on the use of tandem mass spectrometry for newborn screening and clinical testing. *Clinical Biochemistry* **2005,** *38* (4), 296-309.

77. Vogl, J.; Pritzkow, W., Isotope Dilution Mass Spectrometry - A Primary Method of Measurement and Its Role for RM Certification. *Mapan-Journal of Metrology Society of India* **2010,** *25* (3), 135-164.

78. Cajka, T.; Fiehn, O., Toward Merging Untargeted and Targeted Methods in Mass Spectrometry-Based Metabolomics and Lipidomics. *Analytical Chemistry* **2016,** *88* (1), 524-545.

79. Link, H.; Fuhrer, T.; Gerosa, L.; Zamboni, N.; Sauer, U., Real-time metabolome profiling of the metabolic switch between starvation and growth. *Nature Methods* **2015,** *12* (11), 1091-1097.

80. Vuckovic, D., Current trends and challenges in sample preparation for global metabolomics using liquid chromatography-mass spectrometry. *Analytical and Bioanalytical Chemistry* **2012,** *403* (6), 1523-1548.

81. Gonzalez-Dominguez, R.; Garcia-Barrera, T.; Gomez-Ariza, J. L., Using direct infusion mass spectrometry for serum metabolomics in Alzheimer's disease. *Analytical and Bioanalytical Chemistry* **2014,** *406* (28), 7137-7148.

82. Peng, J.; Guo, K.; Xia, J. G.; Zhou, J. J.; Yang, J.; Westaway, D.; Wishart, D. S.; Li, L., Development of Isotope Labeling Liquid Chromatography Mass Spectrometry for Mouse Urine Metabolomics: Quantitative Metabolomic Study of Transgenic Mice Related to Alzheimer's Disease. *Journal of Proteome Research* **2014,** *13* (10), 4457-4469.

83. Willenberg, I.; Ostermann, A. I.; Schebb, N. H., Targeted metabolomics of the arachidonic acid cascade: current state and challenges of LC-MS analysis of oxylipins. *Analytical and Bioanalytical Chemistry* **2015,** *407* (10), 2675-2683.

84. Jin, S. N.; Song, C. W.; Jia, S. L.; Li, S.; Zhang, Y.; Chen, C.; Feng, Y. L.; Xu, Y.; Xiong, C. M.; Xiang, Y.; Jiang, H. L., An integrated strategy for establishment of curcuminoid profile in turmeric using two LC-MS/MS platforms. *Journal of Pharmaceutical and Biomedical Analysis* **2017,** *132*, 93-102.

85. Gika, H. G.; Theodoridis, G. A.; Plumb, R. S.; Wilson, I. D., Current practice of liquid chromatography-mass spectrometry in metabolomics and metabonomics. *Journal of Pharmaceutical and Biomedical Analysis* **2014,** *87*, 12-25.

86. Lu, W.; Bennett, B. D.; Rabinowitz, J. D., Analytical strategies for LC-MS-based targeted metabolomics. *Journal of Chromatography B-Analytical Technologies in the Biomedical and Life Sciences* **2008,** *871* (2), 236-242.

87. Buszewski, B.; Noga, S., Hydrophilic interaction liquid chromatography (HILIC)-a powerful separation technique. *Analytical and Bioanalytical Chemistry* **2012,** *402* (1), 231-247.

88. Heaton, J.; Smith, N. W., Advantages and disadvantages of HILIC: A brief overview. Chromatography Today 2012; Vol. 5, pp 44-47.

89. Makarov, A., Electrostatic axially harmonic orbital trapping: A high-performance technique of mass analysis. *Analytical Chemistry* **2000,** *72* (6), 1156-1162.

90. Rajski, L.; Gomez-Ramos, M. D.; Fernandez-Alba, A. R., Large pesticide multiresidue screening method by liquid chromatography-Orbitrap mass spectrometry in full scan mode applied to fruit and vegetables. *Journal of Chromatography A* **2014,** *1360*, 119-127.

91. Rousu, T.; Herttuainen, J.; Tolonen, A., Comparison of triple quadrupole, hybrid linear ion trap triple quadrupole, time-of-flight and LTQ-Orbitrap mass spectrometers in drug discovery phase metabolite screening and identification in vitro - amitriptyline and verapamil as model compounds. *Rapid Communications in Mass Spectrometry* **2010,** *24* (7), 939-957.

92. Eldridge, S. L.; Higgins, L. A.; Dickey, B. J.; Larive, C. K., Insights into the Capillary Electrophoresis Separation of Heparin Disaccharides from Nuclear Magnetic Resonance, pK(a), and Electrophoretic Mobility Measurements. *Analytical Chemistry* **2009,** *81* (17), 7406-7415.

93. Dinges, M. M.; Solakyildirim, K.; Larive, C. K., Affinity capillary electrophoresis for the determination of binding affinities for low molecular weight heparins and antithrombin-III. *Electrophoresis* **2014,** *35* (10), 1469-77.

94. Zhang, X.; Sweedler, J. V., Ultraviolet native fluorescence detection in capillary electrophoresis using a metal vapor NeCu laser. *Analytical Chemistry* **2001,** *73* (22), 5620-5624.

95. Matczuk, M.; Aleksenko, S. S.; Matysik, F. M.; Jarosz, M.; Timerbaev, A. R., Comparison of detection techniques for capillary electrophoresis analysis of gold nanoparticles. *Electrophoresis* **2015,** *36* (9-10), 1158-1163.

96. Garcia, A.; Godzien, J.; Lopez-Gonzalvez, A.; Barbas, C., Capillary electrophoresis mass spectrometry as a tool for untargeted metabolomics. *Bioanalysis* **2017,** *9* (1), 99-130.

97. Gonzalez-Pena, D.; Dudzik, D.; Garcia, A.; de Ancos, B.; Barbas, C.; Sanchez-Moreno, C., Metabolomic Fingerprinting in the Comprehensive Study of Liver Changes Associated with Onion Supplementation in Hypercholesterolemic Wistar Rats. *International Journal of Molecular Sciences* **2017,** *18* (2).

98. Ramautar, R.; Somsen, G. W.; de Jong, G. J., CE-MS for metabolomics: Developments and applications in the period 2014-2016. *Electrophoresis* **2017,** *38* (1), 190-202.

99. Matsumoto, M.; Kibe, R.; Ooga, T.; Aiba, Y.; Kurihara, S.; Sawaki, E.; Koga, Y.; Benno, Y., Impact of Intestinal Microbiota on Intestinal Luminal Metabolome. *Scientific Reports* **2012,** *2*.

100. Jackson, P. E., Determination of inorganic ions in drinking water by ion chromatography. *Trac-Trends in Analytical Chemistry* **2001,** *20* (6-7), 320-329.

101. Zhang, K.; Cao, M. Y.; Lou, C. Y.; Wu, S. C.; Zhang, P. M.; Zhi, M. Y.; Zhu, Y., Graphene-coated polymeric anion exchangers for ion chromatography. *Analytica Chimica Acta* **2017,** *970*, 73-81.

102. Peng, Y. H.; Hou, Y. J.; Zhang, F. F.; Shen, G. B.; Yang, B. C., A hyperbranched polyethylenimine functionalized stationary phase for hydrophilic interaction liquid chromatography. *Analytical and Bioanalytical Chemistry* **2016,** *408* (13), 3633-3638.

103. Zhao, Q. M.; Wu, S. C.; Zhang, K.; Lou, C. Y.; Zhang, P. M.; Zhu, Y., Hydrothermal carbon nanosphere-based agglomerated anion exchanger for ion chromatography. *Journal of Chromatography A* **2016,** *1468*, 73-78.

104. Wouters, S.; Bruggink, C.; Agroskin, Y.; Pohl, C.; Eeltink, S., Microfluidic membrane suppressor module design and evaluation for capillary ion chromatography. *Journal of Chromatography A* **2017,** *1484*, 26-33.

105. Murrihy, J. P.; Breadmore, M. C.; Tan, A. M.; McEnery, M.; Alderman, J.; O'Mathuna, C.; O'Neill, A. P.; O'Brien, P.; Advoldvic, N.; Haddad, P. R.; Glennon, J. D., Ion chromatography on-chip. *Journal of Chromatography A* **2001,** *924* (1-2), 233-238.

106. Haddad, P. R.; Nesterenko, P. N.; Buchberger, W., Recent developments and emerging directions in ion chromatography. *Journal of Chromatography A* **2008,** *1184* (1-2), 456-473.

107. Wu, S.; Anumol, T.; Gandhi, J.; Snyder, S. A., Analysis of haloacetic acids, bromate, and dalapon in natural waters by ion chromatography-tandem mass spectrometry. *Journal of Chromatography A* **2017,** *1487*, 100-107.

108. Gui, J. Y.; Sun, W.; Zhang, C. L.; Zhang, Y. T.; Zhang, L.; Liu, F., An Innovative Approach to Sensitive Artificial Sweeteners Analysis by Ion Chromatography-Triple Quadrupole Mass Spectrometry. *Chinese Journal of Analytical Chemistry* **2016,** *44* (3).

109. Saccenti, E.; Hoefsloot, H. C. J.; Smilde, A. K.; Westerhuis, J. A.; Hendriks, M. M. W. B., Reflections on univariate and multivariate analysis of metabolomics data. *Metabolomics* **2014,** *10* (3), 361-374.

110. Surendiran, B.; Sundaraiah, Y.; Vadivel, A.; Ieee, Classifying Digital Mammogram Masses using Univariate ANOVA Discriminant Analysis. *2009 International Conference on Advances in Recent Technologies in Communication and Computing (Artcom 2009)* **2009**, 175-177.

111. Green, D.; de Leon, S. P.; Leon-Rodriguez, E.; Sosa-Sanchez, R., Adenocarcinoma of the stomach: Univariate and multivariate analysis of factors associated with survival. *American Journal of Clinical Oncology-Cancer Clinical Trials* **2002,** *25* (1), 84-89.

112. Choi, H. K.; Choi, Y. H.; Verberne, M.; Lefeber, A. W. M.; Erkelens, C.; Verpoorte, R., Metabolic fingerprinting of wild type and transgenic tobacco plants by H-1 NMR and multivariate analysis technique. *Phytochemistry* **2004,** *65* (7), 857-864.

113. Wold, S.; Sjostrom, M.; Eriksson, L., PLS-regression: a basic tool of chemometrics. *Chemometrics and Intelligent Laboratory Systems* **2001,** *58* (2), 109-130.

114. Liland, K. H., Multivariate methods in metabolomics - from pre-processing to dimension reduction and statistical analysis. *Trac-Trends in Analytical Chemistry* **2011,** *30* (6), 827-841.

115. Benabid, H.; Naamoune, H.; Nocairi, H.; Rutledge, D. N., Application of chemometric tools to compare Algerian olive oils produced in different locations. *Journal of Food Agriculture & Environment* **2008,** *6* (2), 43-51.

116. Wiklund, S.; Johansson, E.; Sjostrom, L.; Mellerowicz, E. J.; Edlund, U.; Shockcor, J. P.; Gottfries, J.; Moritz, T.; Trygg, J., Visualization of GC/TOF-MS-based metabolomics data for identification of biochemically interesting compounds using OPLS class models. *Analytical Chemistry* **2008,** *80* (1), 115-122.

117. Clarke, L. L., A guide to Ussing chamber studies of mouse intestine. *American Journal of Physiology-Gastrointestinal and Liver Physiology* **2009,** *296* (6), G1151-G1166.

118. Turnbaugh, P. J.; Hamady, M.; Yatsunenko, T.; Cantarel, B. L.; Duncan, A.; Ley, R. E.; Sogin, M. L.; Jones, W. J.; Roe, B. A.; Affourtit, J. P.; Egholm, M.; Henrissat, B.; Heath, A. C.; Knight, R.; Gordon, J. I., A core gut microbiome in obese and lean twins. *Nature* **2009,** *457* (7228), 480-U7.

119. Flint, H. J.; Aberdeen, U. o.; Health, R. I. o. N. a.; h.flint@abdn.ac.uk; Duncan, S. H.; Aberdeen, U. o.; Louis, P.; Aberdeen, U. o., Gut Microbiome and Obesity. **2016**, 73-82.

120. Talbot, C.; Lytle, C., Segregation of Na/H exchanger-3 and Cl/HCO3 exchanger SLC26A3 (DRA) in rodent cecum and colon. **2010**.

121. Backhed, F.; Ley, R. E.; Sonnenburg, J. L.; Peterson, D. A.; Gordon, J. I., Host-bacterial mutualism in the human intestine. *Science* **2005,** *307* (5717), 1915-1920.

122. Jansson, J.; Willing, B.; Lucio, M.; Fekete, A.; Dicksved, J.; Halfvarson, J.; Tysk, C.; Schmitt-Kopplin, P., Metabolomics Reveals Metabolic Biomarkers of Crohn's Disease. *Plos One* **2009,** *4* (7), 10.

CHAPTER TWO

Analytical methods

Abstract: Developing optimal methods for the analysis of biological samples is crucial to obtaining reliable experimental results. Many compounds of interest within a biological sample are present at low concentrations within a complex background, which produces matrix effects. To simplify the analyses and reduce the time required for the measurements, methods with minimal sample preparation, and the sensitivity necessary for quantitative analysis are highly beneficial. This is certainly the case for metabolomics measurements that aim to quantify large numbers of metabolites in a single experiment. Because the metabolome is a complex composite of different classes of compounds, its characterization benefits from the application of complementary analytical methods. The results described in this dissertation rely on method development utilizing the techniques of ion chromatography (IC), nuclear magnetic resonance (NMR), and gas chromatography-mass spectrometry (GC-MS) to provide analytical results for a wide range of metabolites. The comparative advantages of each instrumental platform result in a more complete data set yielding a global view of metabolite composition within a single biological sample.

2.1 Introduction

Biological samples such as serum[1-3], plasma[4-6], urine[7-9], and fecal stool[9-12] have been widely studied in an effort to identify biomarkers, and determine the effects of health stressors. These biological matrices hold a wealth of knowledge that can potentially be correlated to the overall health of a patient, but challenges remain due to the complexity and matrix effects within samples. The field of bioanalysis strives to define better analytical methods to improve measurement selectivity and sensitivity without the need for extensive sample preparation steps.

The work presented in this dissertation describes analytical methods employed for metabolomics analysis with a focus on fecal stool composition. Metabolic profiling provides a quantitative snapshot as a function of a variable like time, dose, or location, and by comparing several snapshots, changes in the metabolome as a function of a perturbation or stressor can be revealed. Many of these changes are subtle, or primarily found in metabolites of relatively low concentrations. For this reason, analytical methods need to be sensitive, robust, and reproducible. In many studies because samples are available in limited quantities, the analytical methods must not only fit these criteria, but also feature minimal sample consumption.

This chapter will describe the analytical methods employed for metabolomics analysis of fecal stool samples obtained from healthy female rats, including ion chromatography (IC) for the analysis of anions and cations, nuclear magnetic resonance (NMR) for the simultaneous analysis of organic compounds, and gas chromatography - mass spectrometry (GC-MS) to provide separation and enhanced sensitivity for measurement of metabolites present at levels too low to be detected by NMR.

2.2 Ion chromatography (IC)

IC is a well-established analytical chromatographic method most commonly used in the study of inorganic ions, and in water quality analysis.[13] Developed in 1975 by Small et al., IC has become a mature technique offering both chromatographic separation and simultaneous analysis of multiple inorganic ions in a short time, with good reproducibility, and high sensitivity.[14-16] The instrument used in this work is a Dionex 1100 ion chromatograph, equipped with Chromeleon software for operation and processing. As this instrument is not capable of performing gradient elution, two isocratic methods were employed in the analysis of anionic and cationic ions separately.

2.2.1 Anion analyses

Stool water samples were kept at -80 ºC after initial extraction (described in greater detail in Chapter 3), and thawed at room temperature prior to IC analysis.[17] Samples were centrifuged at 13.0 rpm for 3 min at 4.0 ºC to pellet the solids.
To preserve the life of the IC column 100 µL of the stool water was transferred to a 2.0 mL Eppendorf, diluted to 2.0 mL and passed through a 3,000 molecular weight cut-off (MWCO) centrifuge filter (Millipore; Billerica, MA USA) to remove bacteria and proteins. Of the filtrate, 300 µL was manually injected into the IC equipped with a 25 µL sample loop via manual injection using a 1.0 mL disposable syringe to ensure optimal rinsing and reduced carry-over. The remaining sample was frozen at -80ºC for analysis of cations.

Anions were separated using a Dionex IonPac AG14A RFIC 4x50 mm guard column, an IonPac AS14A RFIC 4x250 mm column and AERS 500 4 mm suppressor. (Thermofisher; Waltham, MA) In IC it is important that concentration of mobile phase (eluent) is constant day-to-day so a 500 mL stock solution of 800 mM sodium carbonate and 100 mM sodium bicarbonate was prepared prior to these analyses. Fresh eluent consisting of 8.0 mM sodium carbonate and 1.0 mM sodium bicarbonate was prepared daily by adding 10.0 mL of stock solution to a 1.0 L volumetric flask and diluting to the mark with milli-Q ultrapure water (Millipore; Billerica, MA, USA). Air bubbles in the eluent can easily destroy column efficiency in this system, so the eluent was degassed for approximately 30 min after preparation.

A flow rate of 1.2 mL/min was used, producing a system pressure of 1800-1900 psi and a total run time of 20 min. As IC separates components via a displacement mechanism, anions are eluted based on the strength of their interaction with the positively charged stationary phase. Using this method the elution order of the well-resolved anions of interest is: propionate, chloride, butyrate, phosphate, and sulfate (Figure 2.1). Two peaks believed to be nitrate and oxalate based on retention times, were too low in intensity to meet the 10:1 signal-to-noise ratio required for quantitative analysis. The peak labeled short chain fatty acids (SCFA's) is comprised mostly of acetate, but due to co-elution with formate and citrate, we were unable to use this peak for our analyses. If we had access to an instrument capable of gradient elution, we would likely have been able to resolve and quantify these components by IC.[18]

Calibration plots for each anion were completed at the beginning and end of a batch of samples. A quality control standard composed of a known concentration of each anion, and a blank of milli-Q water were run at the beginning and end of each day to confirm column efficiency and the quality of the data recorded.

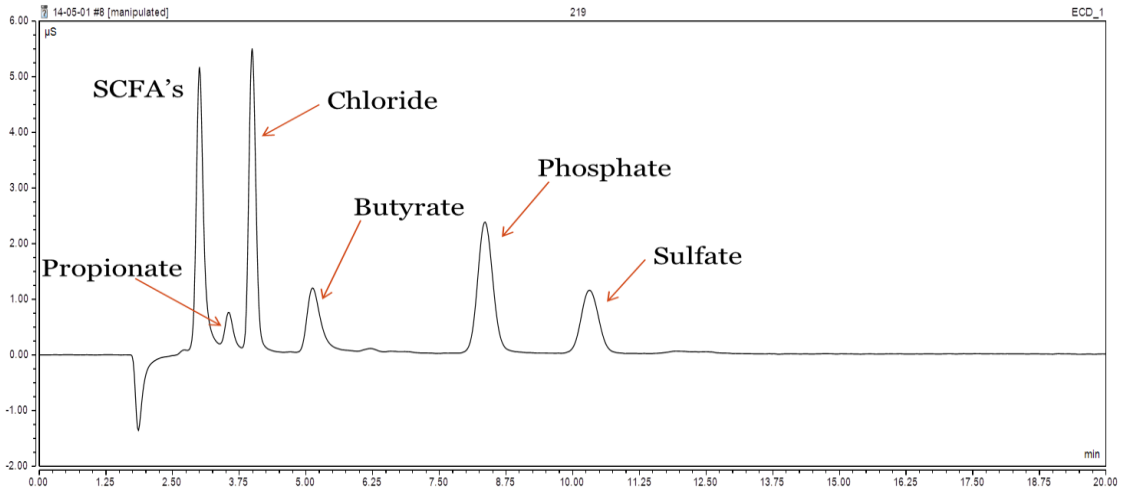

Figure 2.1. Anion chromatogram depicting the resolution of propionate, chloride, butyrate, phosphate, and sulfate. The peak labeled short chain fatty acids (SCFA's) is comprised mostly of acetate, but due to co-elution with formate and citrate, we were unable to use the peak in our analyses.

2.2.2 Cation analyses

Cation analyses were performed as a batch after the analyses of anions were completed due to the necessary but time-consuming reconfiguration of the ion chromatography system's instrumental components, which includes changing the guard and separation columns and replacement of the suppressor. After reconfiguration, the system was flushed with the cation eluent for 10-12 h until stable separation conditions were achieved. The stool water samples previously prepared for anion analysis, were kept at -80 °C and thawed at room temperature before injection using the procedure described in Section 2.2.1.

Cations were separated using a Dionex IonPac CG12A cation-exchange 3x30 mm guard column, IonPac CS14A cation-exchange 3x150 mm column and CERS 500 3 mm suppressor. (Thermofisher; Waltham, MA) The eluent selected for the cation analysis was 20 mM methanesulfonic acid (MSA). This eluent was prepared fresh daily by dilution of a 100 mM MSA stock solution purchased from Sigma-Aldrich by transferring 200 mL of stock solution into a 1.0 L volumetric flask and diluting with Milli-Q ultrapure water. (Millipore; Billerica, MA, USA) To avoid gas in the system, eluent was degassed for 30 min prior to use.

The optimal flow rate was determined to be 0.5 mL/min with a system pressure of approximately 2000 psi and a total run time of 20 min. The elution order of identified and well-resolved cations is: sodium, ammonium, potassium, magnesium, and calcium (Figure 2.2). Unfortunately, due to sample handling and the volatility of ammonia, it was not possible to quantify the ammonium concentration using this method.

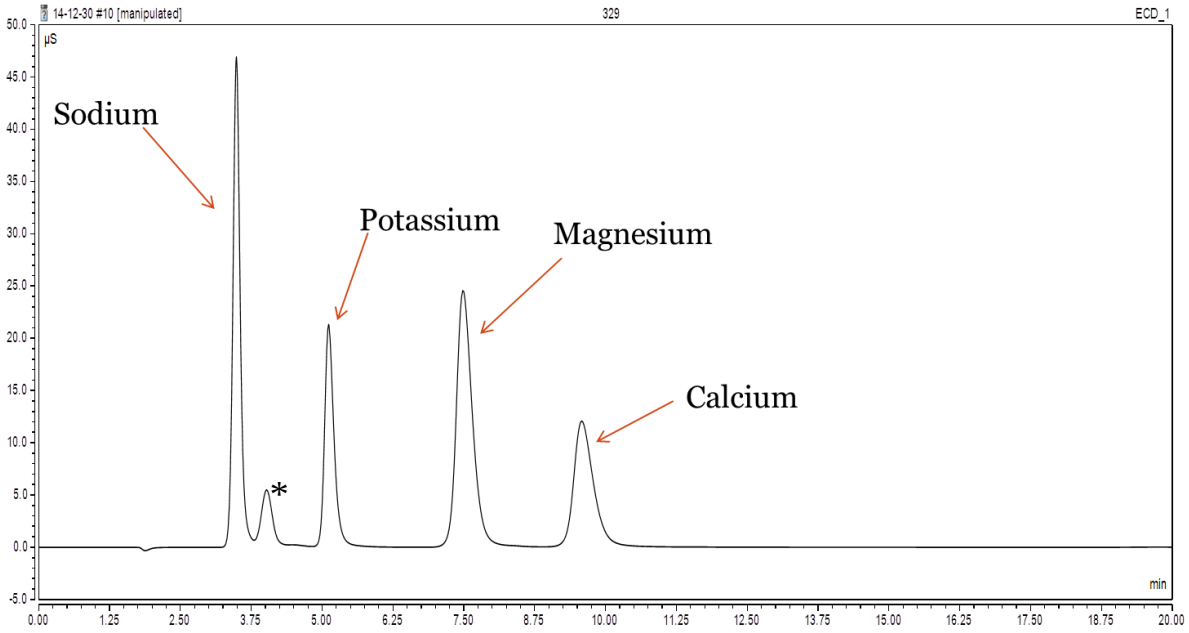

Figure 2.2. Cation chromatogram of sodium, potassium, magnesium, and calcium. The peak at approximately 4 min (*) was determined to be ammonium (NH_4^+). Unfortunately, due to sample handling and the volatility of ammonia, it was not possible to quantify this component.

Calibration plots for each cation were completed at the beginning and end of each batch of samples. A quality control standard composed of a known concentration of each cation, and a blank of milli-Q water were run at the beginning and end of each day to confirm column efficiency and quality of data.

2.2.3 Conductivity detection and ion suppression

Conductivity is a relatively simple detection method, consisting of two electrodes positioned within a flow cell. An alternating current is applied to avoid electrolysis across the two electrodes which act as the impedance component in one arm of a Wheatstone bridge. Changes in the ionic composition within the cell change the impedance of the circuit reflected as an "out of balance" signal in the bridge. The signal is reported as conductance, in units of Siemens.

One complication to conductivity detection in this system is that separation is achieved based on ion exchange. For example, in an anion separation the stationary phase is positively charged to retain the negatively charged anions of interest. The mobile phase is a carbonate/bicarbonate mixture that is attracted to the stationary phase as well. Competitive binding of the mobile phase displaces the anions of interest from the stationary phase causing them to elute.

The conductivity detector has to distinguish the presence of dilute analytes against the high background produced by the mobile phase, reducing sensitivity. To overcome this problem, a suppressor is used to reduce the high background produced by the mobile phase. Suppressors differ depending on the type of mobile phases used, meaning different suppressors must be employed depending on whether anion or cation analysis is performed.

For anion analysis the carbonate/bicarbonate mobile phase is protonated to form carbonic acid in the suppressor prior to conductivity detection. The conductivity of the neutral carbonic acid is substantially lower than the carbonate and bicarbonate species. After detection, the mobile phase is recycled back into the suppressor, but this time to be deprotonated back to the original composition of carbonate and bicarbonate before being removed from the system as waste. This recycling function allows the suppressor to be used long term.

2.2.4 IC data processing

Ion chromatography is a separation technique in which identifications are made by comparing retention times to those of standards. Once peaks were identified, standard solutions were prepared and the response determined for each analyte. Peak areas were extracted using Chromeleon software (Thermofisher; Waltham, MA), and plotted to produce a calibration curve. The linear portion of the curve was fit by linear regression and used for the concentration determinations in Chapter 3.

To account for any degradation of column or detector efficiency, a quality control sample was run at the beginning and end of the day, and a fresh blank was measured every day. Samples were measured in a random order to avoid systematic errors arising from carry-over, baseline drift, bias in processing or additional difficulties that could affect the integrity of analysis over time.

Though ion chromatography is a well-defined and robust technique that is especially useful for detecting inorganic ions, its pitfall in the field of metabolomics is the inability to study neutral molecules. Thus, to get a full understanding of the metabolic profile it is necessary to use complementary analytical instrumentation such as NMR and mass spectrometry (MS) which of each provides unique abilities to aid in a global determination of small molecules within the colon.

2.3 Nuclear magnetic resonance (NMR)

The research described in this dissertation relies on the analysis of one-dimensional ^{1}H-NMR spectra, taking advantage of the robustness of NMR and its ability to obtain unbiased quantitative data with minimal sample preparation. A unique advantage of NMR is that the response factor is directly proportional to the number of nuclei, in this case protons, and is equal for all compounds. As a result, components in a complex sample can be quantified using a single standard without the need for calibration plots for each analyte.

NMR spectra also provide structural information. This can aid in the identification of unknown metabolites, especially when supplemented by 2D NMR spectra.

2.3.1 NMR sample preparation

Sample preparation refers to how the sample is treated prior to analysis. This is an important step to ensure robustness of results and prevent the incorporation of error. In this dissertation two sample preparation techniques were used for metabolic profiling of stool extracts, and the analysis of transport using the Ussing chamber.

2.3.1.1 Sample preparation for metabolic profiling of stool extracts

Samples for metabolic profiling experiments (Chapter 3) were prepared by delivering a 100 µL aliquot of the stool sample extracts filtered prior to ion chromatography analysis (Section 2.2.1) into a 2.0 mL Eppendorf centrifuge tube. The samples were diluted by addition of 500 µL of deuterium oxide (D_2O, 99.9% D; Cambridge Isotopes, Tewksbury, MA) buffer containing 50 mM sodium phosphate pD 7.4, 0.5 mM DSS (sodium-2,2 dimethyl-2-silapentane-5-sulfonate-*d6*) (Cambridge Isotope Laboratories, Tewksbury, MA) and 0.2 mM EDTA (ethylenediaminetetraacetic acid-*d16*) (Sigma Aldrich, St. Louis, MO). A 600 µL aliquot of this solution was transferred to a 5 mm glass NMR tube (Wilmad 535-pp or equivalent), sonicated to remove air bubbles, and capped for analysis.

2.3.1.2 Sample preparation for Ussing chamber sample analysis

A 65 µL aliquot of deuterated 50 mM sodium phosphate buffer (pH 7.4, Sigma Aldrich, St. Louis, MO) in D_2O containing 0.35 or 0.45 mM 3-(trimethylsilyl)propane-1-sulfonic acid (DSS, Cambridge isotopes, Tewksbury, MA) as a chemical shift (0 ppm) and quantitation reference, and 0.2 mM ethylenediaminetetraacetic acid-d_{16} (EDTA, Sigma Aldrich, St. Louis, MO) was added to the 585 µL of sample obtained from the Ussing chamber in a 5 mm tube. The DSS concentration was determined in a separate NMR experiment relative to the concentration of the primary standard potassium hydrogen phthalate (KHP, minimum 99.95% purity; Sigma Aldrich, St. Louis, MO) as described by Larive et al.[19]

2.3.2 Acquisition parameters

2.3.2.1 Shimming

Shimming is a process fundamental to NMR in which adjustments are made to improve magnetic field homogeneity narrowing resonances and improving peak shape. Since the perfect magnet has not been built, a mechanism is needed to correct for imperfections in the magnetic field and induced perturbations by the environment and the sample. Shimming is the act of trying to homogenize the magnetic field as much as possible so that all the spins in the sample have the same Larmor frequency.

Shims that affect the field along the vertical axis are referred to as axial or Z shims, while the shims that acts in a horizontal plane are radial or X/Y shims. Bathed in liquid helium and surrounding the magnetic coil are a set of three cryoshims that are adjusted after the magnet is brought to field. To provide further refinement to the magnetic field homogeneity, the NMR probe is inserted into a housing that contains a set of room temperature shim coils (26 for the magnet used in this work). Adjusting the electric currents in each of the shim coils produces magnetic fields that reduce the spatial inhomogeneity in magnetic field felt by the sample.

Prior to the shimming process it is important to let the sample reach thermal equilibrium in the spectrometer so that convection currents are avoided. It is also important to select an indicator to use as a gauge for progress in achieving field homogeneity. This can be the lock level, the shape of the free induction decay (FID), or the shape of the NMR resonance of a well-resolved singlet resonance. While all 3 methods have been used in conjunction to shim the magnet, the peak width at half-height and at the base of NMR resonance itself are the ultimate measures of field homogeneity.

It is also important to note that magnetic field differences not only come from imperfections in the magnet that can be reduced by shimming, but can also arise from local magnetic fields produced by intramolecular and intermolecular interactions in the sample, referred to as “genuine” or “natural” transverse relaxation processes.

The observed relaxation time constant, T_2^*, is used to describe the combination of the natural transverse relaxation of a nucleus and that arising from magnetic field inhomogeneity:

$$\frac{1}{T_2^*} = \frac{1}{T_2} + \frac{1}{T_{2\ (\Delta B_0)}} \tag{1}$$

where T_2 refers to the contributions from natural relaxation processes, and $T_{2\ (\Delta B0)}$ is that from field inhomogeneity. The peak width at half height of an NMR resonance is inversely proportional to T_2^* with a short T_2^* corresponding to a faster decay of the FID. Upon Fourier transformation of the FID, the resonances of the NMR spectrum have a Lorentzian line shape with the peak width at half height, ($\Delta\nu_{1/2}$), determined by T_2* as shown in Equation 2.

$$\Delta\nu_{1/2} = \frac{1}{\pi T_2^*} \tag{2}$$

For low-viscosity solutions of small, rapidly tumbling molecules with spin ½ nuclei, such as protons, it is the magnetic field homogeneity that contributes most to the observed linewidths.

When comparing the large number of samples, as in a metabolomics study, it is critical that each sample is measured under similar conditions including optimized magnetic field homogeneity. Figure 2.3 shows the comparison of the DSS resonance at 0.0 ppm both before (blue) and after (red) shimming to a peak width at half-height $\leq$1.0 Hz. The resonance in red is not only narrower, but has greater intensity.

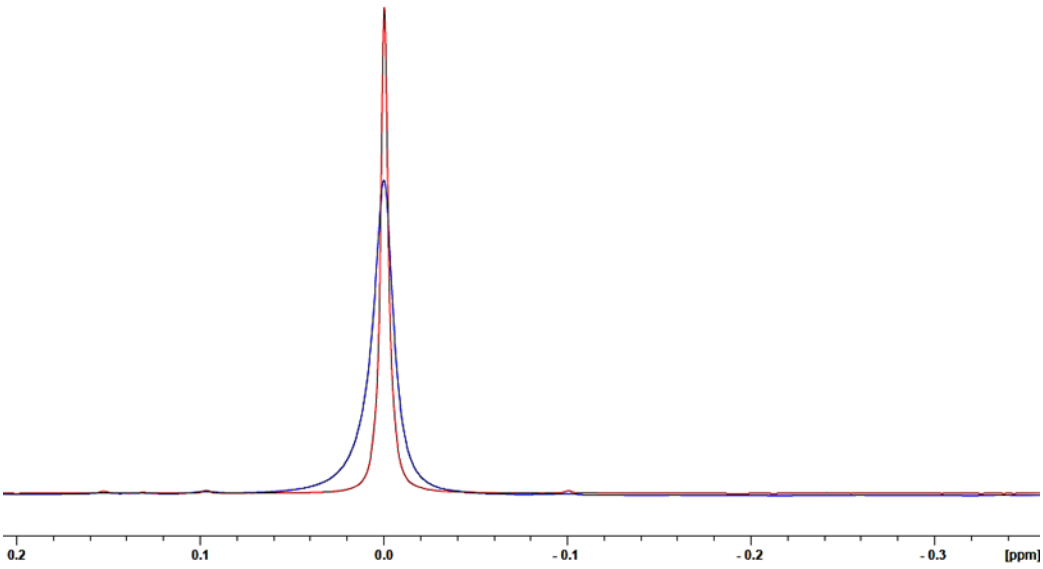

Figure 2.3. Overlays of two ^{1}H-NMR spectra of DSS showing how shimming affects peak shape and resolution. The spectra in blue has a fairly Lorentzian peak shape, but a width at half-height of about 1.5 Hz, while the spectra in red has a peak width at half-height <1.0 Hz and is much narrower at its base.

The improved peak shape not only improves resolution, but provides greater intensity and S/N. In metabolomics studies, we aim to detect as many metabolites as possible with some metabolites being detectable, but without the proper S/N for quantitative analyses making good shimming parameters important for our analysis. In the case that shims do not remain consistent between samples, resolution is greatly affected due to the broadening of the peak shape. This is especially problematic in the complex spectra obtained for biological samples used for metabolomics and metabolic profiling experiments. Poor resolution and non-Lorentzian peak shapes contribute to resonance overlap in an already complicated spectrum and greatly reduce the confidence of peak deconvolution and integration.

Several factors influence line shape including the quality of the NMR tube, sample concentration, dissolved oxygen, and paramagnetic impurities. In these cases, shimming can be difficult and time consuming, often without success unless problem can be identified and corrected. To avoid these issues only high quality NMR tubes that are rated for 600 MHz or above are used, samples are degassed to remove bubbles, and EDTA is added to buffer solution to scavenge any paramagnetic metal ions in the sample. Spectra for which the peak width at half height of the DSS resonance was not within the acceptable range of less than 1.0 Hz, and/or did not have a symmetrical peak shape were thrown out prior to statistical analysis.

2.3.2.2 Solvent suppression

Most biological samples are in an aqueous matrix and ^{1}H-NMR detects the protons of H_2O producing a large signal proportional to the amount of water present. Even when extracts of biological samples are measured in D_2O, the resulting solutions typically contain a substantial component of protonated water, most of which will be present as HOD. If the concentration of H_2O or HOD is far greater than the analyte concentration, a dynamic range problem is created in measuring the FID. Even the most modern NMR spectrometers have only 18 bit analog-to-digital converters (ADCs). To prevent the intense solvent resonance from overflowing the ADC and improperly digitizing the FID, a very low receiver gain must be used. Suppressing the water signal allows use of maximum receiver gain, and in return increases the S/N of the spectrum allowing for better quantitation of low abundance resonances.

Another concern that solvent suppression addresses is radiation damping, which is a common problem in high quality factor (Q-factor) probes. Radiation damping occurs in conditions where the amount of protons in the solvent greatly outnumbers the protons in the solute which is common when running experiments with 90% H_2O and 10% D_2O. In radiation damping, the precession of the solvent nuclei disturbs the amplitude and phase of the radio frequency (RF) pulse. Radiation damping causes peak broadening, peak asymmetry, and phase shifting that interfere with our ability to perform quantitative analyses.[20-22]

To counter these problems, a variety of solvent suppression methods have been introduced, but most have the disadvantage that they not only suppress the solvent signal, but also analyte resonances close in frequency to the solvent peak. This is a concern for reliable quantitation using these methods, and in metabolomics and metabolic profiling experiments the region adjacent to the solvent resonance is typically omitted from the spectral analysis.

The simplest and most common type of solvent suppression, presaturation, is a selective saturation method that uses a low power pulse at the same frequency of the solvent resonance.[23] One of the largest pitfalls of the use of presaturation in metabolomics studies is that it often causes baseline distortions that negatively impact quantitation. Another disadvantage is the transfer of saturation to exchangeable protons, such as amides, altering the ability to detect or quantify these resonances.

An improved method of presaturation is the one-dimensional ^{1}H nuclear Overhauser effect spectroscopy (NOESY1D) with presaturation pulse program. This robust method is frequently used in the field of metabolomics due to its ability to yield adequate solvent suppression with very little optimization required.[24] The NOESY sequence produces a selective inversion of the solvent peak. Central to this pulse sequence is a double pulsed field gradient spin echo (DPFGSE) which provides a cleaner spectrum and more level baseline than the basic presaturation pulse program. However, the NOESY1D with presaturation has similar pitfalls as the basic presaturation methods in that the resonances close to the solvent resonance can be effected by the selective inversion, resulting in poor quantitative results.

Alternative methods of solvent suppression that provide better quantitation and less baseline distortions than presaturation are desirable for metabolomics studies. One option is water suppression enhanced through T_1 effects (WET). WET is a pulsed-field gradient (PFG) based suppression technique that uses a selective pulse to excite the solvent resonance which is then attenuated using dephasing gradients.[25] Because WET avoids baseline distortions and uses a shorter pulse compared to presaturation, it is less likely to attenuate exchangeable protons. One major advantage of WET is its ability to simultaneously suppress multiple solvent signals. Unfortunately, as with all methods, there are disadvantages including the need to create a shaped pulse, and optimization of gradient powers. If these parameters are not set correctly, baseline distortions will occur, and complicate the ability to quantify metabolite resonances. As a result, WET lacks the robustness needed for the large sample sets analyzed in metabolomics and metabolic profiling studies.

The WATERGATE (water suppression by gradient-tailored excitation) pulse sequence employs PFG's to attenuate the water resonance similarly to WET, however, in this method a nonselective excitation pulse followed by a gradient pulse dephases all resonances. A composite pulse is then applied to invert all of the resonances except for the solvent. A second gradient pulse further dephases the solvent resonance, while rephasing the analyte resonances.[26] Watergate is a useful suppression technique for the study of exchangeable protons, but the delays used can cause "nulls" or regions in which the spectrum is not fully rephased.

This results in attenuated resonance intensity in the regions around the nulls. As the nulls are located at frequencies distant from the solvent resonance but still within the spectral window, problems can be encountered in reliable quantification in WATERGATE spectra of biological samples. Another disadvantage of WATERGATE is its potential adverse effects on strongly coupled spin systems, which can cause baseline distortions as well.

Excitation sculpting is an alternative approach that uses selective 180° pulses and gradients to dephase the solvent resonance while analyte resonances remain in the detection plane.[27] Excitation sculpting does not have the baseline issues common with other solvent suppression methods and in contrast to WATERGATE produces a uniform excitation profile, making it an excellent candidate for quantitative and metabolic analysis.

Several solvent suppression methods were evaluated using a stool extract test sample in 10% H_2O and 90% D_2O. Figure 2.4 shows comparison of (from top to bottom) a basic 90° pulse with no solvent suppression (A), excitation sculpting (B), WATERGATE (C), Noesy1D with presaturation (D), and presaturation (E). The solvent resonance is at approximately 4.7 ppm, and when comparing the results obtained by each pulse sequence, the excitation sculpting spectrum has the best solvent suppression and is free of baseline distortions. It is also clear that when comparing the other resonances, spectrum 2.4B has no visible "nulls" that would cause irregularity in signal intensity and complicate quantitation.

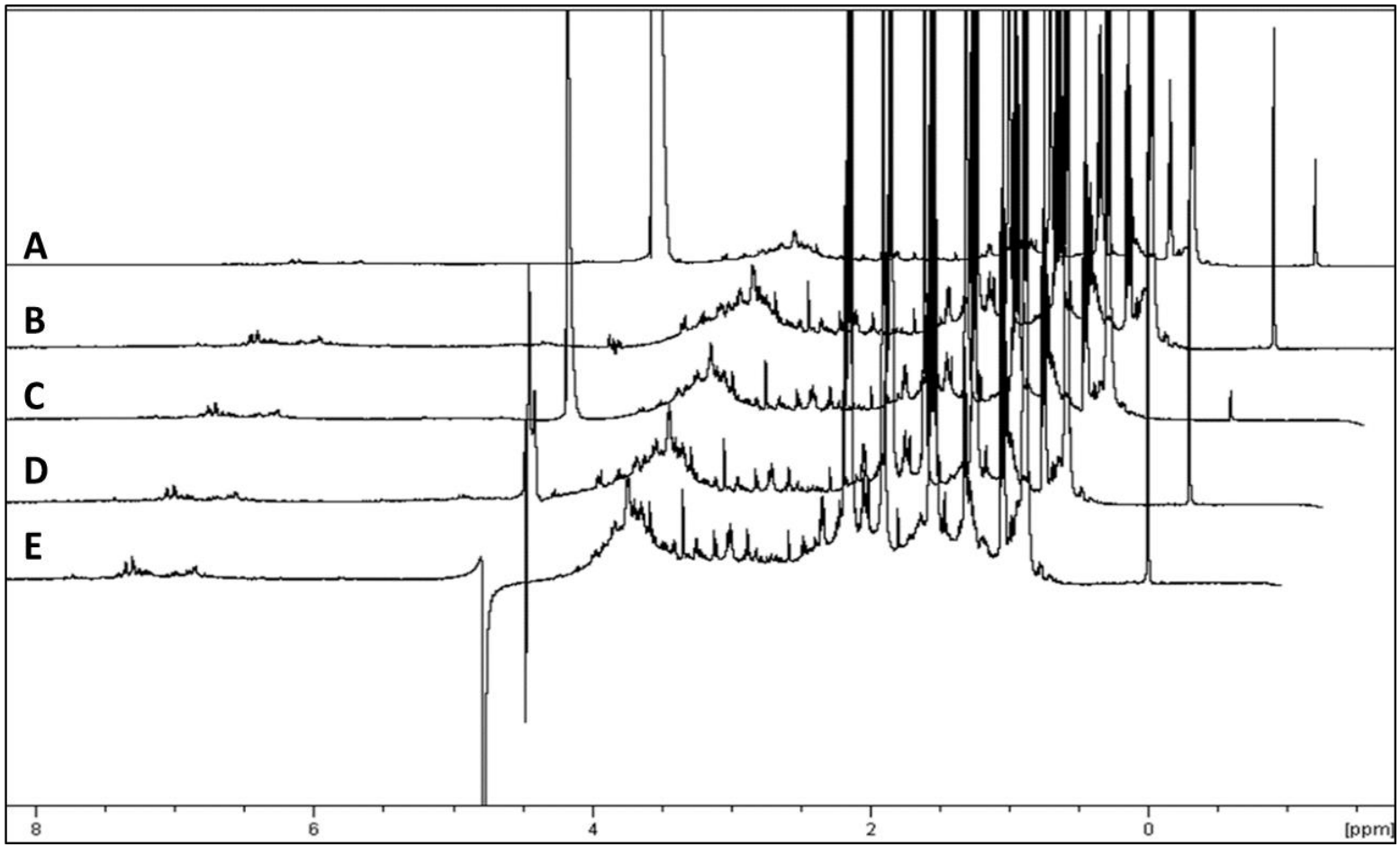

Figure 2.4. ^{1}H-NMR spectra of a stool water extract sample in 90% D_2O/10 % H_2O sodium phosphate buffer solution containing 0.4 mM DSS. Spectra are overlaid to compare solvent (4.7 ppm) suppression techniques including a basic 90° pulse with no solvent suppression (A), excitation sculpting (B), WATERGATE (C), Noesy1D with presaturation (D), and presaturation (E).

2.3.2.3 Data acquisition parameters

All ^{1}H-NMR spectra were acquired at 25°C using a 90º pulse and excitation sculpting (zgesgp)[27] of the solvent resonance with a Bruker Avance NMR spectrometer (Bruker, Billerica, MA, USA) equipped with a BBI probe and operating at 599.52 MHz.

Spectra obtained for metabolic profiling discussed in Chapter 3 were measured by coaddition of 256 transients using 32 dummy scans, a relaxation delay of 2.0 s and acquisition time of 2.38 s. Spectra were processed using Bruker Topspin 3.2 using zero-filling to 131072 points and line broadening equivalent to 1.0 Hz.

For Ussing chamber analyses discussed in Chapter 4, spectra were acquired into 131072 points with coaddition of 4096 transients, 128 dummy scans, and a relaxation delay of 0.05 s and acquisition time of 2.38 s for a total experiment time of 11 hr 19 min.

2.3.3 Spectral pre-processing

Spectra were pre-processed using Bruker Topspin 3.2 for initial phasing and referencing of DSS to 0.000 ppm. Further pre-processing was done using Mnova 10.0 (Mestrelab Research, Bajo, Spain). Free induction decays (FIDs) were apodized by multiplication by an exponential decay equivalent to 1.0 Hz line broadening, zero-filled to 32768 points, manually phased and 2.31 Hz (Whittaker smoothing) baseline correction applied prior to all analysis. Preliminary assignments of ^{1}H-NMR resonances were performed by comparison with the Human Metabolome Database,[28-30] Chenomx,[31] and various literature reports[32-35]

Most resonance assignments were confirmed using an in-house spectral library of authentic metabolite standards measured under similar conditions to those employed in this work, and confirmed by two-dimensional (2D) NMR experiments, as illustrated in Chapter 3. In the event metabolite standards are hard to obtain or the compound has only a singlet resonance for which the ^{1}H chemical shift does not provide conclusive identification, 2D heteronuclear single quantum correlation spectroscopy (HSQC) experiments were performed. The ^{1}H-^{13}C HSQC adds a second dimension with carbon chemical shifts coupled to the proton spectrum, improving spectral resolution, and providing additional evidence for confident identification.

2.3.4 Processing

Mnova 10.0 was used for peak-fitting analysis of all spectra. Pre-processed data were fit using a Lorentzian-Gaussian algorithm and corresponding data sets were uploaded into Microsoft Excel. Metabolite resonances were identified in each sample and peak area was uploaded into a table for comparison across samples. Peak area was normalized to the DSS peak area adjusted for T_1 relaxation effects (Section 2.3.5.1) and the known DSS concentration for each sample followed by a normalization to stool weight. This data was uploaded into R and processed used the metabolomics package "muma". PCA, PLS-DA, and OPLS-DA analysis were subsequently performed.

Upon further examination of data, it was determined that a statistical package with the ability to combine multivariate analysis across different instrumentation data sets, the ability to produce 3-dimensional multivariate plots, and produce high quality images with user friendly controls was essential for additional analysis. The software package SIMCA (Sartorius stedim biotech, Umea, Sweden) was obtained, and was used for the statistical analyses in Chapter 3.

2.3.5 Quantitative analysis

NMR is a well-established method for quantitative analysis, having the advantage that a single standard at known concentration can be used to quantify all the components in a complex mixture, provided care is taken to account for the longitudinal or transverse (T_1) relaxation times of the interrogated nuclei.[36]

2.3.5.1 T_1 determinations and concentration calculations for Ussing chamber analysis

To determine the DSS concentration, the primary standard KHP (Sigma Aldrich, St. Louis, MO) was dried in an oven for 24 hours at approximately 100°C. A known quantity of 513.01 mg KHP was weighed and diluted to 25 mL in a volumetric flask with H2O equaling 100.5 mM KHP. Of this solution, 15 µL was pipetted using a calibrated pipette to ensure accuracy into to an aliquot of 600 µL of the NMR deuterated buffer containing DSS.

Once a fully relaxed NMR spectrum (applied delay of 90 seconds to ensure full relaxation) of the solution containing KHP and DSS has been acquired, Eq.3 can be used to determine the concentration of DSS using the known concentration of KHP calculated from the mass and solution volume, the integral values for resonances of KHP and DSS with their respective normalization factor (NF). The normalization factor corresponds to the number of protons that give rise to the resonance.[19]

$$[DSS] = [KHP] \times \frac{(integral_{DSS} \times NF_{DSS})}{(integral_{KHP} \times NF_{KHP})} \quad (3)$$

Once the concentration of the DSS is determined for the buffer, it can be used in a similar equation (Eq. 4) to determine the metabolite concentration [M] in a sample, being careful to consider dilution.

$$[M] = [DSS] \times \frac{(integral_{M} \times NF_{M})}{(integral_{DSS} \times NF_{DSS})} \quad (4)$$

Due to the large number of scans necessary to reach a sufficient signal-to-noise ratio for quantitative measurements of 10:1, a short delay time of 0.05 s was used to reduce the total experiment time for Ussing chamber samples. Many quantitative NMR measurements use repetition times that are at least 5 times the longest T_1 relaxation time to ensure complete relaxation. In these experiments, a shorter repetition time (2.43 s) was used and a correction factor was applied to compensate for incomplete T_1 relaxation. To determine the correction factors necessary for quantitative analysis, T_1 values were calculated for each compound of interest using the inversion-recovery experiment.[37]

Inversion recovery spectra were measured using standard solutions of the metabolites identified in test solutions including: sodium acetate (Sigma Aldrich, St. Louis, MO), sodium butyrate (Alfa Aesar, Ward Hill, MA), sodium propionate (Sigma Aldrich, St. Louis, MO), lithium acetoacetate (Sigma Aldrich, St. Louis, MO), sodium citrate (Fisher, Pittsburg, PA), choline chloride (Sigma Aldrich, St. Louis, MO), phenylalanine (Fisher, Pittsburg, PA), tyramine (Sigma Aldrich, St. Louis, MO), tyrosine (Fisher, Pittsburg, PA), hydrocinnamic acid (3-phenylpropionate, Acros Organics, Fisher, Pittsburg, PA), DL-β-hydroxybutyric acid sodium salt (3-hydroxybutyric acid, Sigma Aldrich, St. Louis, MO), sodium formate (Fisher, Pittsburg, PA), succinic acid (Spectrum chemical, Gardena, CA), sodium pyruvate (Sigma Aldrich, St. Louis, MO), oxaloacetic acid (Alfa Aesar, Ward Hill, MA), lactic acid (Sigma Aldrich, St. Louis, MO), L-alanine (Sigma Aldrich, St. Louis, MO), valine (Sigma Aldrich, St. Louis, MO), lysine (Sigma Aldrich, St. Louis, MO), isoleucine (Fisher, Pittsburg, PA), arabinose (Sigma Aldrich, St. Louis, MO), aspartic acid (Fisher, Pittsburg, PA), benzoate (Sigma Aldrich, St. Louis, MO), ethanol (Fisher, Pittsburg, PA), glycine (Fisher, Pittsburg, PA), methanol (Fisher, Pittsburg, PA), nicotinic acid (Sigma Aldrich, St. Louis, MO) and the internal standard DSS.

The NMR spectra for the standard solutions were measured under the same conditions as the Ussing chamber samples, including the same composition of Parson's and phosphate buffer. Inversion recovery spectra were measured with the coaddition of 96 scans, recovery delays between 0.01 and 60.0 s, and repetition times equal to the largest recovery delay plus the acquisition time of 2.38 s (Figure 2.5). In individual experiments, the maximum recovery delay and the corresponding relaxation delay varied from 50 to 60 s, however, in all experiments the total relaxation time was more than 10 times the greatest T_1 relaxation time.

Data were processed using Mnova software with 1.0 Hz apodization, and 2.31 Hz Whittaker smoothing baseline correction applied. Resonances for each compound were selected for quantitation purposes based on the spectral resolution and signal-to-noise, and were fit to obtain peak areas as described in section 2.3.4.

To extract the T_1 relaxation times from these spectra, peak areas were plotted versus recovery delay time in Mathematica (Wolfram Research, Champaign, IL) as illustrated in Figure 2.6. T_1 relaxation times were calculated for each resonance used for quantification by fitting Eq. 5 to the inversion recovery data.

$$M(t) = M\left(1 - 2e^{\frac{-t}{T_1}}\right) \quad (5)$$

In Eq. 5 M(t) is the observed peak area for a particular resonance in a spectrum, and M is the peak area of the fully relaxed spectrum. The recovery time is denoted by t and the relaxation time constant is T_1.

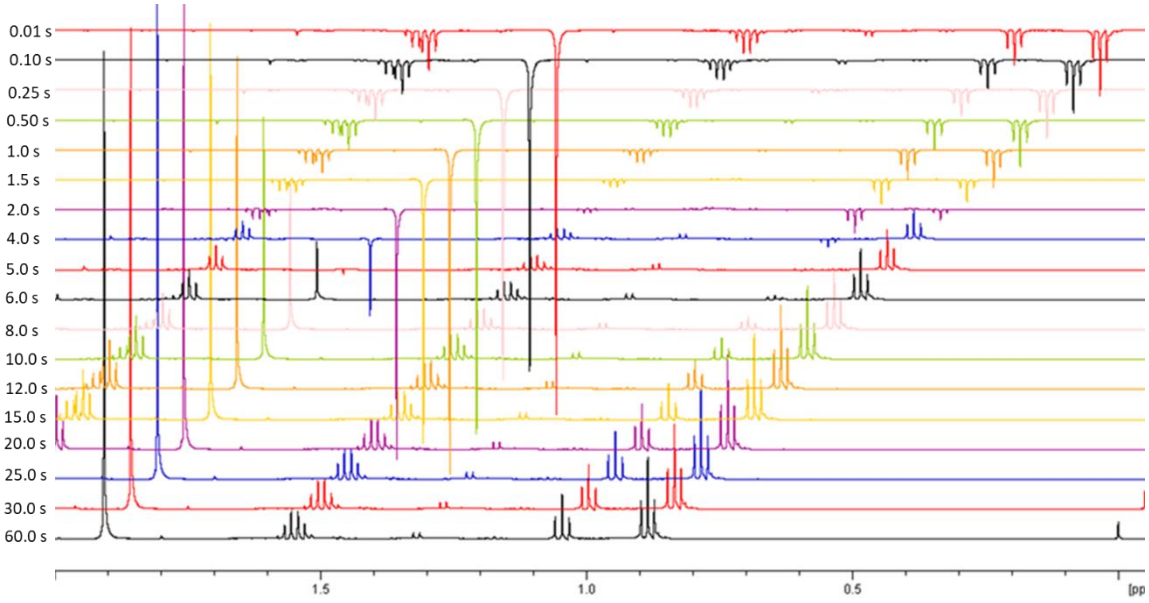

Figure 2.5. Representative inversion-recovery spectra used to calculate T1 values. Each spectrum represents a different recovery delay from 0.01 to 60.0 seconds (top to bottom)

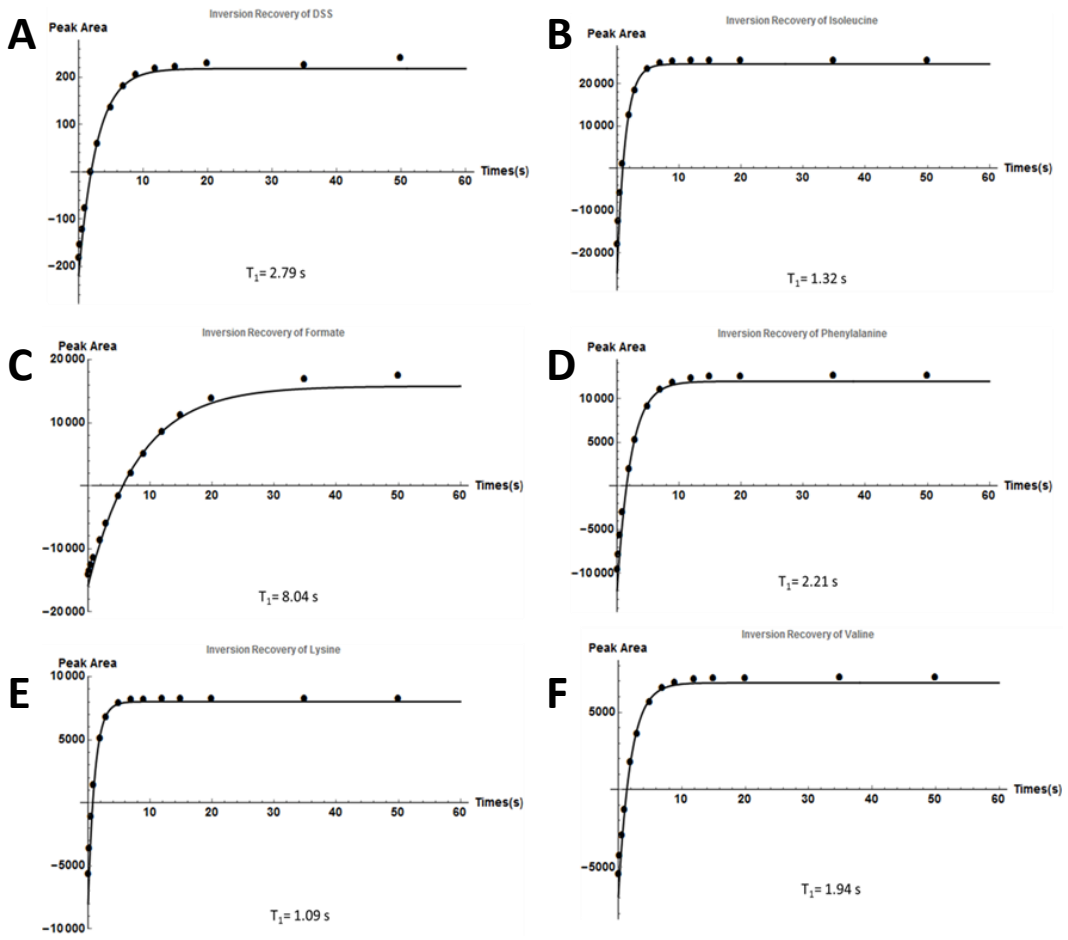

Figure 2.6. Integrated peak areas (Y-axis) obtained from the inversion recovery spectra plotted against the recovery times (X-axis) for the ^{1}H-NMR resonances of DSS (A), isoleucine (B), formic acid (C), phenylalanine (D), lysine (E), and valine (F). The T_1 relaxation time is determined from the fit of the line in Mathematica.

The T_1 relaxation time constants summarized in Table 1 were used to correct integrals measured for each metabolite quantified as illustrated by Eq. 6, where t is the recovery time used in the acquisition of the 1D NMR spectrum.

$$M = \left[\frac{M(t)}{\left(1-2e^{\frac{-t}{T_1}}\right)}\right] \times \frac{1}{P} \quad (6)$$

$$[MET] = \left(\frac{[DSS] \times M_{MET}}{M_{DSS}}\right) \times \mathrm{D} \quad (7)$$

Eq. 6 uses values determined previously in Eq. 5, as well as the number of protons (P) for the corresponding resonance to solve for M. This will correct the peak area due to T_1 values, and provide a per proton value which can be converted to concentration using Eq 7. Here we use the ratio of predetermined DSS concentration and its corresponding peak area (M_{DSS}) to determine the concentration of the metabolite of interest ($[MET]$), taking into consideration the dilution factor (D) applied when deuterated buffer is added to the sample prior to NMR analysis.

2.4 Gas chromatography – mass spectrometry (GC-MS)

Complementary to NMR analysis, GC-MS offers improved resolution and enhanced sensitivity that allows for the quantification of less abundant metabolites.[38] GC-MS offers a robust and reproducible gas chromatographic separation coupled with the sensitivity of a mass analyzer, making it a useful tool in the field of metabolomics and metabolic profiling.[39]

Table 2.1. Metabolite standards measured using inversion recovery experiments to determine the corresponding T_1 values used to calculate peak intensity correction factors due to incomplete relaxation in the Ussing chamber NMR experiments.

	Metabolite	T_1 Value (s)
1	3-hydroxybutyric acid	1.51
2	Acetate	5.30
3	Acetoacetate	5.85
4	Alanine	1.93
5	Arabinose	2.43
6	Aspartate	1.34
7	Benzoate	5.16
8	Butyrate	2.84
9	Choline	2.42
10	Citrate	0.84
11	DSS	3.06
12	Ethanol	5.92
13	Formate	8.17
14	Glycine	3.43
15	Hydrocinnamic acid	1.76
16	Isoleucine	1.47
17	Lactic acid	1.78
18	Lysine	1.31
19	Methanol	6.81
20	Nicotinate	5.61
21	Oxaloacetic acid	5.43
22	Phenylalanine	2.55
23	Propionate	4.89
24	Pyruvate	4.76
25	Succinate	2.47
26	Tyramine	2.74
27	Tyrosine	2.12
28	Valine	2.48

2.4.1 GC-MS sample preparation

Samples of stool water extracts were removed from storage at -80°C and thawed. A 20 µL aliquot of sample was transferred to a 350 µL glass GC flat bottom insert (Phenomenex, Torrence, CA) in a 1.5 mL Eppendorf centrifuge tube and dried by centrifuging under vacuum for approximately 3 hr at ambient temperature using a Thermo-Savant SC110 model speed vacuum equipped with an RVT400 refrigerated vapor trap attached to a GP110 gel pump. Dried samples were stored at -20°C until derivatized for GC-MS analysis.

2.4.2. Derivatization

Dried samples were removed from the freezer and spiked with 200 µL of methanol, and centrifuged under vacuum until dry (~30 min) to ensure no water was present in the sample before derivatization. Dried extracts were treated using the methods provided by Lee and Fiehn.[40] To each sample, 30 µL of methoxyamine (20 µg/µL in pyridine) was added and the samples were shaken on the Eppendorf Thermomixer C (Eppendorf; Hamburg, Germany) at 1200 rpm and 40°C for 90 min.[41] This was followed by the addition of 90 µL *N*-Methyl-*N*-(trimethylsilyl)-trifluoroacetamide (MSTFA) and the samples were maintained at 40°C on the thermomixer at 500 rpm for 30 min to undergo the silylation reaction.

After the reaction was complete, 4 µL of 0.8 mg/mL methyl octacosanoate (FAMES: C28, Sigma-Aldrich) was added as an internal standard, followed by the direct transfer of the glass inserts to a wide-mouth crimp top vial (Phenomenex, Torrance, CA) which was sealed with an 11 mm crimp cap. All samples were analyzed within 24 hr of derivatization.

2.4.3 GC separation

An Agilent 7683B autosampler equipped with a 10 µL Agilent syringe (Agilent Technologies; Santa Clara, CA) was used to inject 1 µL of derivatized sample into a splitless, singletapered MS-certified injector liner with glass wool (Agilent Technologies) heated to 230°C. The liner was changed daily (25-30 samples) to ensure efficient analyte transfer to the column. After each injection, the syringe was rinsed 3 times with methylene chloride in preparation for the next run.

The injector was operated in pulsed-splitless mode with helium (99.998% purity) pressure of 35.0 PSI for 0.5 min, after which the flow was reduced to a stable 1.0 mL/min. for the duration of the method. The GC separation was carried out using an Agilent 7890A gas chromatograph equipped with an Agilent DB-5MS column, 0.250 mm i.d. and 30 m length.

The sample was introduced at an oven temperature of 60°C with a hold of 1 min and ramped at 10.00°C/min to reach a final temperature of 320°C followed by a hold of 5.00 min for a total run time of 32 min. All instrument operations were controlled by Waters MassLynx software version 4.1 (Waters Corporation; Milford, MA).

2.4.4 MS detection

The sample was introduced from the GC to the MS at a transfer line temperature of 320 °C. Electron impact ionization was used at 70 eV with a source temperature of 220 °C. The filament was turned on after 7.0 min and mass spectra were recorded using a time of flight (TOF) mass analyzer over a m/z range of 50 to 600 at a scan rate of 10 spectra per s, and operated at 2700 V. Mass spectral data were collected and stored in Waters file format (*.raw), prior to conversion to *.cdf format for processing with the Automated Mass Spectral Deconvolution and Identification System (AMDIS, NIST, Gaithersburg, MD). Deconvolution settings used a component width of 17 scans, high resolution, high sensitivity, and medium shape. For compound identification, AMDIS queried the Golm Metabolome Database mass spectral library, by matching mass fragmentation patterns and retention indices (RI).[42]

MarkerLynx XS (Waters Corporation) was used for data preprocessing to collect integration values for identified metabolites. Peaks were detected without smoothing from an initial retention time of 7.00 min and final retention time of 32.00 min, with a low-mass cutoff of 73.5 Da, a high-mass cutoff of 600 Da, and a mass accuracy of 0.10 Da.

The peak width at 5% was overestimated as 2 s to ensure peak detection. A peak-to-peak baseline noise value of 1.0, a marker intensity threshold of 25 counts, and a mass and retention time window of 0.1 Da/min were also used. A noise elimination level of 3.0 was chosen and data was deisotoped. The results were exported to Excel (Microsoft, Redmond, WA) where the retention times and the extracted masses were matched with identified metabolites. One mass-retention time pair with the corresponding area for each metabolite was used for data normalization and statistical analysis. The mass-retention time pair with the highest relative abundance was chosen to represent each metabolite, excluding the silylation-related fragments 73 and 147 m/z.[43]

2.5 Summary

Development and optimization of analytical methods aimed at studying small molecules is the key for reliable and successful metabolomics experiments. The methods described in this dissertation were selected in an effort to identify as many metabolites as possible in stool water extracts and to map their change along the length of the colon (Chapter 3), and to identify and quantify metabolites that are involved in transport and transformation across the colonic epithelium with Ussing chamber experiments (Chapter 4). These methods have proven to be robust and complementary, yielding large datasets that provided compelling evidence for segmental stratification of the colon, as well as evidence of transport and transformation of metabolites and the ability to quantify the change exhibited.

2.6 References

1. Nolen, B. M.; Langmead, C. J.; Choi, S.; Lomakin, A.; Marrangoni, A.; Bigbee, W. L.; Weissfeld, J. L.; Wilson, D. O.; Dacic, S.; Siegfried, J. M.; Lokshin, A. E., Serum biomarker profiles as diagnostic tools in lung cancer. *Cancer Biomark* **2011,** *10* (1), 3-12.

2. Kosaka, P. M.; Pini, V.; Ruz, J. J.; Silva, R. A. d.; González, M. U.; Ramos, D.; Calleja, M.; Tamayo, J., Detection of cancer biomarkers in serum using a hybrid mechanical and optoplasmonic nanosensor. *Nature Nanotechnology* **2014,** *9*, 1047-1053.

3. Chen, X.; Ba, Y.; Ma, L. J.; Cai, X.; Yin, Y.; Wang, K. H.; Guo, J. G.; Zhang, Y. J.; Chen, J. N.; Guo, X.; Li, Q. B.; Li, X. Y.; Wang, W. J.; Zhang, Y.; Wang, J.; Jiang, X. Y.; Xiang, Y.; Xu, C.; Zheng, P. P.; Zhang, J. B.; Li, R. Q.; Zhang, H. J.; Shang, X. B.; Gong, T.; Ning, G.; Zen, K.; Zhang, J. F.; Zhang, C. Y., Characterization of microRNAs in serum: a novel class of biomarkers for diagnosis of cancer and other diseases. *Cell Research* **2008,** *18* (10), 997-1006.

4. Zhu, C.; Ren, C.; Han, J.; Ding, Y.; Du, J.; Dai, N.; Dai, J.; Ma, H.; Hu, Z.; Shen, H.; Xu, Y.; Jin, G., A five-microRNA panel in plasma was identified as potential biomarker for early detection of gastric cancer. *British Journal of Cancer* **2014,** *110* (9), 2291-2299.

5. Zhang, A. H.; Sun, H.; Qiu, S.; Wang, X. J., NMR-based metabolomics coupled with pattern recognition methods in biomarker discovery and disease diagnosis. *Magnetic Resonance in Chemistry 51* (9), 549-556.

6. Zupancic, K.; Blejec, A.; Herman, A.; Veber, M.; Verbovsek, U.; Korsic, M.; Knezevic, M.; Rozman, P.; Turnsek, T. L.; Gruden, K.; Motaln, H., Identification of plasma biomarker candidates in glioblastoma using an antibody-array-based proteomic approach. *Radiology and Oncology* **2014,** *48* (3), 257-266.

7. Tokushige, N.; Markham, R.; Crossett, B.; Ahn, S. B.; Nelaturi, V. L.; Khan, A.; Fraser, I. S., Discovery of a novel biomarker in the urine in women with endometriosis. *Fertility and Sterility* **2011,** *95* (1), 46-49.

8. Thomas, S.; Hao, L.; Ricke, W. A.; Li, L. J., Biomarker discovery in mass spectrometry-based urinary proteomics. *Proteomics Clinical Applications* **2016,** *10* (4), 358-370.

9. Ganti, S.; Weiss, R. H., Urine metabolomics for kidney cancer detection and biomarker discovery. *Urologic Oncology-Seminars and Original Investigations* **2011,** *29* (5), 551-557.

10. Yang, J. Y.; Sun, Y. W.; Liu, D. J.; Zhang, J. F.; Li, J.; Hua, R., MicroRNAs in stool samples as potential screening biomarkers for pancreatic ductal adenocarcinoma cancer. *American Journal of Cancer Research* **2014,** *4* (6), 663-673.

11. Huang, J. X.; Zhou, Y.; Wang, C. H.; Yuan, W. W.; Zhang, Z. D.; Zhang, X. F., Tumor M2-pyruvate kinase in stool as a biomarker for diagnosis of colorectal cancer: A meta-analysis. *Journal of Cancer Research and Therapeutics* **2014,** *10* (7), C225-C228.

12. Yamaguchi, S.; Takeuchi, Y.; Arai, K.; Fukuda, K.; Kuroki, Y.; Asonuma, K.; Takahashi, H.; Saruta, M.; Yoshida, H., Fecal calprotectin is a clinically relevant biomarker of mucosal healing in patients with quiescent ulcerative colitis. *Journal of Gastroenterology and Hepatology* **2016,** *31* (1), 93-98.

13. Haddad, P. R.; Nesterenko, P. N.; Buchberger, W., Recent developments and emerging directions in ion chromatography. *Journal of Chromatography A* **2008,** *1184* (1-2), 456-473.

14. Fritz, J. S., Factors affecting selectivity in ion chromatography. *Journal of Chromatography A* **2005,** *1085* (1), 8-17.

15. Small, H.; Stevens, T. S.; Bauman, W. C., NOVEL ION-EXCHANGE CHROMATOGRAPHIC METHOD USING CONDUCTIMETRIC DETECTION. *Analytical Chemistry* **1975,** *47* (11), 1801-1809.

16. Haddad, P. R.; Jackson, P. E.; Shaw, M. J., Developments in suppressor technology for inorganic ion analysis by ion chromatography using conductivity detection. *Journal of Chromatography A* **2003,** *1000* (1-2), 725-742.

17. Gratton, J.; Phetcharaburanin, J.; Mullish, B. H.; Williams, H. R. T.; Thursz, M.; Nicholson, J. K.; Holmes, E.; Marchesi, J. R.; Li, J. V., Optimized Sample Handling Strategy for Metabolic Profiling of Human Feces. **2016**.

18. Corporation, D., Determination of Organic Acids and Inorganic Anions in Lithium-Containing Boric Acid-Treated Nuclear Power Plant Waters. *Application note 175* **2016,** *LPN 2569*, 1-7.

19. Larive, C. K.; Jayawickrama, D.; Orfi, L., Quantitative analysis of peptides with NMR spectroscopy. *Applied Spectroscopy* **1997,** *51* (10), 1531-1536.

20. Bloom, S., EFFECTS OF RADIATION DAMPING ON SPIN DYNAMICS. *Journal of Applied Physics* **1957,** *28* (7), 800-805.

21. Bruce, C. R.; Norberg, R. E.; Pake, G. E., RADIATION DAMPING AND RESONANCE SHAPES IN HIGH RESOLUTION NUCLEAR MAGNETIC RESONANCE. *Physical Review* **1956,** *104* (2), 419-420.

22. Krishnan, V. V.; Murali, N., Radiation damping in modern NMR experiments: Progress and challenges. *Progress in Nuclear Magnetic Resonance Spectroscopy* **2013,** *68*, 41-57.

23. Hoult, D. I., SOLVENT PEAK SATURATION WITH SINGLE-PHASE AND QUADRATURE FOURIER TRANSFORMATION. *Journal of Magnetic Resonance* **1976,** *21* (2), 337-347.

24. McKay, R. T., How the 1D-NOESY Suppresses Solvent Signal in Metabonomics NMR Spectroscopy: An Examination of the Pulse Sequence Components and Evolution. *Concepts in Magnetic Resonance Part A 38A* (5), 197-220.

25. Smallcombe, S. H.; Patt, S. L.; Keifer, P. A., WET solvent suppression and its applications to LC NMR and high-resolution NMR spectroscopy. *Journal of Magnetic Resonance Series A* **1995,** *117* (2), 295-303.

26. Piotto, M.; Saudek, V.; Sklenar, V., GRADIENT-TAILORED EXCITATION FOR SINGLE-QUANTUM NMR-SPECTROSCOPY OF AQUEOUS-SOLUTIONS. *Journal of Biomolecular Nmr* **1992,** *2* (6), 661-665.

27. Hwang, T. L.; Shaka, A. J., WATER SUPPRESSION THAT WORKS - EXCITATION SCULPTING USING ARBITRARY WAVE-FORMS AND PULSED-FIELD GRADIENTS. *Journal of Magnetic Resonance Series A* **1995,** *112* (2), 275-279.

28. Wishart, D. S.; Jewison, T.; Guo, A. C.; Wilson, M.; Knox, C.; Liu, Y.; Djoumbou, Y.; Mandal, R.; Aziat, F.; Dong, E.; Bouatra, S.; Sinelnikov, I.; Arndt, D.; Xia, J.; Liu, P.; Yallou, F.; Bjorndahl, T.; Perez-Pineiro, R.; Eisner, R.; Allen, F.; Neveu, V.; Greiner, R.; Scalbert, A., HMDB 3.0--The Human Metabolome Database in 2013. *Nucleic Acids Res* **2013,** *41* (Database issue), D801-7.

29. Wishart, D. S.; Knox, C.; Guo, A. C.; Eisner, R.; Young, N.; Gautam, B.; Hau, D. D.; Psychogios, N.; Dong, E.; Bouatra, S.; Mandal, R.; Sinelnikov, I.; Xia, J.; Jia, L.; Cruz, J. A.; Lim, E.; Sobsey, C. A.; Shrivastava, S.; Huang, P.; Liu, P.; Fang, L.; Peng, J.; Fradette, R.; Cheng, D.; Tzur, D.; Clements, M.; Lewis, A.; De Souza, A.; Zuniga, A.; Dawe, M.; Xiong, Y.; Clive, D.; Greiner, R.; Nazyrova, A.; Shaykhutdinov, R.; Li, L.; Vogel, H. J.; Forsythe, I., HMDB: a knowledgebase for the human metabolome. *Nucleic Acids Res* **2009,** *37* (Database issue), D603-10.

30. Wishart, D. S.; Tzur, D.; Knox, C.; Eisner, R.; Guo, A. C.; Young, N.; Cheng, D.; Jewell, K.; Arndt, D.; Sawhney, S.; Fung, C.; Nikolai, L.; Lewis, M.; Coutouly, M. A.; Forsythe, I.; Tang, P.; Shrivastava, S.; Jeroncic, K.; Stothard, P.; Amegbey, G.; Block, D.; Hau, D. D.; Wagner, J.; Miniaci, J.; Clements, M.; Gebremedhin, M.; Guo, N.; Zhang, Y.; Duggan, G. E.; Macinnis, G. D.; Weljie, A. M.; Dowlatabadi, R.; Bamforth, F.; Clive, D.; Greiner, R.; Li, L.; Marrie, T.; Sykes, B. D.; Vogel, H. J.; Querengesser, L., HMDB: the Human Metabolome Database. *Nucleic Acids Res* **2007,** *35* (Database issue), D521-6.

31. Weljie, A. M.; Newton, J.; Mercier, P.; Carlson, E.; Slupsky, C. M., Targeted profiling: Quantitative analysis of H-1 NMR metabolomics data. *Analytical Chemistry* **2006,** *78* (13), 4430-4442.

32. Le Gall, G.; Noor, S. O.; Ridgway, K.; Scovell, L.; Jamieson, C.; Johnson, I. T.; Colquhoun, I. J.; Kemsley, E. K.; Narbad, A., Metabolomics of Fecal Extracts Detects Altered Metabolic Activity of Gut Microbiota in Ulcerative Colitis and Irritable Bowel Syndrome. *Journal of Proteome Research* **2011,** *10* (9), 4208-4218.

33. Jacobs, D. M.; Deltimple, N.; van Velzen, E.; van Dorsten, F. A.; Bingham, M.; Vaughan, E. E.; van Duynhoven, J., H-1 NMR metabolite profiling of feces as a tool to assess the impact of nutrition on the human microbiome. *Nmr in Biomedicine* **2008,** *21* (6), 615-626.

34. Lamichhane, S.; Yde, C. C.; Schmedes, M. S.; Jensen, H. M.; Meier, S.; Bertram, H. C., Strategy for Nuclear-Magnetic-Resonance-Based Metabolomics of Human Feces. *Analytical Chemistry* **2015,** *87* (12), 5930-5937.

35. Munoz-Gonzalez, I.; Jimenez-Giron, A.; Martin-Alvarez, P. J.; Bartolome, B.; Victoria Moreno-Arribas, M., Profiling of Microbial-Derived Phenolic Metabolites in Human Feces after Moderate Red Wine Intake. *Journal of Agricultural and Food Chemistry* **2013,** *61* (39), 9470-9479.

36. Barding, G. A., Jr.; Salditos, R.; Larive, C. K., Quantitative NMR for bioanalysis and metabolomics. *Analytical and Bioanalytical Chemistry* **2012,** *404* (4), 1165-1179.

37. Vold, R. L.; Waugh, J. S.; Klein, M. P.; Phelps, D. E., Measurement of Spin Relaxation in Complex Systems. **1968**.

38. Weckwerth, W., Metabolomics in systems biology. *Annual Review of Plant Biology* **2003,** *54*, 669-689.

39. Shiomi, Y.; Nishiumi, S.; Ooi, M.; Hatano, N.; Shinohara, M.; Yoshie, T.; Kondo, Y.; Furumatsu, K.; Shiomi, H.; Kutsumi, H.; Azuma, T.; Yoshida, M., GCMS-based Metabolomic Study in Mice with Colitis Induced by Dextran Sulfate Sodium. *Inflammatory Bowel Diseases* **2011,** *17* (11), 2261-2274.

40. Lee, D. Y.; Fiehn, O., High quality metabolomic data for Chlamydomonas reinhardtii. *Plant Methods* **2008,** *4*.

41. Abbiss, H.; Rawlinson, C.; Maker, G. L.; Trengove, R., Assessment of automated trimethylsilyl derivatization protocols for GC-MS-based untargeted metabolomic analysis of urine. *Metabolomics* **2015,** *11* (6), 1908-1921.

42. Kopka, J.; Schauer, N.; Krueger, S.; Birkemeyer, C.; Usadel, B.; Bergmuller, E.; Dormann, P.; Weckwerth, W.; Gibon, Y.; Stitt, M.; Willmitzer, L.; Fernie, A. R.; Steinhauser, D., GMD@CSB.DB: the Golm Metabolome Database. *Bioinformatics* **2005,** *21* (8), 1635-1638.

43. Barding, G. A.; Beni, S.; Fukao, T.; Bailey-Serres, J.; Larive, C. K., Comparison of GC-MS and NMR for Metabolite Profiling of Rice Subjected to Submergence Stress. *Journal of Proteome Research* **2013,** *12* (2), 898-909.

Chapter 3

Metabolic profiling of the rat colon

Abstract:

The large intestine is vitally important to human health. Also referred to as the "gut microbiome", the large intestine contains more than 800 species of bacteria that help harvest energy, synthesize vitamins, and shape the immune system. Though it is critically important for human health and has been implicated in many diseases including obesity, diabetes, colorectal cancer, allergies, autism, and Crohn's disease, the mechanism of metabolic communication between the gut microbiome and its human host remains poorly understood. In this chapter, NMR, GC-MS, and IC are used to identify and quantify major metabolites in extracts of fecal material isolated from the rat ileum, cecum, proximal, mid, and distal colon. These metabolites include short chain fatty acids that are the preferred energy source for colonocytes, amino acids, polyamines, bile acids, choline metabolites, phenolic compounds, and inorganic ions. This study provides a wealth of new information on the metabolome, its stratification along the colon, and the assortment of metabolites available to absorptive transporters within each segment.

3.1 Introduction

The colon cultivates a vast community of beneficial microbes that generates a diverse mix of more than 500 small molecules.[1] A systematic effort, using a combination of approaches, is urgently needed to delineate the subset of metabolites that most impact health and gain understanding of how these bioactive molecules exert their systemic effects. Progress in identifying microbial metabolites has been hampered by the chemical complexity of the gut microbiome and the preponderance of metabolomic studies performed using voided stool.[2, 3] The rat colon can be thought of as several different segments including the ileum (end of the small intestine), cecum (acts as a fermenting chamber), proximal, mid, and distal colon. Throughout these different locations the composition of stool varies significantly due to the fermentation, bacterial metabolism, and absorption and secretion of metabolites across the epithelial tissue. Therefore, voided stool samples reflect the metabolic endpoint of digestion and lack information about the transient metabolic complexity introduced by the segmental stratification of the colon.

This study aims to profile the changes in metabolic composition that occur as the stool travels through the colon, highlighting why voided stool studies cannot provide a complete picture of colonic function. The colon is not merely a waste packing organ, but a highly complex system housing the gut microbiome and acting as the last vital point in digestion through which the human body can retain water, electrolytes, and nutrients before eliminating the contents as waste.

The gut microbiome encompasses a large and diverse cluster of microorganisms and coevolves with the host to provide a wide range of functions including digestion of complex dietary macronutrients to produce nutrients and vitamins, defend against pathogens, and aid in maintaining the immune system.[4-6]

Disturbances in the gut microbiome have been implicated in many diseases including allergies,[7] autism,[8, 9] colorectal cancer,[10, 11] Crohn's disease,[12, 13] diabetes,[14, 15] and obesity.[16] Exactly how the gut microbiome communicates metabolically with its host remains unclear, but there is evidence for a two-way dialogue across the colonic epithelium. The work described in this chapter aims to identify which metabolites are afforded access to transport across the colonic epithelium in an effort to better understand colonic function and segmental differentiation.

3.2 Materials and methods

3.2.1 Stool samples

A total of 20 healthy female rats obtained from the University of California-Riverside vivarium were used in this study. They were anesthetized before undergoing surgery for the removal of portal vein blood, and then euthanized with isoflurane. The colon of the rat was surgically removed from the ileum to the anus. Stool was removed from various positions of the colon yielding 101 discrete samples placed into a previously weighed centrifuge tube to measure the sample weight.

A known volume of deionized water (approximately 1.0 mL) was added to each sample, followed with mixing by vortexing. Centrifugation was used to separate the solid matter, and the aqueous phase was removed, immediately frozen and stored at -80°C.

Due to limited sample volume, some samples could not be analyzed by all three analytical methods: ion chromatography (IC), nuclear magnetic resonance (NMR), and gas chromatography-mass spectrometry (GC-MS). For IC analysis, the same 101 samples from 15 rats were measured twice to analyze for anions and cations, each with a run time of 20 min because the IC instrument used was not equipped with an autosampler, each sample was injected manually. ^{1}H-NMR experiments included 97 of the same 101 samples run on the IC, however 4 samples did not meet the quality control standards for peak fitting due to poor peak resolution or non-Lorentzian peak shape, leaving ^{1}H-NMR analysis of 93 samples. Each ^{1}H-NMR spectrum was acquired over 45 min. GC-MS was performed with a total of 81 stool water extract samples, with only 20 of the samples being the same as previously run on IC and NMR. Due to insufficient sample volumes remaining from the first batch of samples collected, new samples for GC-MS were extracted from 5 rats. Each GC-MS analysis had a run time of 32 min in addition to the oven cool down time, amounting to a total measurement time of around 55 min per sample.

3.2.2 Sample preparation

Sample preparations are discussed in full detail for IC, NMR, and GC-MS experiments in Chapter 2.2.1, 2.3.1.1, and 2.4.1 and 2.4.2 respectively.

3.2.3 Instrumental methods

Instrumental methods including those IC, NMR, and GC-MS are discussed in detail in Chapter 2.2, 2.3, and 2.4 respectively.

3.3 Results and discussion

Segmental stratification along the colon is observed by metabolic profiling using IC, ^{1}H-NMR, and GC-MS. A total of 106 metabolites from stool water extracts were profiled throughout the ileum, cecum, proximal, mid, and distal colon and their changes along the length are evaluated with a combination of univariate and multivariate statistical analyses. The compositional changes observed are a combination of processes taking place in the colon including, but not limited to, fermentation, bacterial metabolism, and absorptive/secretory forms of transport. As stool travels from the cecum to the proximal colon there is a large influx of water followed by the subsequent removal along the remainder of the colon (Figure 3.1). This influx of water is necessary to maintain an appropriate level of luminal fluidity that aids in digestion and transport of metabolites.[17]

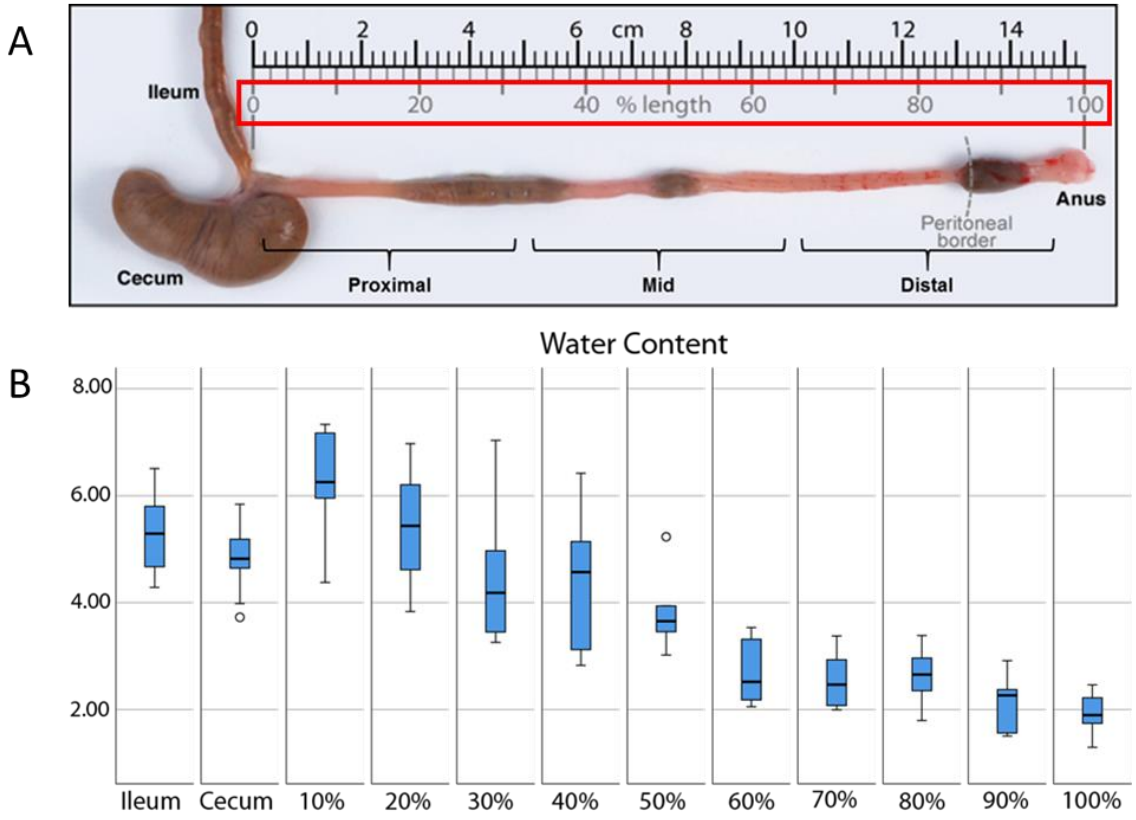

Figure 3.1. Example of a female rat colon removed before stool extraction. Segments of the colon are labeled including the ileum, cecum, and approximate location of the proximal, mid, and distal colon with an example of % length highlighted in red. (A) Graph of water content (µL/mg dry weight; y-axis) obtained from the corresponding locations within the colon (x-axis) displayed as a box plot (B).

Figure 3.1 represents water content previously determined by our collaborator UCR Professor Christian Lytle through stool removal from rats in which weight of stool was recorded before and after drying to calculate the weight of water in the sample. The data obtained from this analysis is depicted in the form of box plots with each box representing data collected from the corresponding location including the ileum, cecum, proximal (10-30%), mid (40-60%), distal (70-100%) which includes void samples.

Figure 3.1 also includes a picture of a representative rat colon illustrate how the % location (highlighted in the red box) is determined. Stool found within the first 10% of the colon, not including the cecum, is binned into the 10% category followed by stool found within the next 10.1%-20% is binned into 20% and so on.

Due to the large variations of water content between samples along the length of the colon, we opted to normalize all data to dry stool weight for analysis to provide information about the amount of metabolite present rather than the concentration driven by water content. Discussions of metabolite profiling is presented several sections pertaining to the chemical classes of each metabolite, beginning with inorganic ions.

3.3.1 Inorganic ions

Inorganic ions have historically played an important role in the discovery of the colon as a heterogeneous organ, with function and transport capacities varying significantly along its length.[18, 19] Both cationic and anionic inorganic ions including sodium, potassium, magnesium, calcium, chloride, phosphate, and sulfate can be measured using the IC methods described in sections 2.2.1 and 2.2.2 (Figure 3.2). Resulting peak areas from the corresponding chromatograms can be obtained and converted to concentrations using calibration curves obtained from standards.

Using the multivariate analysis technique orthogonal projections to latent structures (OPLS-DA)[20] of just the inorganic ions (omitting propionate and butyrate), we can observe how concentrations differ between the locations along the length of the colon. For OPLS-DA analysis data was sorted into 5 locations including the ileum, cecum, proximal, mid and distal colon.

Figure 3.3 presents the OPLS-DA score and loadings plots which show good clustering and correlation of samples within the same groups (locations). Principal component 2 (PC2) along the y-axis of the score plot provides good visual separation of the ileum and cecum samples from those of the proximal, mid, and distal colon. The loadings plot provides information about the metabolites contributing to the separation along that axis (principal component), and as Figure 3.3 indicates, differences in sodium and calcium levels contribute most to the separation of the ileum and cecum samples along PC 2.

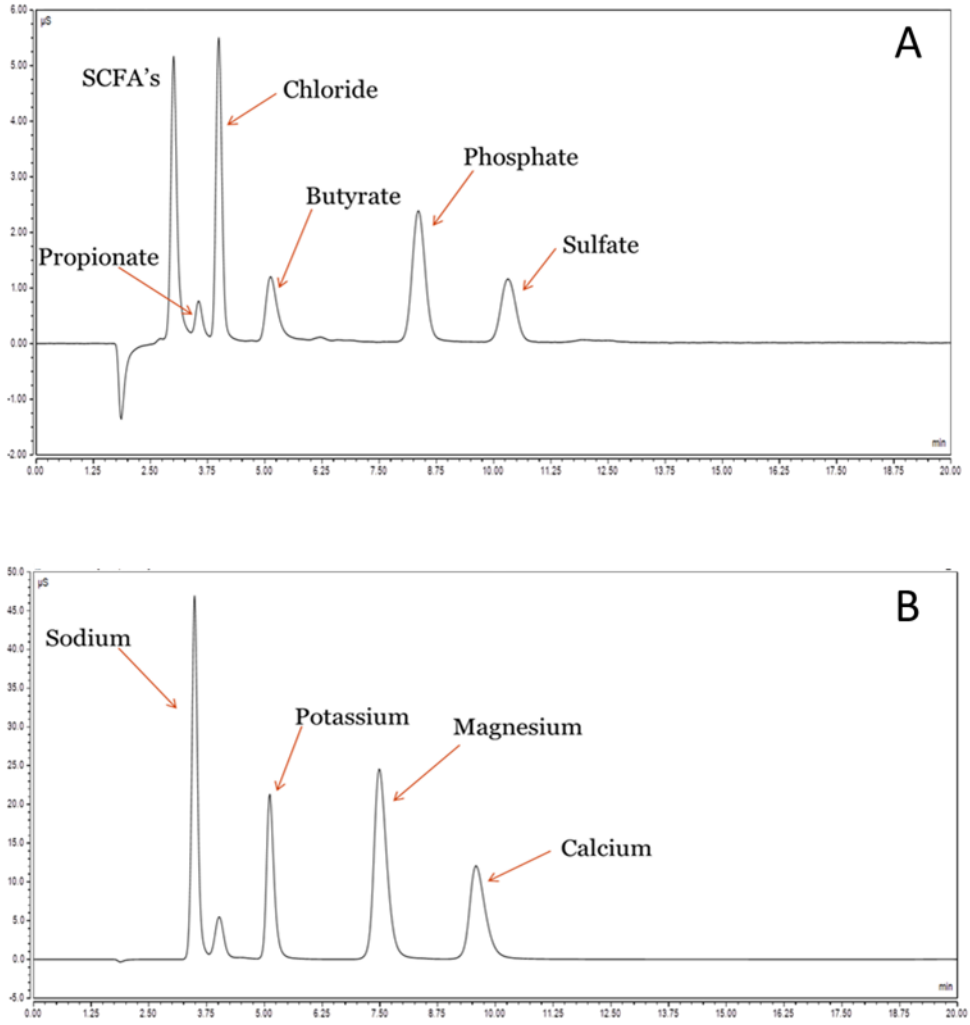

Figure 3.2. Anion chromatogram depicting the resolution of propionate, chloride, butyrate, phosphate, and sulfate. The peak labeled short chain fatty acids (SCFA's) is comprised mostly of acetate, but due to co-elution with formate and citrate, we were unable to use the peak in our analyses.(A) Cation chromatogram of sodium, potassium, magnesium, and calcium. (B)

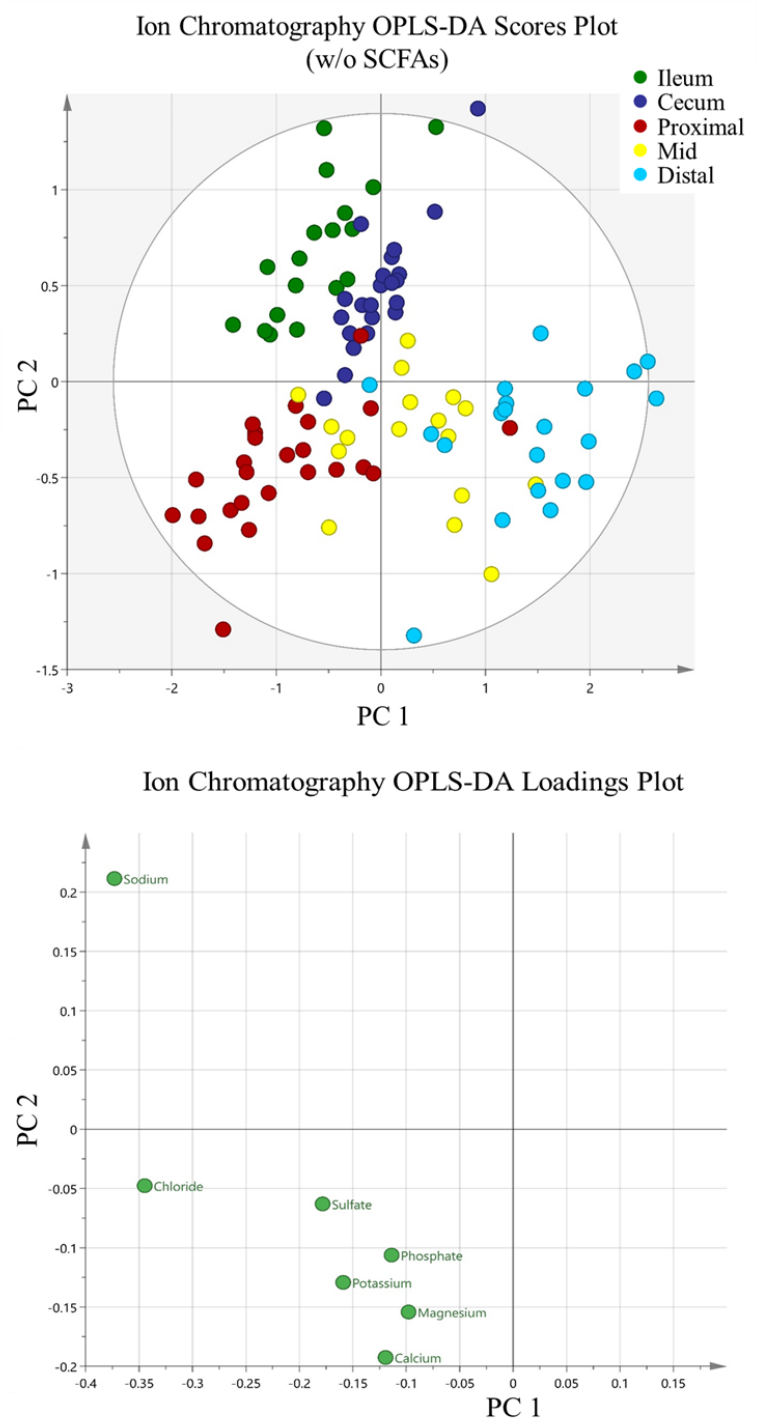

Figure 3.3. OPLS-DA score and loadings plot of the 7 inorganic ions obtained from IC.

Principal component PC1 (x-axis) by definition explains the greatest variance of the dataset compared to the other PC's, and in this dataset is driven by the amount of sodium and chloride in the corresponding sections of the colon. As we work left to right along PC1 we see that the cecum samples have the most negative PC1 values (furthest left), and the distal colon samples are most positive in PC1 (furthest right) with the samples from other locations interspersed between these groupings. Upon examination, it is notable that all the ions appear left of 0.0 along PC1. This is due to the ions behaving similarly along the length of the colon. This is a case where multivariate analysis may not be necessary.

Though multivariate analysis tells us that there is variance in the levels of these ions that causes the groups to segregate, a positive or negative PC value does not explain how they vary in abundance, i.e. increasing or decreasing concentrations. If we examine the data using a type of univariate analysis with box plots, we can better observe what is happening to inorganic cation (Figure 3.4) and anion (Figure 3.5) concentrations along the length of the colon. This univariate analysis indicates that the inorganic ions may be behaving in a similar manner.

Figure 3.4 shows us that sodium, as well as sulfate and chloride (Figure 3.5) have higher than average concentrations within the ileum, but with a large standard deviation. Once the stool enters the cecum, a slight decrease in concentration is observed and the standard deviation decreases.

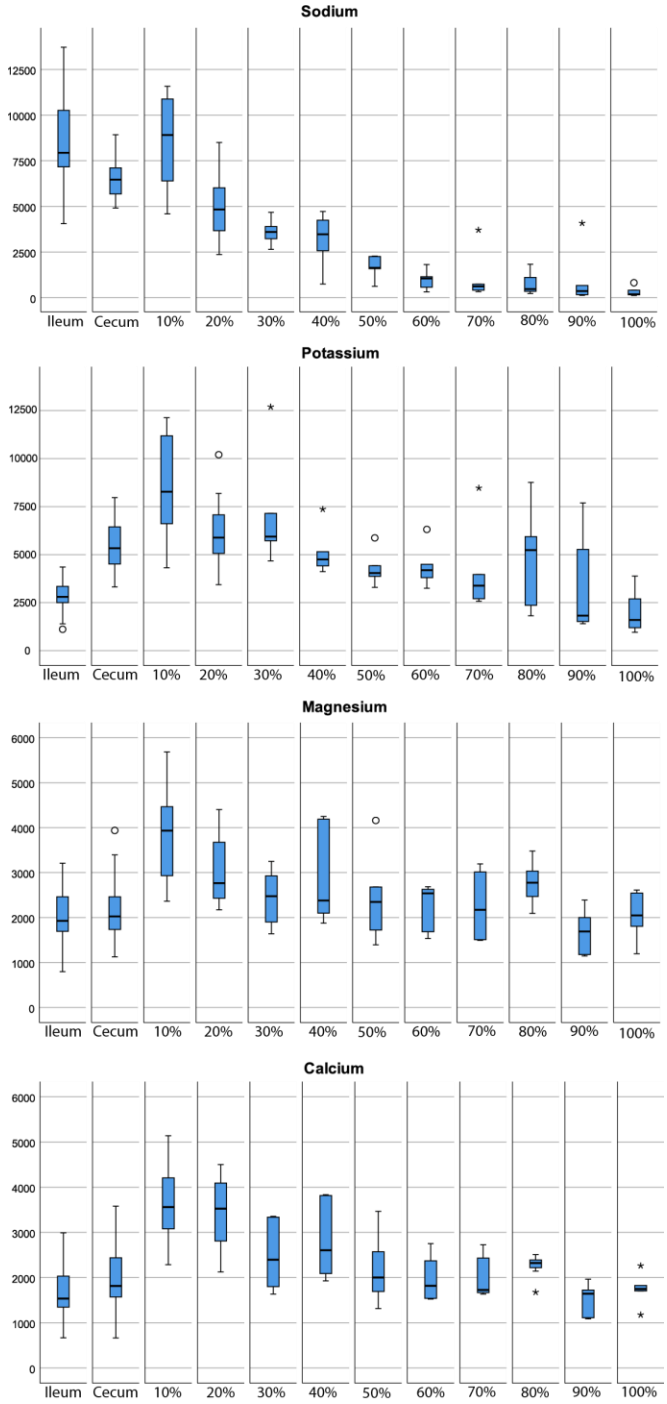

Figure 3.4. Box plots of IC concentration (mM; normalized to mg dry stool) data for cations including sodium, potassium, magnesium, and calcium obtained from corresponding locations of the colon including ileum, cecum, proximal (10-30 %), mid (40-60%) and distal colon (70-100%)

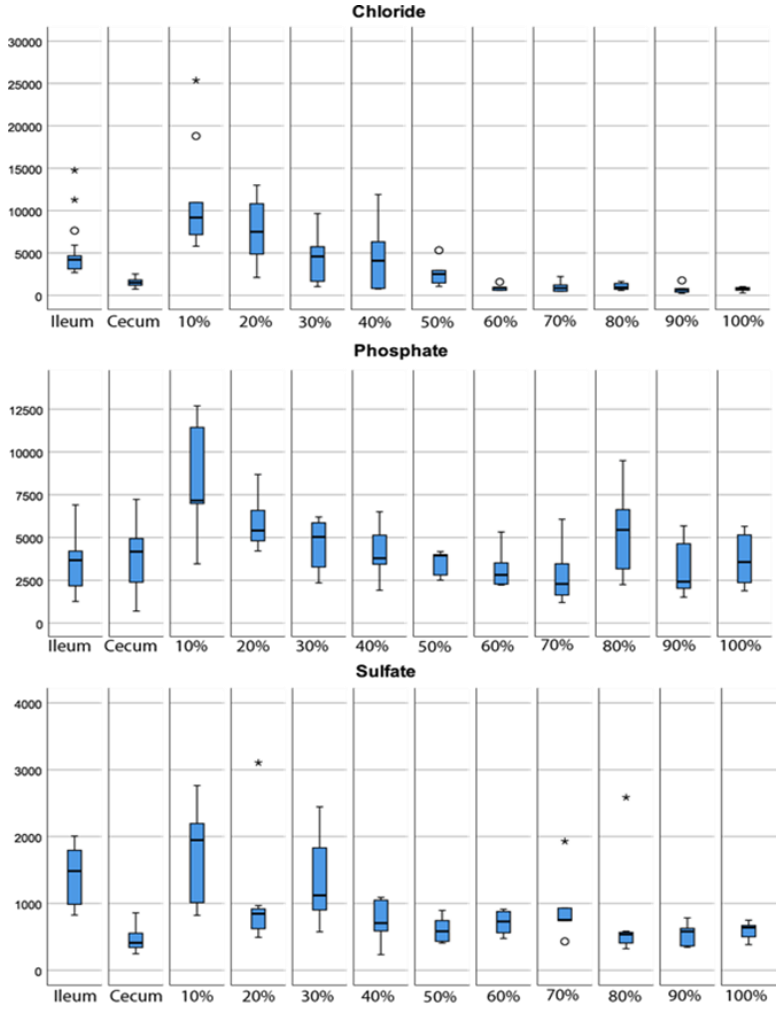

Figure 3.5. Box plots of IC concentration (mg/L; normalized to mg of dry stool) data for anions including chloride, phosphate and sulfate obtained from corresponding locations of the colon including ileum, cecum, proximal (10-30 %), mid (40-60%) and distal colon (70-100%)

The concentrations of these ions increase in concentration in the proximal colon, followed by significant decreases along the remaining length of the colon. The other ions have a similar trend with the difference being that concentrations are initially lower in the ileum and cecum prior to an increase in concentration in the proximal colon and subsequent decreases along the remaining length.

Observing correlations between samples in plots like those shown in Figures 3.4 and 3.5 becomes difficult as the number of metabolites increases. For this reason, a heat map (Figure 3.6), can allow for easier comparisons of changes in concentration between groups of metabolites along the length of the colon. The heat map represents samples similarly to the box plots with corresponding locations separated into 12 total segments including the ileum, cecum, with the remaining proximal, mid, and distal colon segmented into 10 locales each corresponding to 10% block of total length.

The heat map shown in Figure 3.6 displays concentrations as percentiles relative to the average value of each individual metabolite along the length of the colon. The colors along a row are calculated using blue as the 10^{th} percentile (lowest abundance), white as 50^{th} percentile (the average value), and red as the 90^{th} percentile (highest abundance).

Using the heat map we can examine the changes of sodium and chloride along the length of the colon. The concentrations start out above average in the ileum and decrease a bit in the cecum.

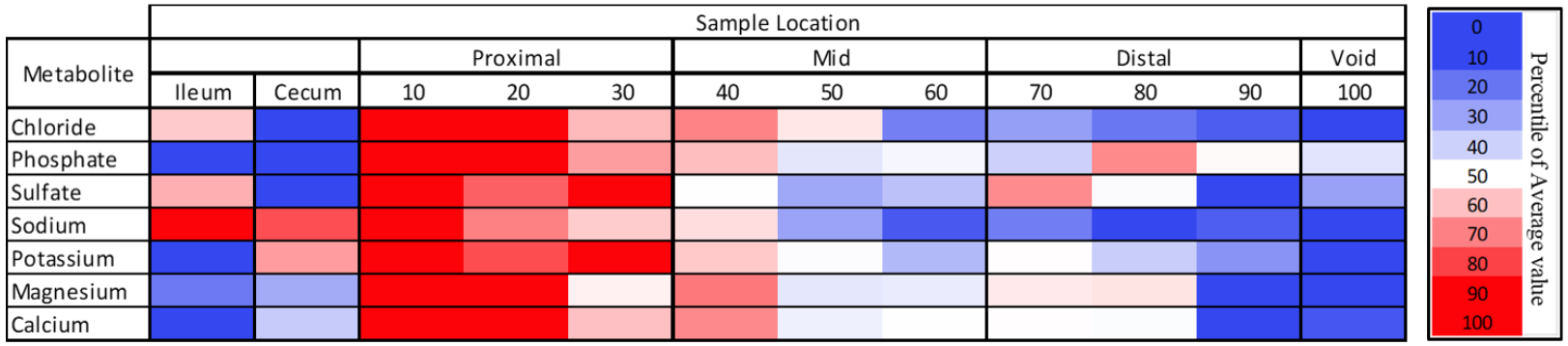

Figure 3.6. Heat map of inorganic ion concentrations along the length of the colon displayed in the form of averages for each segment, color coded to display the change in averages for each metabolite as presented as percentiles.

Upon entering the proximal colon the concentrations both ions increase to values within the 90th percentile (red) followed by a decrease in concentration throughout the mid and distal colon until reaching values in the 10th percentile (blue) within the voided stool region. This observation matches the separation observed in the OPLS-DA analysis of the inorganic ions along PC1 of Figure 3.3.

This change in ion concentration is indicative of the absorptive and secretory processes of the colon. *Rechkemmer et al.* state that the secretagogues of the large intestinal segments stimulate chloride and potassium secretion and in addition inhibit sodium and chloride absorption in the proximal colon. This inhibition of sodium and chloride absorption could be responsible for the high concentrations of both ions present in the proximal colon.

Other ions such as phosphate, potassium, magnesium, and calcium show a similar trend as sodium and chloride with a significant increase in the proximal colon and a pattern of decreasing concentration along the length of the colon until reaching low values in the distal colon. However, when looking at the data provided by the heat map, sulfate and phosphate show above average values in the distal colon.

If we look back at the box plots for sulfate and phosphate (Figure 3.5), we can see that in these locations there are increases in standard deviation that could be attributing to the rise in average values. This is often attributed to biovariability. Though we try to control as many factors as possible, it is not possible in animal experiments to control rates of digestion, gastrointestinal motility including peristaltic and antiperistaltic movements, or the composition of the gut microbiome.

3.3.2 Short chain fatty acids (SCFAs)

Transport of both water and various inorganic ions such as sodium and chloride across the colonic epithelium have been observed in previous studies[21] and establishes proof of concept for our extraction method, the subsequent integrity of samples, and our analysis protocols. Further IC analyses showed the ability to study another group of charged organic compounds important in colonic health, short chain fatty acids (SCFAs). Due to the anionic carboxylic acid group of SCFAs, their concentrations can be measured using IC. However, with the methods used herein, which were limited to isocratic separations, we were unable to resolve formate and acetate limiting the IC analyses of SCFAs to only propionate and butyrate. If we include propionate and butyrate data in the multivariate analyses of samples run on IC (Figure 3.7) we obtain quit a different view on variance between groups.

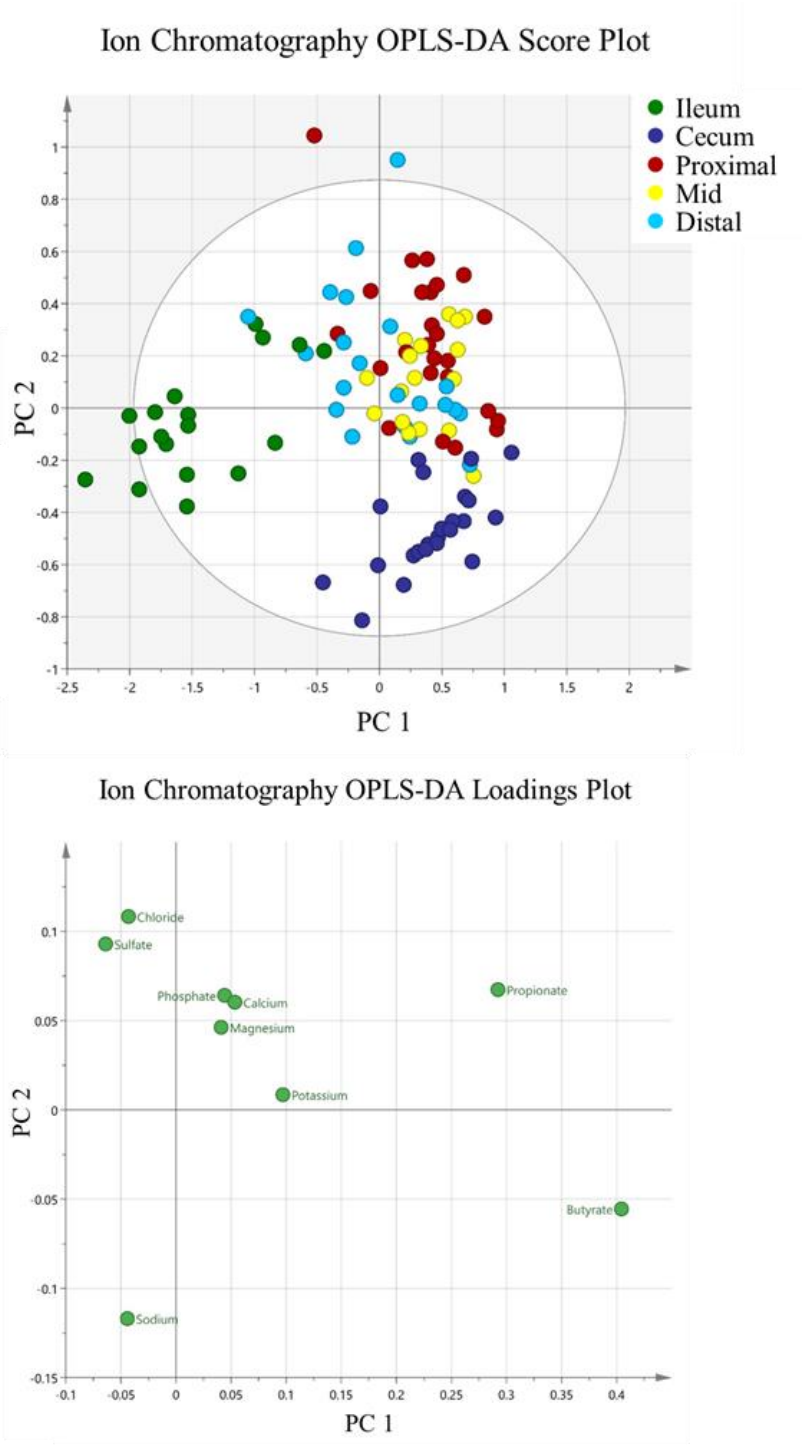

Figure 3.7. OPLS-DA score and loadings plot of the 9 metabolites detected by IC including inorganic ions and organic acids.

The loadings plot of Figure 3.7 reveals that the SCFAs contribute significantly to the separation observed along PC1. The score plot shows separation between the ileum samples and those from the rest of the colon, with some overlap observed between samples of the ileum with the distal colon along PC1. This overlap is a result of similar amounts of propionate and butyrate present within these samples.

We can again use univariate analysis (Figure 3.8) to determine what changes in butyrate and propionate are causing this separation of samples in the loadings plot. Both butyrate and propionate follow a similar trend with low concentrations in the ileum, and concentrations increasing in the cecum and proximal colon as the bacteria break down starch and other complex carbohydrates to form SCFAs. Importantly, SCFAs are the preferred energy source of the colonocyte and have been found as a link to healthy gut function.[22, 23] SCFAs are not only utilized by the colonocyte, but are involved in transport across the colonic epithelium into the portal vein to aid in gluconeogenesis and lipogenesis within the liver,[24, 25] causing concentrations to decrease along the length of the colon. SCFAs have been reported to be 95% absorbed by the colonocytes.[26, 27] By the time the stool reaches the distal colon the SCFAs content is dramatically decreased and levels fall below average to values similar to the ileum.

The study of SCFAs and their generation by the gut microbiome is of great importance in understanding gut health. While IC provides a platform to observe ionic components along the colon, it is beneficial to obtain a broader view of the metabolites present.

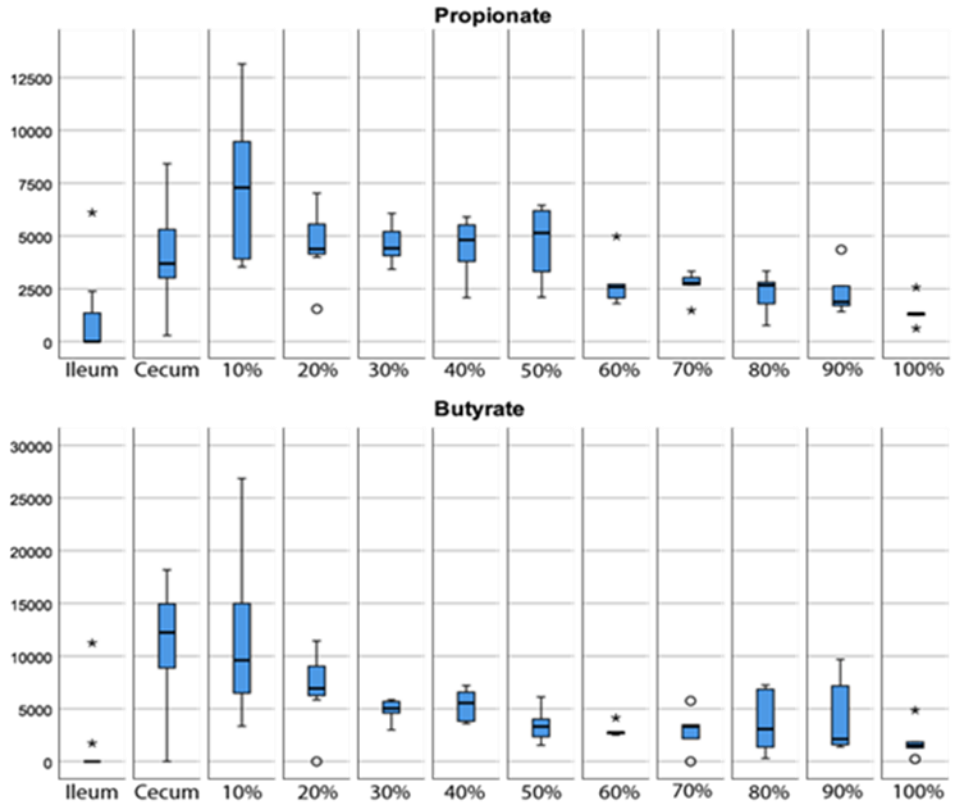

Figure 3.8. Box plots of data for propionate and butyrate concentrations (mg/L; normalized to mg stool) obtained from IC corresponding to locations of the colon including ileum, cecum, proximal (10-30 %), mid (40-60%) and distal colon (70-100%)

In addition to the limitation of IC only detecting ions, it can be challenging to identify unknown peaks because conductivity detection does not provide structural information. Due to these limitations, ^{1}H-NMR was selected as a complementary technique that would allow for the metabolic profiling of a large subset of organic metabolites available for transport within the colon including the acetate and formate that could not be resolved with our IC methods.

3.3.3 ^{1}H-NMR analysis of SCFAs

^{1}H-NMR analysis yielded profiles of 27 metabolites along the length of the colon. In order to profile concentrations of metabolites using ^{1}H-NMR, data was first gathered in an effort to identify as many metabolites as possible in the various positions of the colon. Almost 50 metabolites were identified within the 97 samples, but due to insufficient signal-to-noise in the spectra of the sample set many metabolites could not be used for profiling. Attempts were made to overcome the signal to noise limitations by signal averaging more spectra, but it was found that dynamic range was an issue. In spectra such as those taken from the cecum, resonances of SCFAs are of high abundance. Acetate, for example, is a singlet at 1.91 ppm (Figure 3.9) and often is the most intense metabolite in the spectra. This large peak affects the receiver gain, which is how much the raw FID is amplified,[28] creating the issue of dynamic range between types of samples.

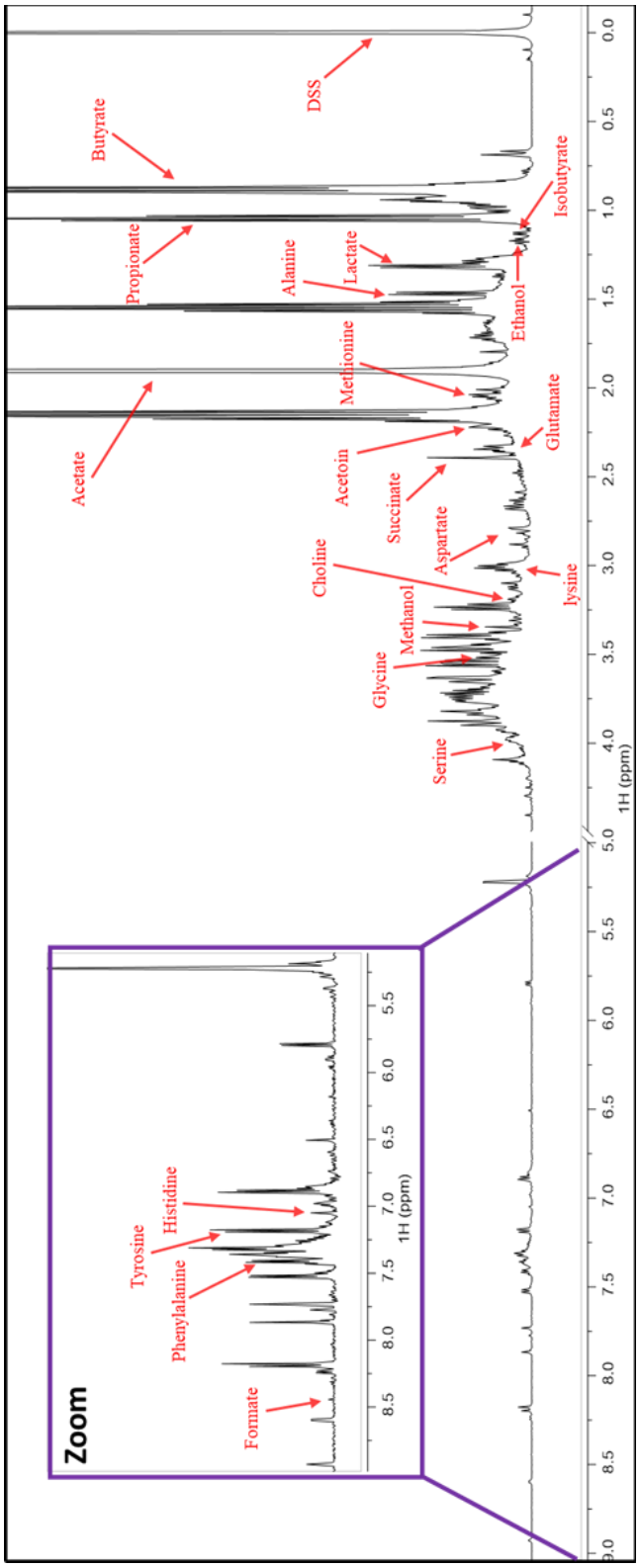

Figure 3.9. ^{1}H-NMR spectrum of a stool water extract of sample removed from the cecum of a rat with identified metabolites shown in red. The aromatic region (5.0- 9.0) was zoomed to better show identifications within the region.

Adding to the complexity of analysis is that some metabolites are not found in every location making it necessary to comb through spectra from each location. It is also crucial to check each sample within a location, because biovariability can complicate analysis even further with some samples not containing enough of a metabolite to reach the limit of detection. For these reasons, only 27 metabolites were selected for metabolic profiling.

Figure 3.9 represents a sample from the cecum containing 22 of the 27 metabolites. These metabolites were identified using a combination of methods including cross referencing previously published literature on stool analysis, and the use of databases such as the human metabolome database in which chemical shifts can be used as the search criteria, or metabolites can be searched by name with an attached NMR spectra to be used as reference.[29, 30]

To confirm tentative assignments, metabolite standards were run for each of the 27 metabolites under the same buffered conditions, ensuring pH, temperature, and processing parameters did not alter observed chemical shifts. The proton chemical shifts for every resonance pertaining to each metabolite was compiled in a table. (Table 1) This also includes the multiplicity of each resonance, and the resonance that was selected to use for metabolic profiling. These resonances were carefully selected as the best for peak fitting/integration based on resolution as well as signal intensity.

Table 3.1. Metabolites identified by ^{1}H-NMR analysis with corresponding chemical shifts of resonances observed. (**) denotes the resonance that was selected for quantitative analysis.

Compound	^{1}H-NMR Chemical shift (multiplicity)
Acetate	1.91 (s)**
Acetoacetate	2.27 (s)**, 3.34 (s)
Acetoin	1.37 (d), 2.22 (s)**, 4.42 (q)
Alanine	1.47 (d)**, 3.78 (q)
Allantoin	5.38 (s)**
Asparagine	2.84 (dd)**, 2.94 (dd), 3.99 (dd)
Aspartate	2.66 (dd), 2.81 (dd)**, 3.88 (dd)
Butyrate	0.88 (t)**, 1.55 (m), 2.15 (t)
Choline	3.19 (s)**, 3.52 (m), 4.07 (m)
Ethanol	1.17 (t)**, 3.64 (q)
Formate	8.44 (s)**
Glucose	3.23 (dd), 3.40 (m), 3.46 (m), 3.52 (dd), 3.71 (m), 3.82 (m), 3.89 (dd), 4.62 (d), 5.22 (d)**
Glutamate	2.05 (m), 2.12 (m), 2.34 (m)**, 3.74 (q)
Glycine	3.55 (s)**
Histidine	3.13 (dd), 3.23 (dd), 3.97 (dd), 7.06 (s)**, 7.80 (s)
Isobutyrate	1.13 (d)**, 2.57 (m)
Lactate	1.32 (d)**, 4.10 (q)
Lysine	1.47 (m), 1.72 (m), 1.90 (m), 3.02 (t)**, 3.74 (t)
Methanol	3.34 (s)**
Methionine	2.13 (m)**, 2.63 (t), 3.85 (dd)
Oxaloacetate	2.37 (s)**
Phenylalanine	3.20 (m), 3.98 (dd), 7.32 (d), 7.36 (m), 7.42 (m)**
Propionate	1.05 (t)**, 2.17 (m)
Serine	3.83 (dd), 3.95 (m)**
Stachyose	3.52 (t), 3.56 (dd), 3.79 (m), 3.99 (m), 4.05 (m), 4.14 (dd), 4.22 (d), 4.00 (m), 5.42 (d)**
Succinate	2.40 (s)**
Tyrosine	3.05 (dd), 3.19 (dd), 3.93 (dd), 6.89 (m), 7.18 (m)**

In the event that a metabolite's only ^{1}H NMR resonance was a singlet, the two-dimensional (2D) NMR experiment [^{1}H-^{13}C] heteronuclear single quantum correlation spectroscopy (HSQC) was employed for confirmation. This includes metabolites such as acetate, succinate, methanol, formate, etc. The [^{1}H-^{13}C] HSQC spectrum provides correlations that connect the chemical shift of a carbon to that of its directly coupled proton (Figure 3.10).

Upon multivariate analysis of the ^{1}H-NMR data using OPLS-DA (Figure 3.11) a clear separation of the ileum samples from those of the colon can be observed along PC1. The loadings plot indicates that acetate, propionate, and butyrate contribute most to this separation, in agreement with the IC results. With closer examination of SCFAs using the heatmap (Figure 3.12), changes in the levels of acetate, butyrate, and propionate in the ^{1}H-NMR data correlate quite well with IC data of propionate and butyrate showing that concentrations are extremely low in the ileum with a rapid increase upon entering the cecum and proximal colon. Once stool travels through the proximal colon the SFCA concentrations start to decrease due to rapid absorption by the colonocyte.

Short chain fatty acids have been studied in both stool[31-33] and blood[34, 35] as a way of determining their rates of transport. Literature reports indicate that SCFAs are produced and found at a molar ratio of 60:20:20 for acetate, propionate, and butyrate respectively, but references suggest this data is collected from voided stool and/or blood.[36-38]

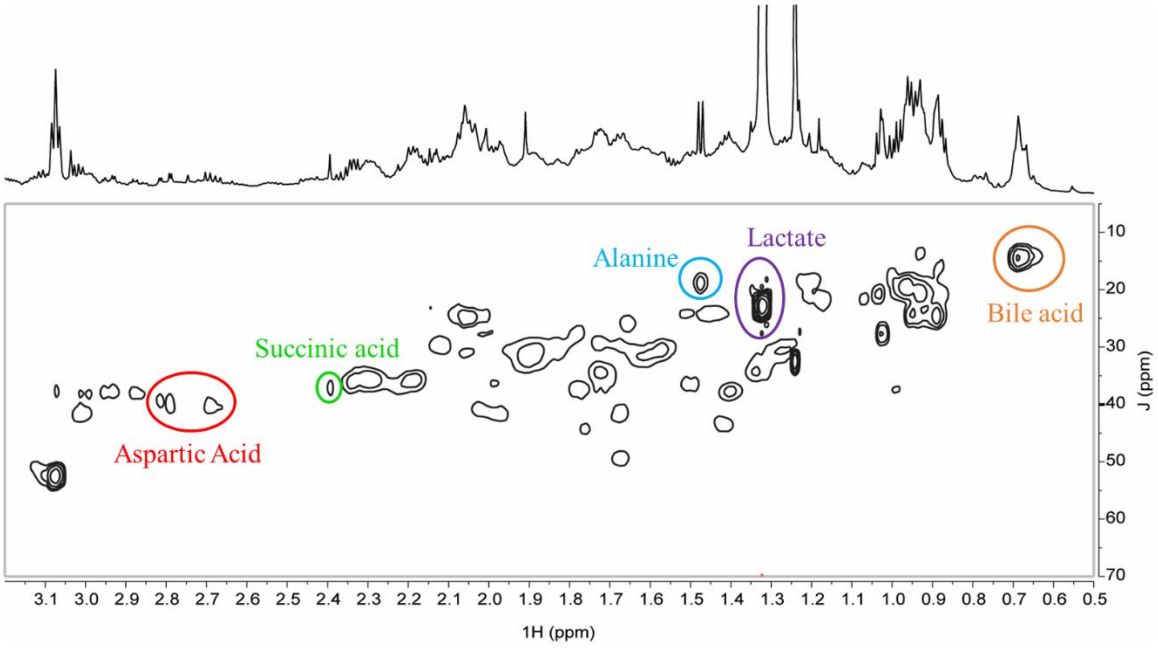

Figure 3.10. [^{1}H, ^{13}C] HSQC spectra of a representative ileum stool extract sample used to aid in the identification of resonances.

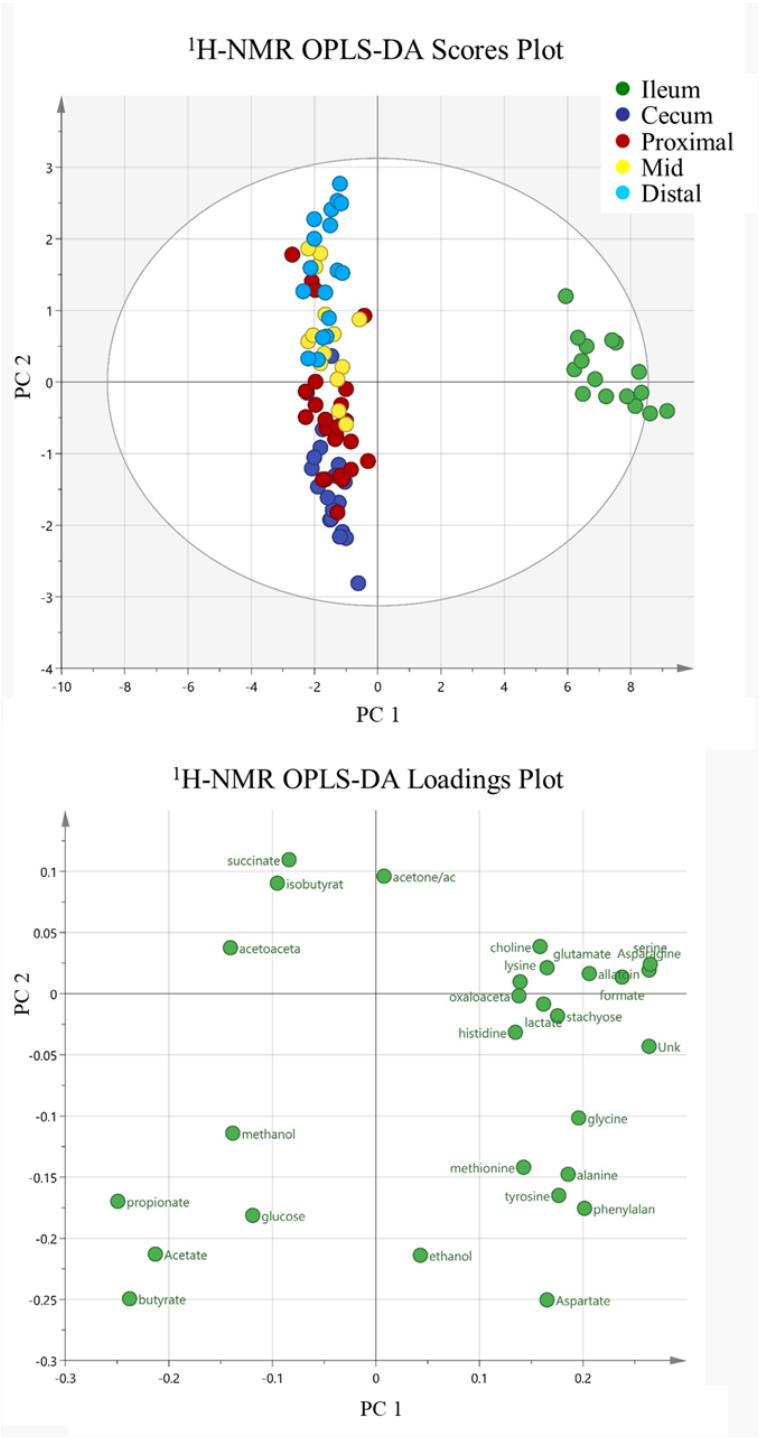

Figure 3.11. OPLS-DA score and loadings pots corresponding to ^{1}H-NMR analysis of 27 metabolites.

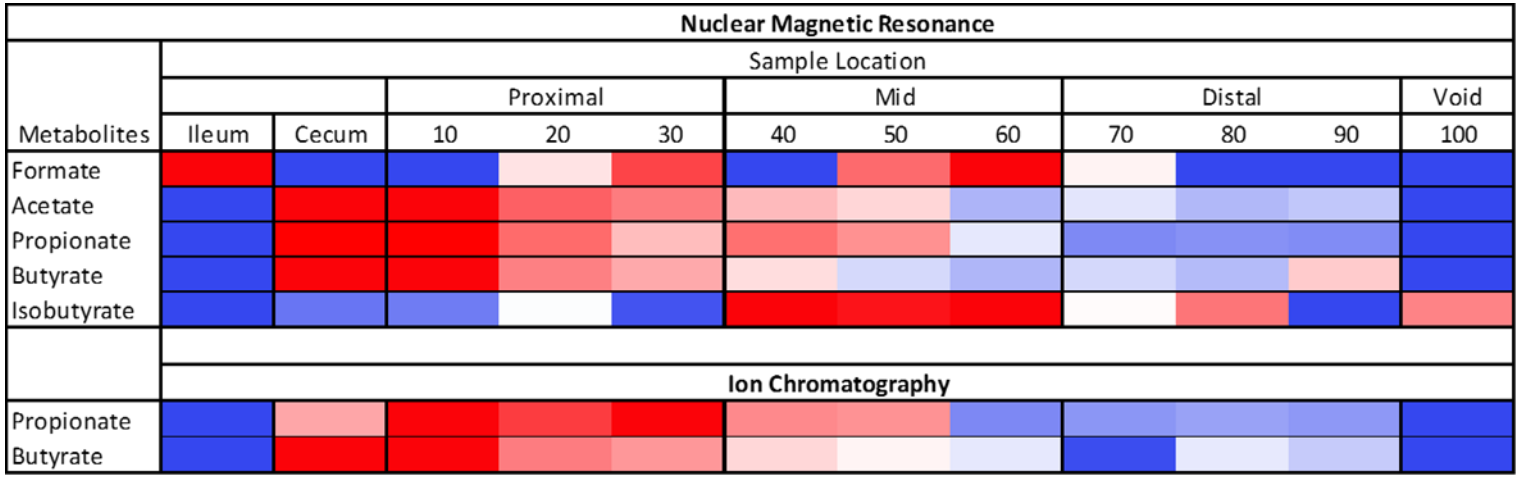

Figure 3.12. Heat map of SCFA concentrations along the length of the colon displayed in the form of averages for each segment, color coded to display change in averages for each metabolite as presented as percentiles.

A closer look at acetate, butyrate, and propionate gathered from our experiments in the form of boxplots (Figure 3.13) suggests that trends are similar, but the compounds are not produced at constant ratios over time. While concentrations of transported SCFAs may be 60:20:20, it does not appear that this ratio is held constant throughout the length of the colon.

It is important to note that SCFAs are defined as fatty acids with 2 to 6 carbons which includes metabolites formate and isobutyrate that were also detected and analyzed by NMR. Both formate and isobutyrate appear to follow a different trend within the colon. (Figure 3.14) For example, formate is found in the ileum and decreases in the cecum and proximal colon until reaching the mid colon where the concentration increases before decreasing again in the distal colon. Isobutyrate also differs, with low concentrations in the ileum, cecum, and proximal colon followed by a large increase within the mid colon. The gut microbiome contains many different types of bacteria with the main purpose of breaking down previously undigested matter in an effort to harvest nutrients that will be absorbed into the bloodstream to be utilized by the host. An increase in isobutyrate concentration in the mid colon could be representative of its formation from the breakdown of other metabolites by the bacteria housed in the mid colon.

The profiles of both formate and isobutyrate do not mimic the profiles of the more common colonic SCFAs, making it important to note for clarity that when referring to SCFAs it is assumed to only include acetate, propionate, and butyrate in the context of colonic function.

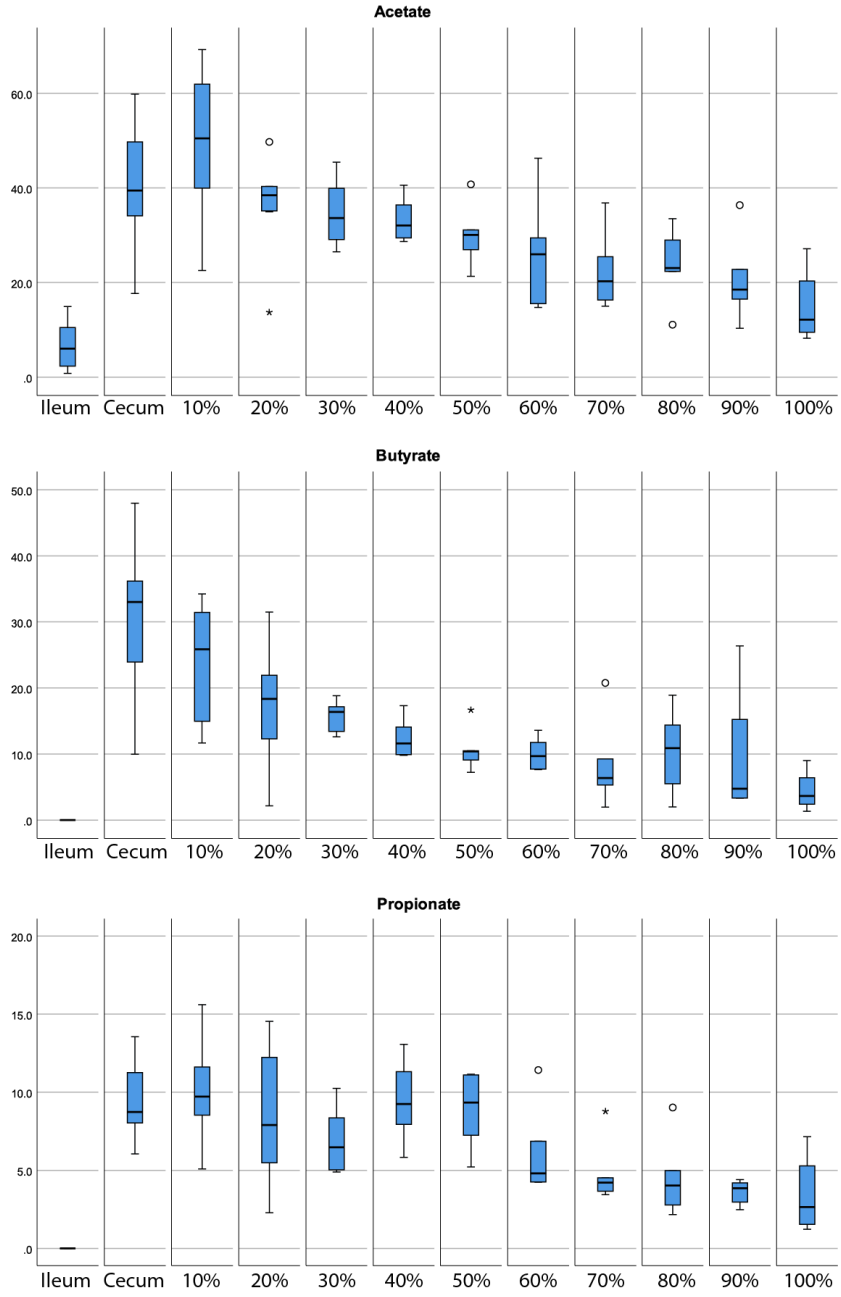

Figure 3.13. Box plots of data for acetate, butyrate, and propionate values (peak area normalized to DSS and mg dry stool) obtained from NMR corresponding to locations of the colon including ileum, cecum, proximal (10-30 %), mid (40-60%) and distal colon (70-100%)

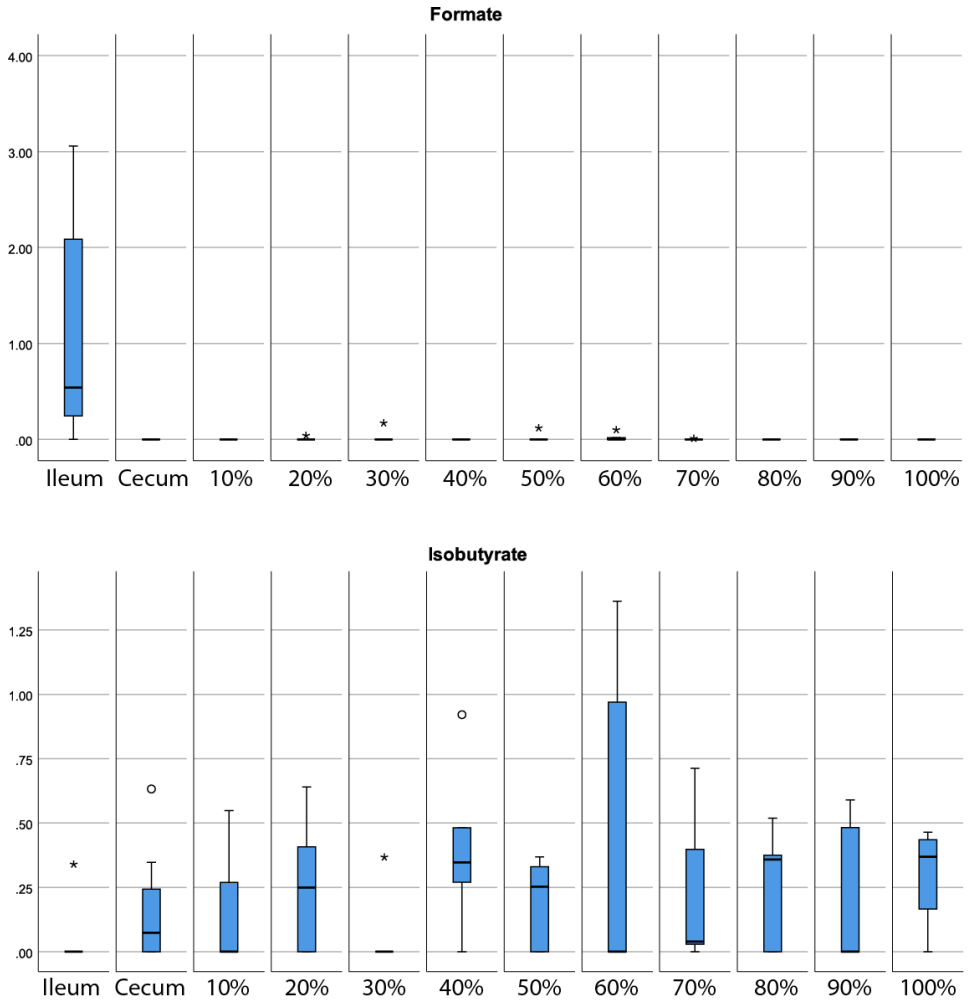

Figure 3.14. Box plots of data for formate and isobutyrate values (peak area normalized to DSS and mg dry stool) obtained from NMR corresponding to locations of the colon including ileum, cecum, proximal (10-30 %), mid (40-60%) and distal colon (70-100%)

3.3.4 Sugars

The SCFAs appear at high levels within the cecum that acts as a large fermenting chamber where bacteria rapidly break down indigestible starch that has survived the stomach and small intestine. This cecum is quite large in the rat and is essential due to the large amounts of starch and fiber in their diet. Through NMR analysis we detected stachyose, a tetrasaccharide found predominantly in seeds and nuts, in samples from the ileum before reaching undetectable amounts within the cecum (Figure 3.15). Stachyose is comprised of 2 galactose, 1 glucose, and 1 fructose sugar monosaccharides. It is possible that the increased presence of glucose in the cecum and proximal colon seen in Figure 3.15 results from the breakdown of stachyose and similar molecules within the cecum. The NMR resonances of sugars often have similar chemical shifts causing overlap within the spectrum and making identification and quantitation difficult. Only the sugar compounds stachyose and glucose could be confidently identified with well resolved resonances necessary for further analysis. To overcome issues of resolution and sensitivity associated with our NMR analysis we conducted GC-MS analysis of the samples, obtaining results for 86 metabolites. (Table 2).

Several sugars were identified in GC-MS analysis that could not be confidently identified in ^{1}H-NMR experiments. One of these sugars, galactose is a component of stachyose and similarly to glucose has an elevated concentration in the cecum that could be a direct result of the bacterial breakdown of stachyose.

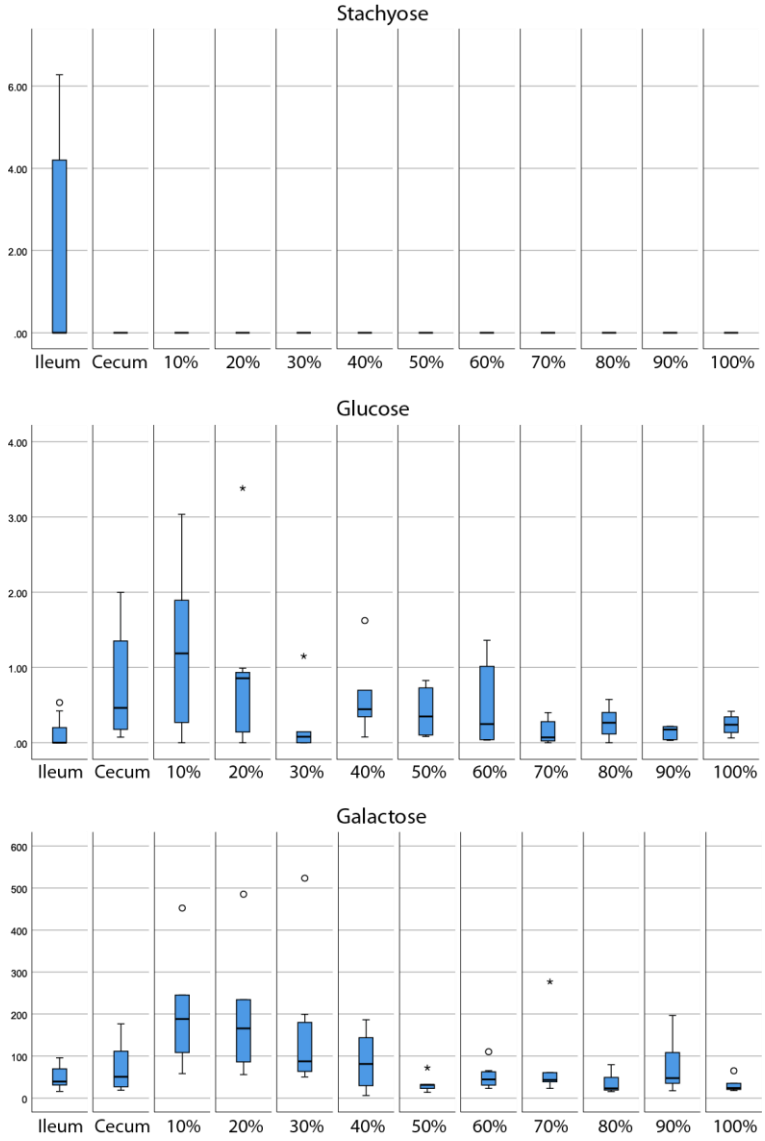

Figure 3.15. Box plots of data for stachyose and glucose values (peak area normalized to DSS and mg dry stool) detected by NMR, and galactose values (ion intensity normalized to internal std and mg dry stool) detected via GC-MS corresponding to locations of the colon including ileum, cecum, proximal (10-30 %), mid (40-60%) and distal colon (70-100%)

Table 3.2. GC-MS detected metabolites including the number of trimethylsilane derivatives detected, retention time, and characteristic ion used for statistical analysis. (**) denotes metabolites also detected by NMR. (Table continues on the next page).

GC-MS Identified Metabolites (1 of 2)			
Compound	# of TMS	Retention time (min.)	Characteristic ion (m/z)
2-deoxy-inosine	3	22.04	209
3-(2-hydroxyphenyl)-propanoic acid	2	13.52	193
3-Hydroxyphenylacetic acid	2	13.10	296
3-Methyl-2-oxopentanoic acid	1	7.72	200
4-Amino-butanoic acid	3	12.13	304
4-Hydroxyphenylacetic acid	2	13.48	252
5-Amino-pentanoic acid	2/3	8.56/13.31	247/174
5-hydroxy-1H-indole-3-acetic acid	3	18.91	290
Alanyl-alanine	2	12.96	116
Allantoin **	4	16.13	331
Allo-Inositol	6	16.79	507
Apigenin	3	24.94	471
Asparagine **	2/3	11.81/13.78	115/231
Aspartic acid **	3	12.00	232
Benzoic acid	1	8.43	179
Cellobiose	8	23.13	361
Cholesterol	1	26.31	329
Creatinine	3	12.41	329
Cysteine	3	12.43	220
Cystine	4	19.95	218
Daidzein	2	24.83	398
D-pantothenic acid	3	17.19	291
Ethanolamine	3	8.64	174
Ferulic acid	2	18.20	338
Galactitol	6	16.55	307
Galactose	5	16.20	319
gamma-Glutamylleucine	4	18.51	431
Gluonic acid	6	16.87	333
Glutamic acid **	2	12.13	276
Glutamine	4	14.48	227
Glutaric acid	2	10.56	261
Glyceric acid	3	9.51	292
Glycerol-3-phosphate	4	14.79	312
Glycine **	3	9.19	276
Glycyl-proline	3	17.10	373
Guanine	3	18.48	441
Guanosine	4	23.79	295
Histidine **	3	16.48	154
Homoserine	3	11.12	218
Hydrocaffeic acid	3	16.74	398

GC-MS Identified Metabolites (2 of 2)			
Compound	# of TMS	Retention time (min.)	Characteristic ion (m/z)
Hydrocinnamic acid	1	10.75	104
Iminodiacetic acid	3	13.15	232
Inosine	4	22.22	230
Isoleucine	2	9.01	158
Lactose	1	23.52	304
Leucine	2	8.71	158
Lysine **	4	16.51	434
Lyxonic acid	5	14.94	217
Lyxose	4	13.84	307
Malic acid	3	11.61	245
Mannitol	6	16.51	174
Methionine **	2	11.99	176
Myo-Inositol	6	18.10	305
N-acetylgalactosamine	5	17.99	319
N-acetyl-glutamic acid	3	14.79	156
N-acetylneuraminic acid	7	22.87	433
N-glycolylneuraminic acid	7	24.00	334
Nicotinic acid	1	9.06	136
Octadecanoic acid	1	19.58	341
Orotic acid	3	14.64	254
O-Toluic-acid	1	10.04	193
Phenylacetic acid	1	9.12	193
Phenylalanine **	2	13.28	218
Pinitol	5	15.51	318
Proline	2	9.07	216
Putrescine	4	14.54	174
Quinic acid	5	15.81	345
Raffinose	11	27.70	361
Serine **	2/3	8.51/9.92	116/204
Shikimic acid	4	15.31	204
Succinic acid **	2	9.33	247
Sucrose	8	22.66	271
Taurine	3	13.76	326
Threitol	4	11.83	205
Threonine	3	10.26	218
Thymine	2	10.47	255
Tryptophan	3	19.28	202
Tyrosine **	3	16.68	280
Uracil	2	9.63	241
Urea	2	8.33	189
Uric acid	4	18.21	441
Uridine	4	21.11	217
Valine	2	7.93	144
Vanillic acid	2	14.88	312

Other indigestible sugars derived from plant matter were detected by GC-MS in samples from the colon including cellobiose and raffinose. (Figure 3.16) These are relatively abundant in the ileum and remain high throughout the proximal colon in which they begin to diminish. Unlike stachyose, these sugars survive the cecum, and are likely digested by a different type of bacterium present in the proximal colon. Cellobiose is a disaccharide of two glucose molecules while raffinose is a trisaccharide of galactose, glucose, and fructose. Looking back at the NMR results for glucose (Figure 3.15) it appears that there is a slight increase in glucose in the mid colon which coincides with the decrease in concentration of cellobiose from the proximal to mid colon.

Several sugars were identified in GC-MS analysis that could not be confidently identified in ^{1}H-NMR experiments. One of these sugars, galactose is a component of stachyose and similarly to glucose has an elevated concentration in the cecum that could be a direct result of the bacterial breakdown of stachyose.

Several sugar alcohols including galactitol, mannitol, pinitol, and threitol were found in colonic samples indicating that they were not fully absorbed in the small intestine. (Figure 3.16) Concentrations of the sugar alcohols start high in the ileum and proximal colon, but before they can reach the mid colon they are likely broken down by the gut bacteria.

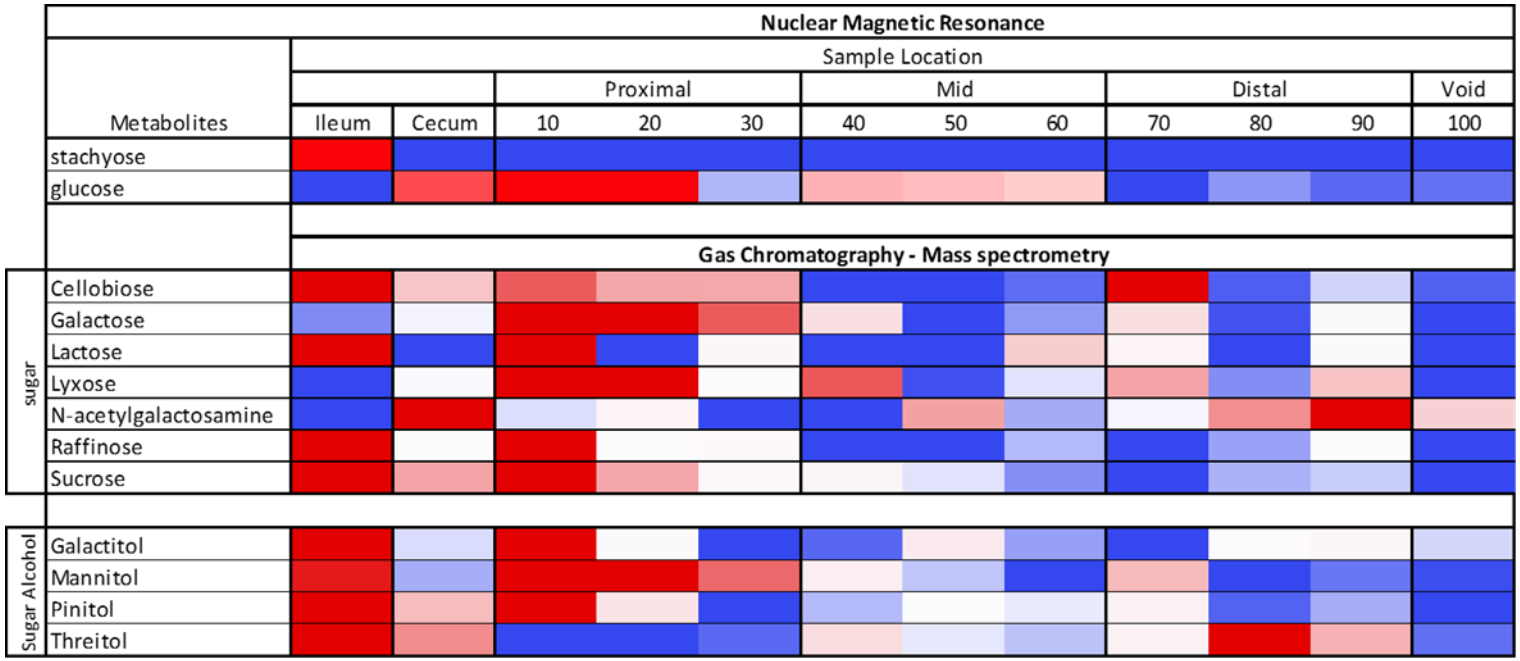

Figure 3.16. Heat map of sugar concentrations along the length of the colon displayed in the form of averages for each segment, color coded to display change in averages for each metabolite as presented as percentiles.

3.3.5 Amino acids

Multivariate analysis of NMR data (Figure 3.11) showed a good separation between the ileum and the remaining segments along PC1, with a loadings plot indicating that SCFAs were a large factor in this separation. Knowing that SCFAs are at high concentrations in the colon, and that they have been well categorized, they were removed from the data set before performing a second round of OPLS-DA. (Figure 3.17) Interestingly, the separation along PC1 remained similar with the ileum being separated from the remaining segments. Examination of the loadings plot reveals that some amino acids such as serine and asparagine contributed to this separation.

For a closer look into how amino acid concentrations are changing along the length of the colon we can examine the heat map. (Figure 3.18) The amino acids appear to all follow a similar trend along the length of the colon with high initial concentrations in the ileum followed by a dip in the cecum before increasing again within the proximal colon. Comparison of the results for the 9 amino acids detected in NMR with the 17 detected by GC-MS we can note some differences between the two analytical platforms. In NMR, several metabolites exhibit a slight increase in the mid colon, while none of the amino acids in the GC-MS exhibit much change. This may be attributed to biovariability, as the same samples were not measured for each NMR, and GC-MS.

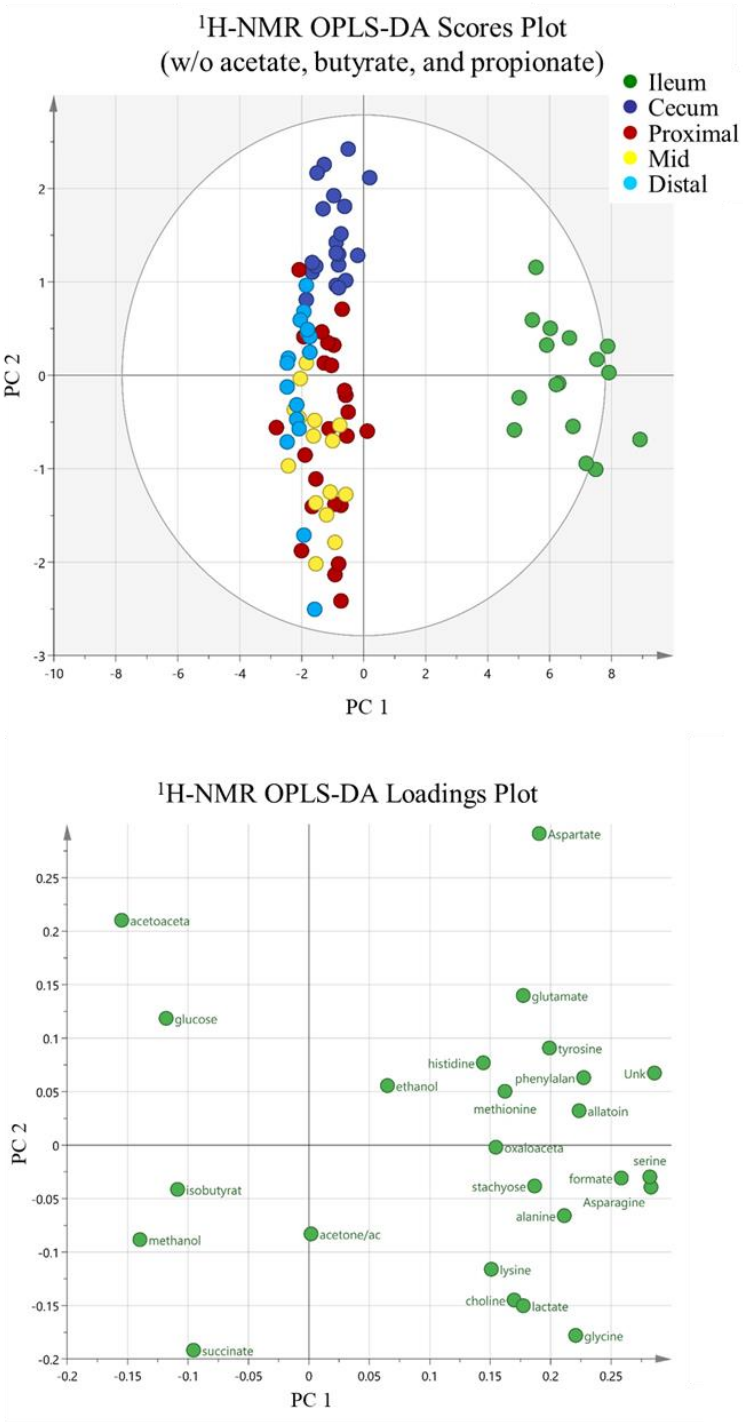

Figure 3.17. OPLS-DA score and loadings plots for NMR data, with acetate, butyrate, and propionate excluded.

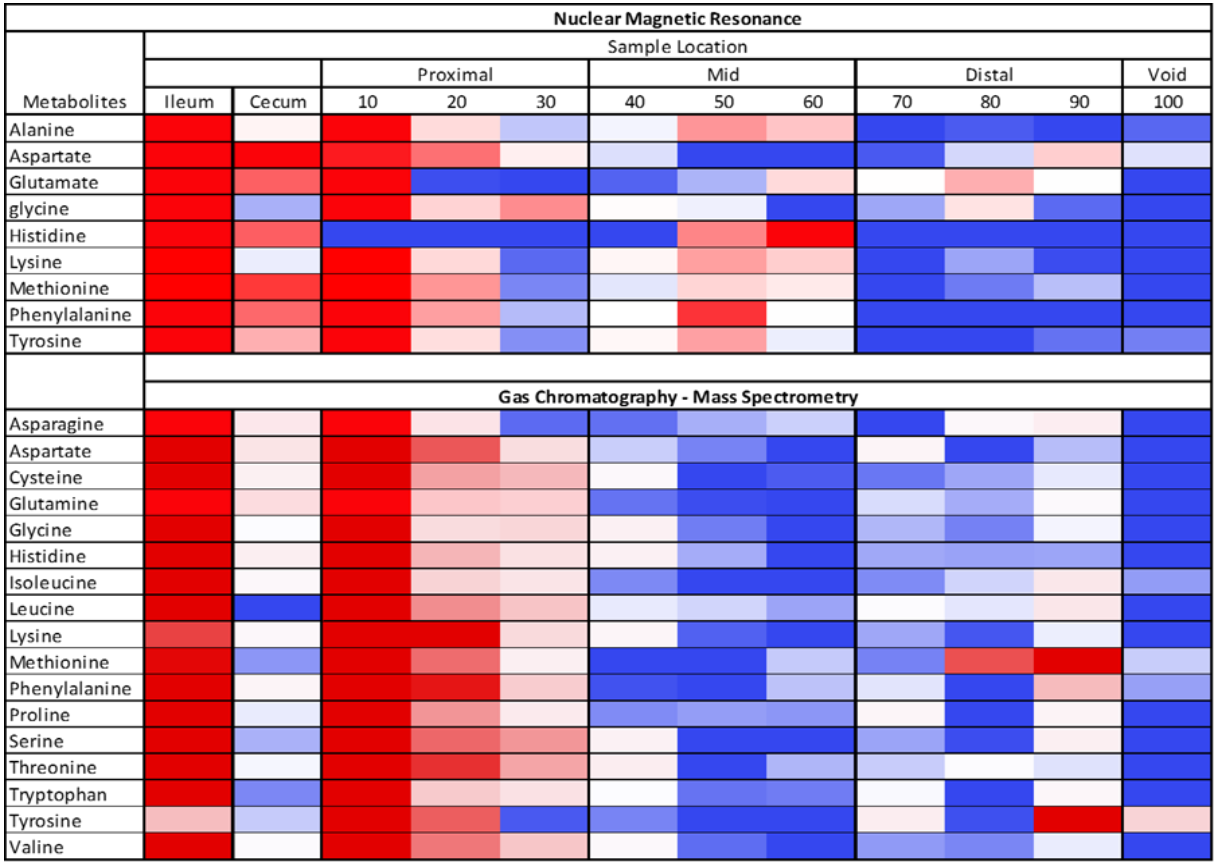

Figure 3.18. Heat map of amino acid concentrations along the length of the colon displayed in the form of averages for each segment, color coded to display change in averages for each metabolite as presented as percentiles.

3.3.6 Aromatic compounds

Several amino acids are metabolized in the colon to produce other important metabolites that can be transported across the epithelium, transformed by the epithelial cell, or further digested by the bacteria and processed as waste. Aromatic amino acids such as tyrosine, tryptophan and phenylalanine are metabolized into other aromatic compounds such as phenylacetic acid, hydrocaffeic acid, and hydrocinnamic acid (Figure 3.19). Due to the similar structure and consequently similar chemical shifts of aromatic compounds, it was difficult to confidently identify any of these compounds by NMR. The use of GC-MS for analysis of aromatic compounds was fruitful, and provided data for 14 compounds. Several compounds including apigenin, daidzein, ferulic acid, and vanillic acid are expected from the diet and have observable high concentrations in the ileum and proximal colon. They are likely digested by the bacteria in the proximal and mid colon resulting in a decrease in concentration. The remaining aromatic compounds are not very abundant in the ileum, and are thus assumed to be metabolic products of aromatic amino acids or other proteins and complex sugars that appear at high levels in the cecum and proximal colon. For example, 3-hydroxyphenylacetic acid is a product of tyrosine metabolism, and 4-hydroxyphenylacetate comes from the bacterial metabolism of tyrosine.[39, 40] Tyrosine, like the other amino acids is at high concentration in the ileum and first 10% of the proximal colon, but diminishes quickly by 20% and 30% of the colon length (Figure 3.19). This same location of 20% of the colon length is where the amount of 3-hydroxyphenylacetate increases, providing evidence of metabolism in this section of the colon.

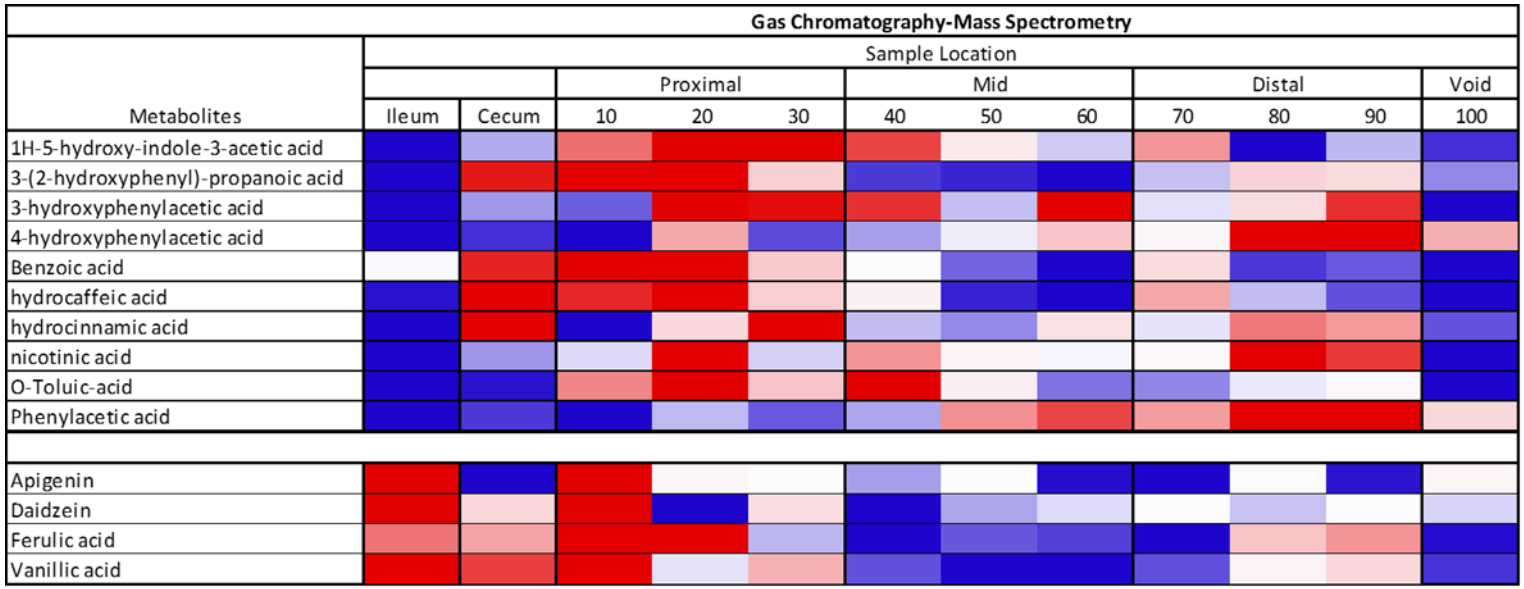

Figure 3.19. Heat map of aromatic compound concentrations along the length of the colon displayed in the form of averages for each segment, color coded to display change in averages for each metabolite as presented as percentiles.

However, it is not until the distal colon that 4-hydroxyphenylacetic acid exhibits a large an increase in abundance. This could be where the types of bacteria responsible for producing 4-hydroxyphenylacetic acid are primarily located. A closer look at the variance of these compounds is provided by Figure 3.20 in which the results are displayed as box plots. These metabolites do appear to be changing as observed, but standard deviations appear too large to say the changes are significant. Many factors relating to diet and movement of stool can create large deviations, making it difficult to observing significance.

As shown in Figure 3.19, four of the aromatic compounds that are not diet related increase in the cecum including 3-(2-hydroxyphenyl)-propanoic acid, benzoic acid, hydrocaffeic acid, and hydrocinnamic acid with both benzoic acid and hydrocinnamic acid being produced from phenylalanine metabolism.[41] The phenylpropionic acids, 3-(2-hyroxyphenyl)-propanoic acid, and hydrocaffeic acid are produce by the gut microflora from the metabolism of both phenylalanine and tyrosine.[42]

Metabolism of tryptophan is also responsible for the production of aromatic compounds like nicotinic acid, a vitamin also referred to as niacin.[43, 44] The ability for gut bacteria to convert tryptophan to nicotinic is quite remarkable, and is believed to contribute to maintaining intestinal homeostasis. [45] Tryptophan metabolism is also responsible for the appearance of 5-hydroxy-1H-indole-3-acetic acid which is a breakdown product of serotonin, however the presence of serotonin in samples was not detected. Upon closer examination between these metabolites,(Figure 3.21) we can determine that standard deviations within nicotinic acid an 5-hydroxy-1H-indole-3-acetic acid are too large to confidently relate them to the loss of tryptophan.

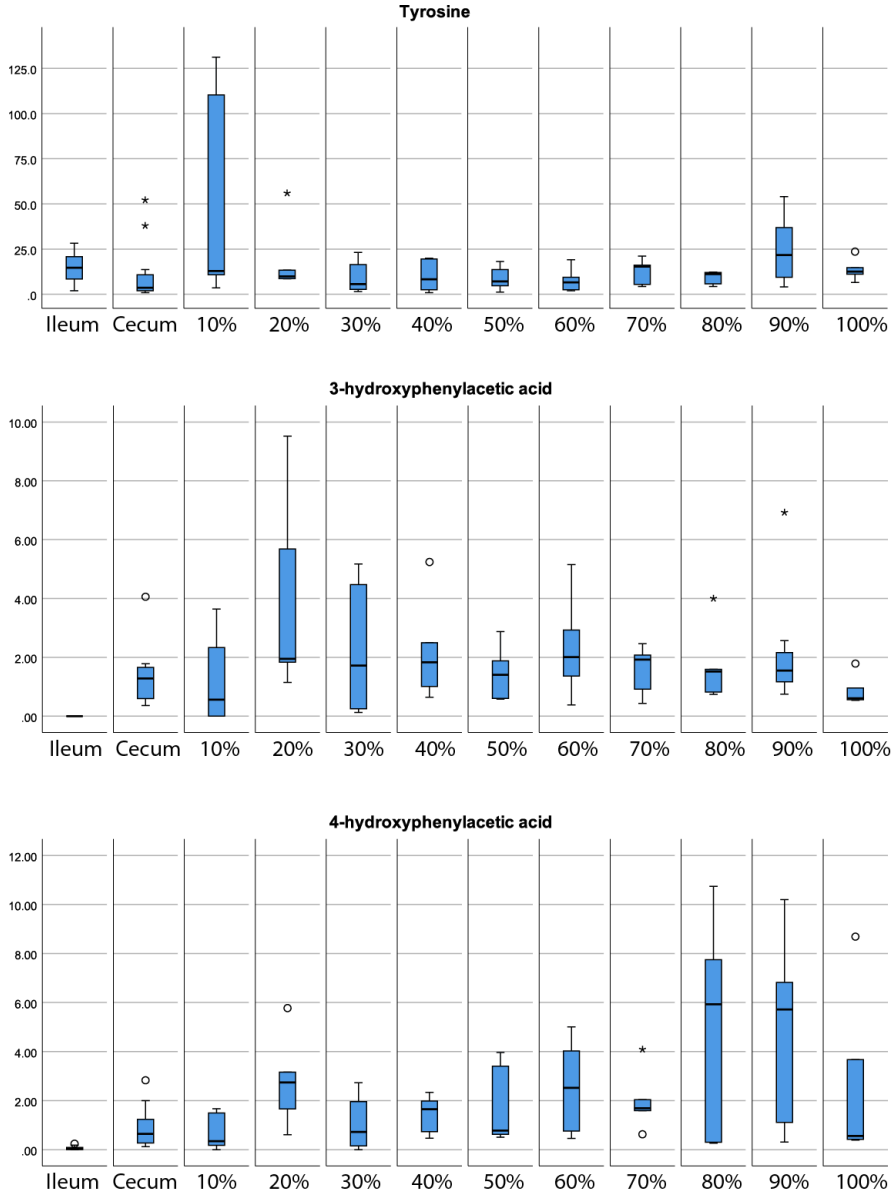

Figure 3.20. Box plots for tyrosine, 3-hydroxyphenylacetic acid, and 4-hydroxyphenylacetic acid values (ion intensity normalized to internal standard and mg dry stool) detected via GC-MS corresponding to locations of the colon including ileum, cecum, proximal (10-30%), mid (40-60%) and distal colon (70-100%).

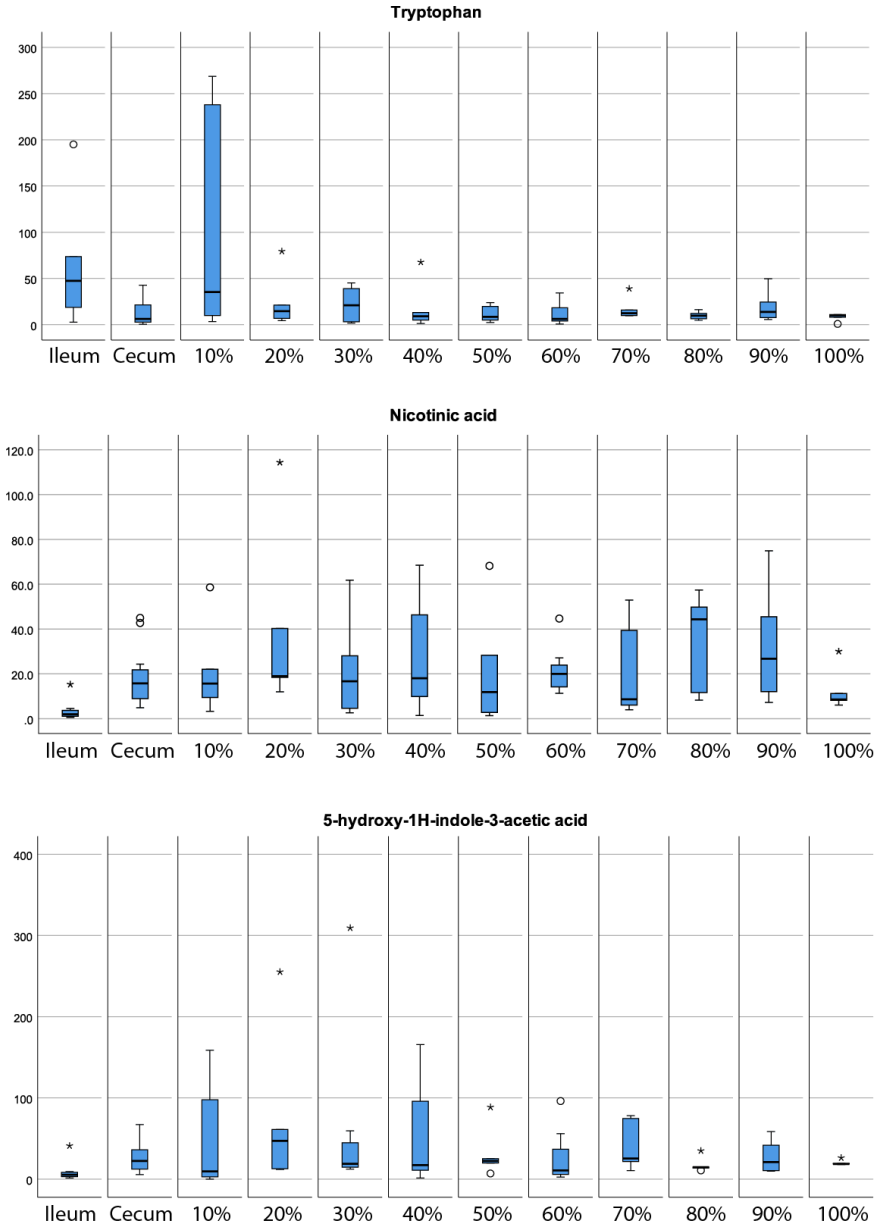

Figure 3.21. Box plots for tryptophan, nicotinic acid, and 5-hydroxy-1H-indole-3-acetic acid values (ion intensity normalized to internal standard and mg dry stool) detected via GC-MS, corresponding to locations of the colon including ileum, cecum, proximal (10-30%), mid (40-60%) and distal colon (70-100%).

3.3.7 Nitrogen containing metabolites

Multivariate analysis of the GC-MS data (Figure 3.22) shows similar separation to that of NMR even without the presence of SCFAs that were not detected with our GC-MS method and with a much larger number (86) of metabolites measured. The addition of these metabolites provides greater insights into the segmental stratification of the colon and the metabolic fate of these compounds. Examination of the OPLS-DA plot in Figure 3.22 indicates that the nitrogen containing compound uridine contributes greatly to the separation along PC2. Uridine is an interesting compound in the field of gut health, as a basic component of ribonucleic acid (RNA) and can found in a normal diet. Recent interest in uridine has grown due to its possible health benefits including the ability to improve memory,[46] anti-inflammatory benefits including the ability to ameliorate the effect of dextran sulfate induced colitis,[47] as well as its use as an antidote for 5-fluorouracil overdose/toxicity.[48, 49]

Uridine can be catabolized to form uracil, which may be happening in the colon as uridine is found at above average levels in the ileum and cecum, before decreasing in concentration in the proximal colon. Figure 3.23 suggests that as uridine concentration decreases, uracil increases. However, closer examination of the uridine and uracil boxplots (Figure 3.24) where standard deviations are included, it can be seen how the heatmap can be misleading. In this case, a handful of samples throughout the colon contain substantially higher amounts of uracil, skewing the average values plotted in the heatmap.

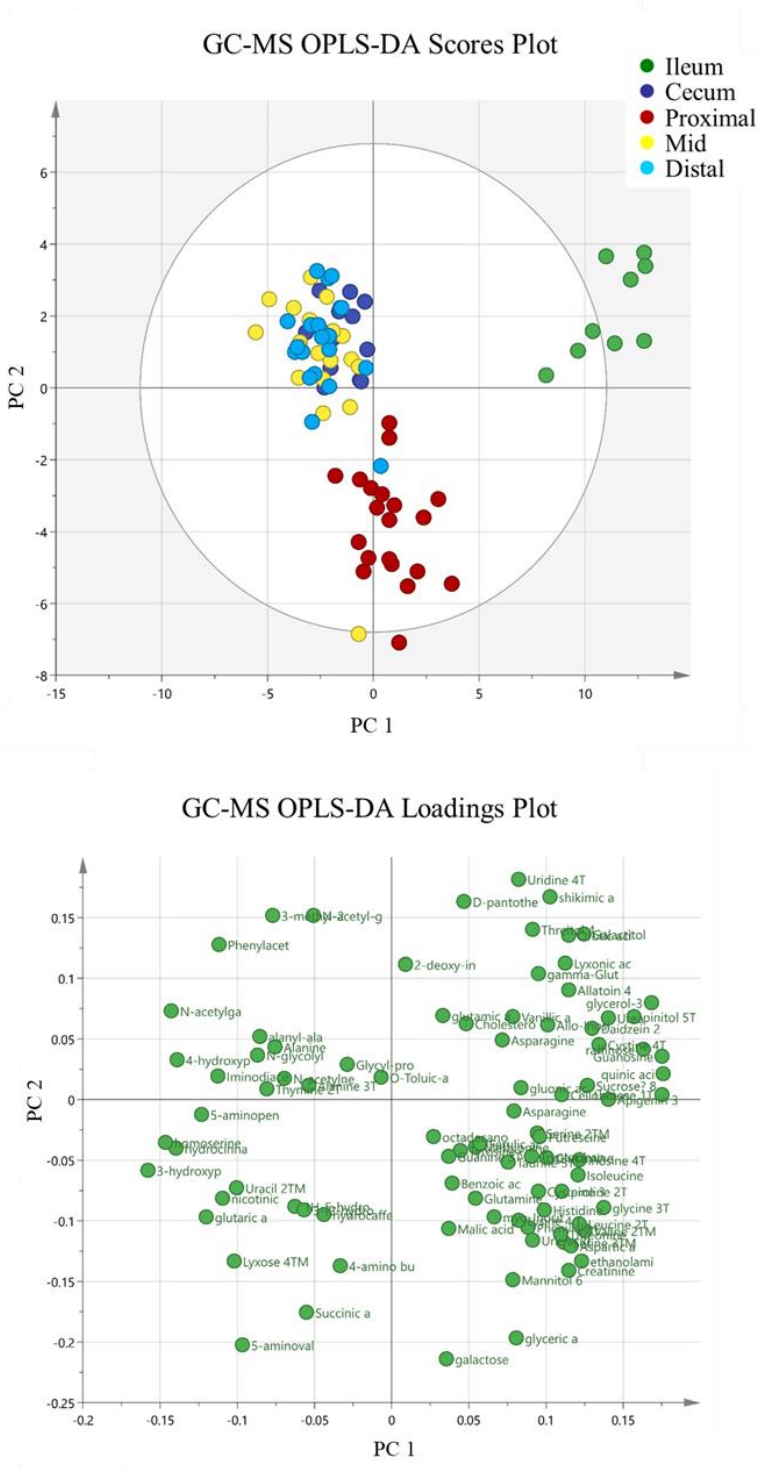

Figure 3.22. OPLS-DA score and loadings plot of data obtained from GC-MS analysis.

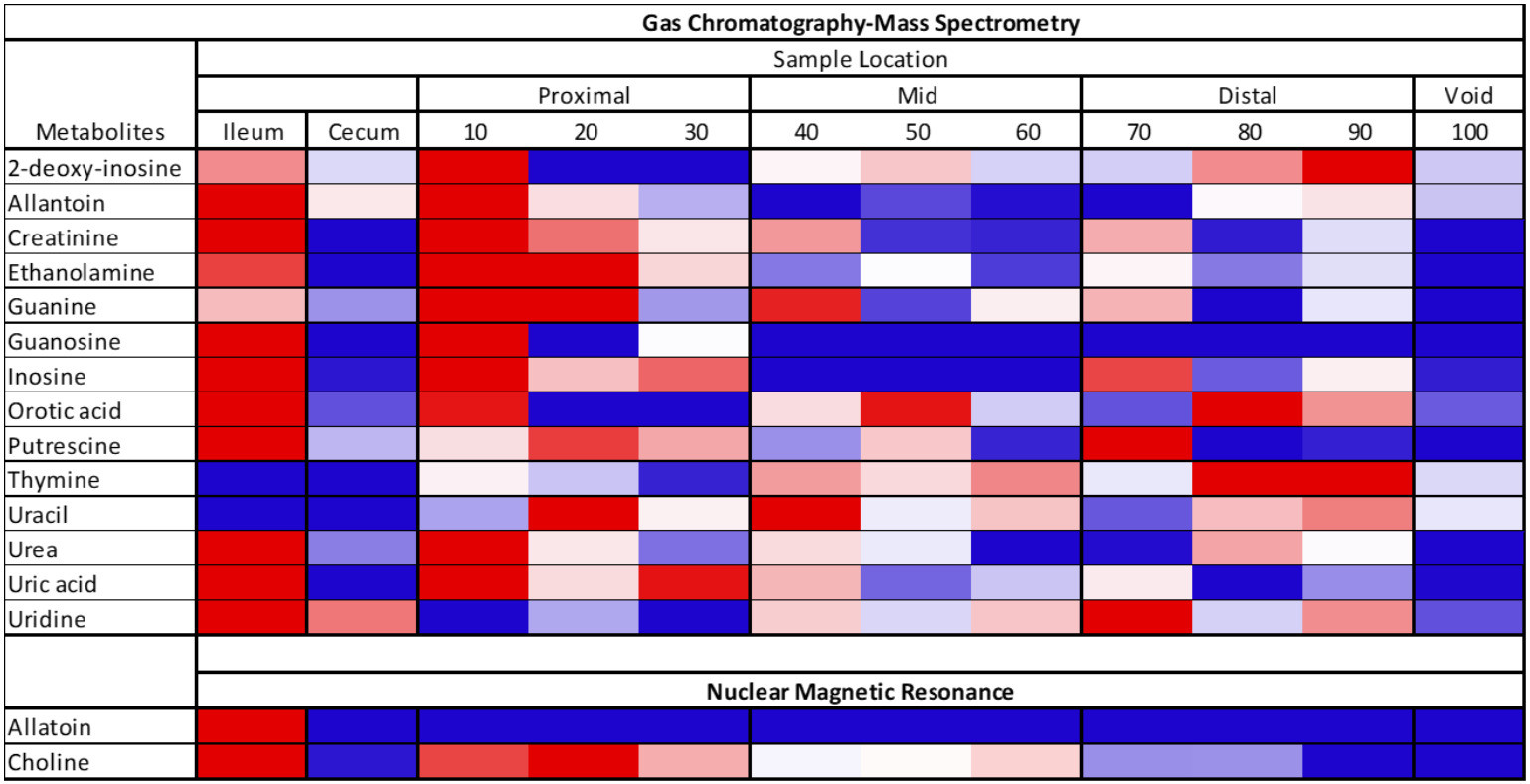

Figure 3.23. Heat map of Nitrogen containing compounds concentrations along the length of the colon displayed in the form of averages for each segment, color coded to display change in averages for each metabolite presented as percentiles.

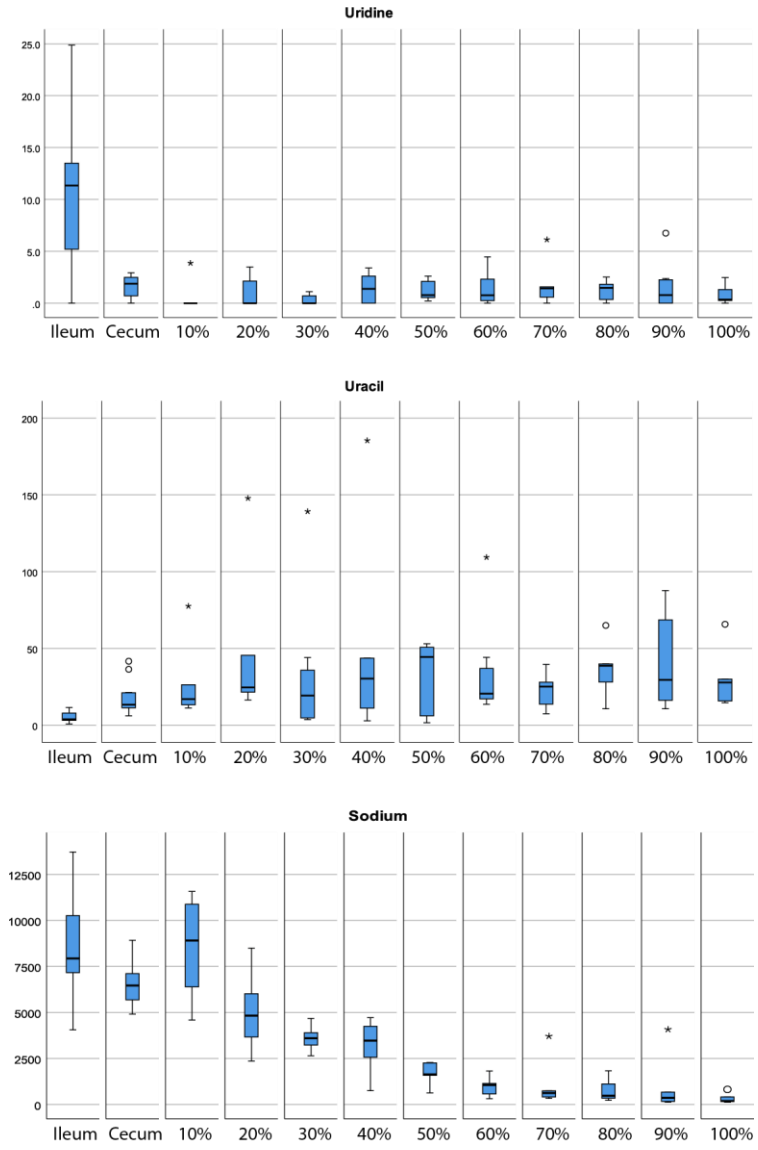

Figure 3.24. Box plots for uridine and uracil values (ion intensity normalized to internal standard and mg dry stool) detected via GC-MS, and sodium values (mM; normalized to mg dry stool) detected via IC corresponding to locations of the colon including ileum, cecum, proximal (10-30 %), mid (40-60%) and distal colon (70-100%).

When processing large batches of data, these outliers can be hard to identify. Interestingly, these observed outliers within the proximal and mid colon (10-60%) all pertain to the same rat.

Uridine and uracil may still be correlated, however, the evidence presented herein suggests that the uridine and uracil levels in the proximal mid and distal colon remain consistent, without any notable changes. The literature suggests uridine is involved in transport across the epithelial tissue. *Pizzorno et al.* discusses a Na^+-dependent transporter for nucleosides found in gut epithelial cells, and its importance for therapeutic opportunities.[50] If we compare the uridine concentration to sodium, uridine concentrations are depleted within the cecum, while sodium concentrations remain quite high in the cecum.

One challenge of comparing data across multiple analytical methods is the ability to compare relative concentrations. In the case of sodium dependent transport, it is probable that the slight decrease in concentration of sodium within the cecum is due to various cases of transport mediated by sodium, perhaps including that of uridine. Even in the ileum, uridine is still at relatively low concentrations, meaning that its transport with sodium, may not result in a statistically significant or detectable loss by these methods.

3.3.7.1 Nitrogen-carboxylic acids

Closer examination of Figure 3.22 suggests that other nitrogen containing compounds contribute to separation along PC2. These include both 5-aminovaleric acid and 4-aminobutyric acid, also referred to as GABA, which can be found within the bottom left quadrant. These compounds contain both nitrogen and carboxylic acid groups. This group of compounds are similar to amino acids and are likely products of amino acid metabolism by the gut bacteria. It is known that both 5-aminovaleric acid and 4-aminobutyric acid are produced endogenously from the catabolism of amino acids; 5-aminovaleric acid stems from the catabolism of lysine,[51] while 4-aminobutyric acid is synthesized from glutamate (glutamic acid).[52] The data provided in Figure 3.25 suggests that concentrations of both 5-aminovaleric acid and 4-aminobutyric acid are low in the ileum and cecum, and do not see an increase until the proximal colon, which is when amino acids concentrations started to decrease. If we compare these metabolites to both lysine and glutamate using the box plots in Figure 3.26, it appears that when lysine concentrations decrease at 20%, there is a subsequent increase in 5-aminovaleric acid concentration. It could be assumed that the observed trend is the catabolism of lysine to 5-aminovaleric acid. On the contrary, glutamic acid do not have a significant difference in concentrations that could be relatable. In this case, both metabolites are of very low abundance and could be exhibiting additional variance due to signal to noise.

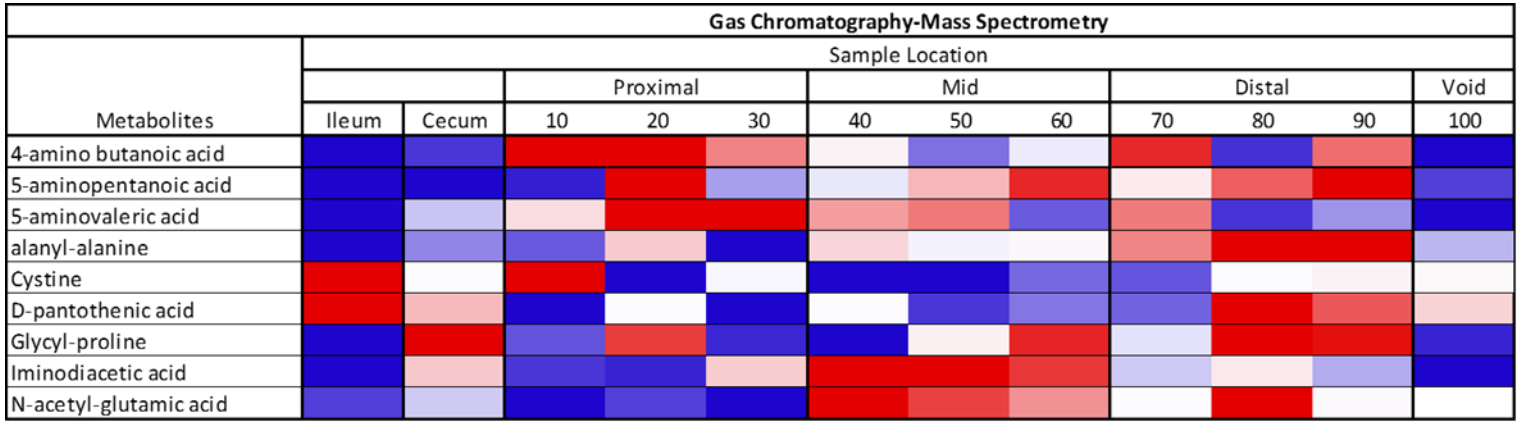

Figure 3.25. Heat map of nitrogen-carboxylic acids concentrations along the length of the colon displayed in the form of averages for each segment, color coded to display change in averages for each metabolite presented as percentiles.

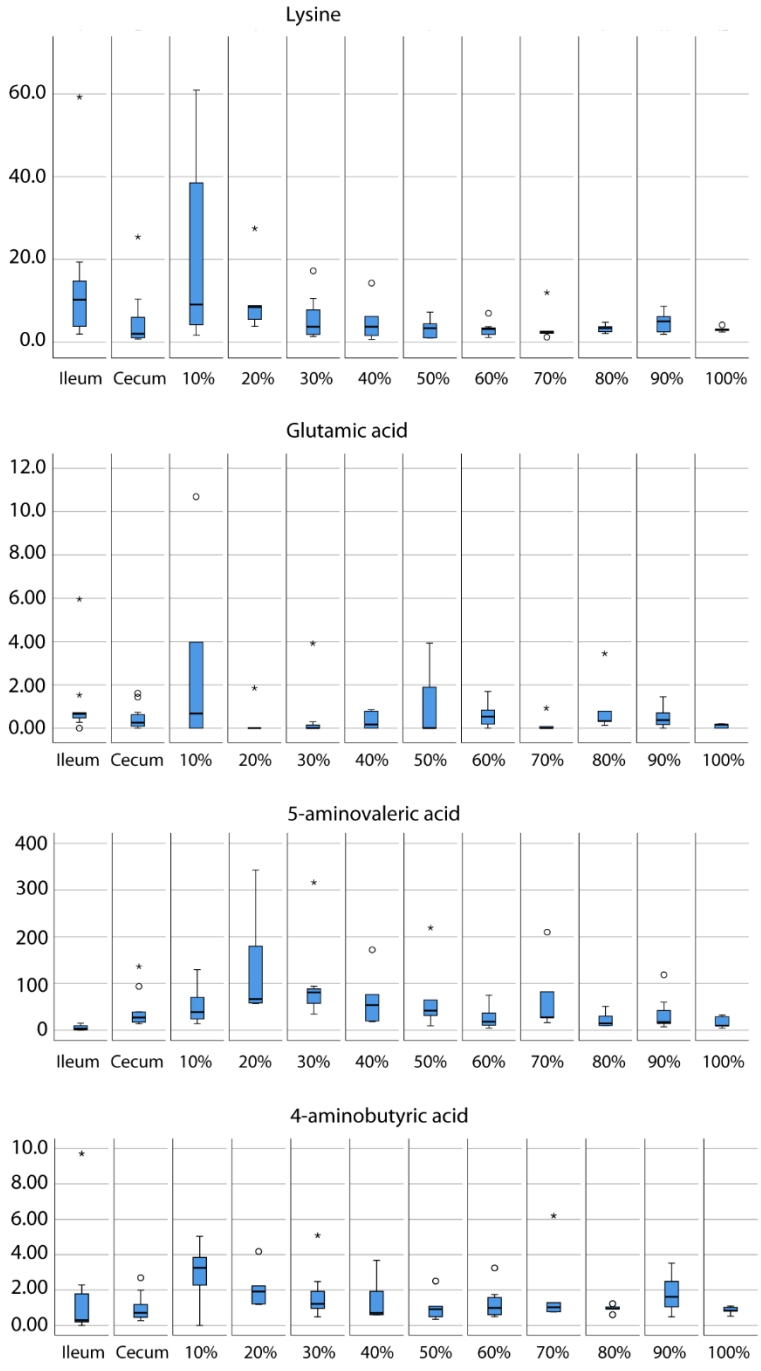

Figure 3.26. Box plots for lysine, glutamic acid, 5-aminovaleric acid, and 4-aminobutyric acid values (ion intensity normalized to internal standard and mg dry stool) detected via GC-MS corresponding to locations of the colon including ileum, cecum, proximal (10-30 %), mid (40-60%) and distal colon (70-100%).

Another interesting compound in this subclass is D-pantothenic acid, also known as vitamin B5. Pantothenic acid is an essential vitamin, but has been found to be synthesized by the gut bacteria.[53] Examination of Figure 3.25 indicates that pantothenic acid is one of the only metabolites in this list that begins at an above average concentration in the ileum and cecum before decreasing in the proximal and mid colons. This decrease may be explained by the presence of sodium dependent active transport. Much like uridine, pantothenic acid transporters have been identified in the colon,[54] allowing for final uptake of this essential vitamin before stool is excreted as waste. In the distal colon, it appears that concentrations increase with levels above average found even in voided stool. Because gut bacteria synthesize vitamin B5, we can imagine that buildup of pantothenic acid would occur once the stool reaches and area void of transporters. This buildup could also be observed even in the presence of transporters due to the packing of the stool in the distal colon. By this point, the stool has lost a substantial amount of water, and transport of pantothenic acid within the solid mass might be impossible.

The other metabolites in this class of compounds do not appear to contribute greatly to separation observed in the multivariate analysis (Figure 3.22). Metabolites that appear to have lowest concentrations within the ileum and cecum followed by observed increase in the remaining sections are most likely metabolites produced by bacteria or the intestinal mucosa. For example, N-acetyl-glutamic acid is a known metabolite produced from glutamate by the intestinal mucosa.[55] Often these metabolites appear to both increase and decrease along the length of the colon, which may be attributed to their constant production and breakdown by the various bacteria making up the gut microbiome.

3.3.8 Carboxylic acids

As observed with the distinct class of SCFAs, carboxylic acids play a crucial role in the overall function of the colon. An additional group of carboxylic acids include linear or branched metabolites that contain a single carboxylic acid group, cyclic carboxylic acids, and the dicarboxylic acids (Figure 3.27).

Gluonic acid is a linear carboxylic acid, found at relatively low concentrations in the colon, but is a known food additive that acts as an acidity regulator. It can also be found naturally in fruit and honey, so it can be assumed that the above average levels exhibited in the ileum, cecum, and proximal colon are due to dietary intake. Gluonic acid is poorly absorbed in the small intestine at only about 20%.[56] The gluonic acid that survives can be utilized by the gut bacteria to produce butyrate.[57]

Cyclic compounds, quinic acid and shikimic acid are both plant metabolites that are come from the diet, and both arrive at above average values in the ileum. Once in the proximal colon, levels decrease. It could be assumed that, like many of the other cyclic sugar compounds, these are metabolized by the bacteria to form other compounds such as SCFAs for transport across the epithelium.

Malate and succinate are both dicarboxylic acids known for their role in the Krebs cycle. These 2 metabolites appear to have opposing trends in Figure 3.27 with malate at high abundance in the ileum and decreasing in the cecum, while succinate has low abundance in the ileum and increases in the cecum. A more detailed picture of the variation of the levels of these compounds can be gleaned from Figure 3.28.

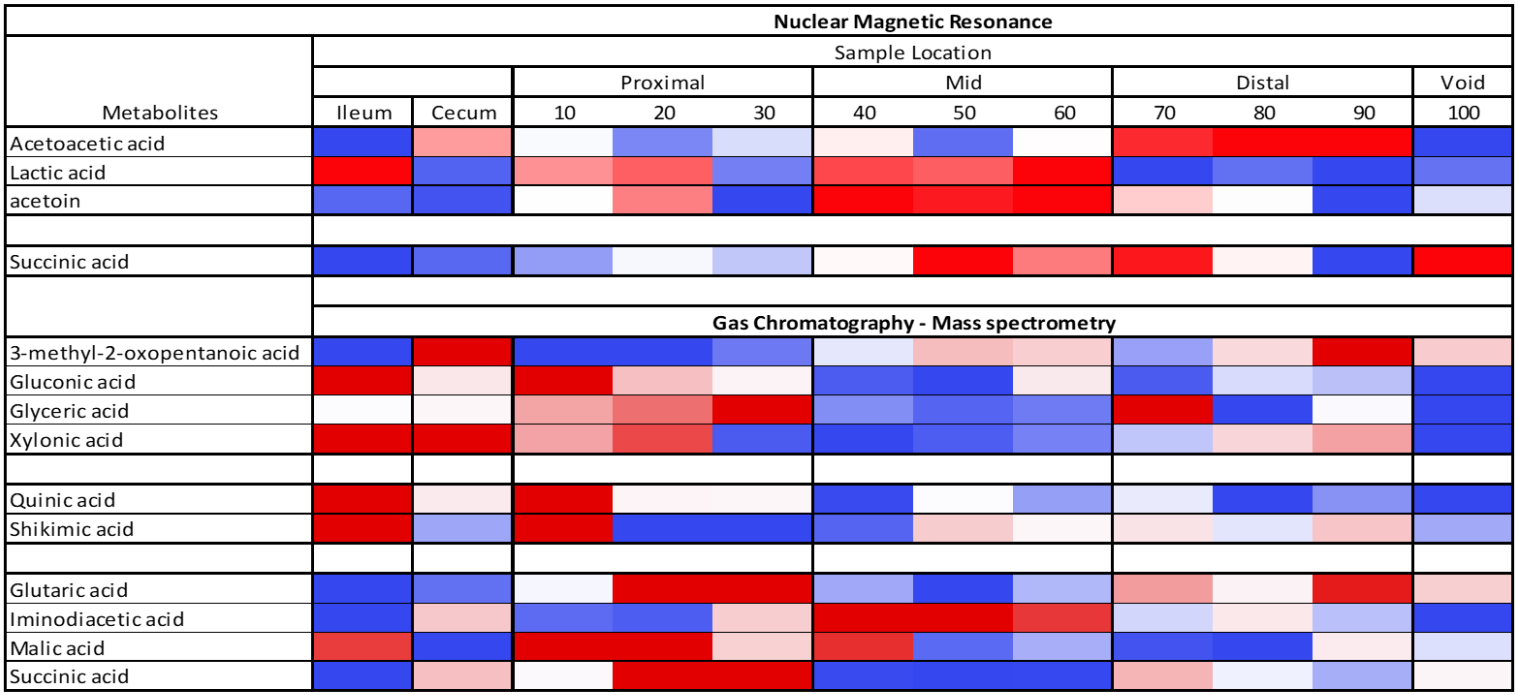

Figure 3.27. Heat map of carboxylic acid concentrations along the length of the colon displayed in the form of averages for each segment, color coded to display change in averages for each metabolite as presented as percentiles.

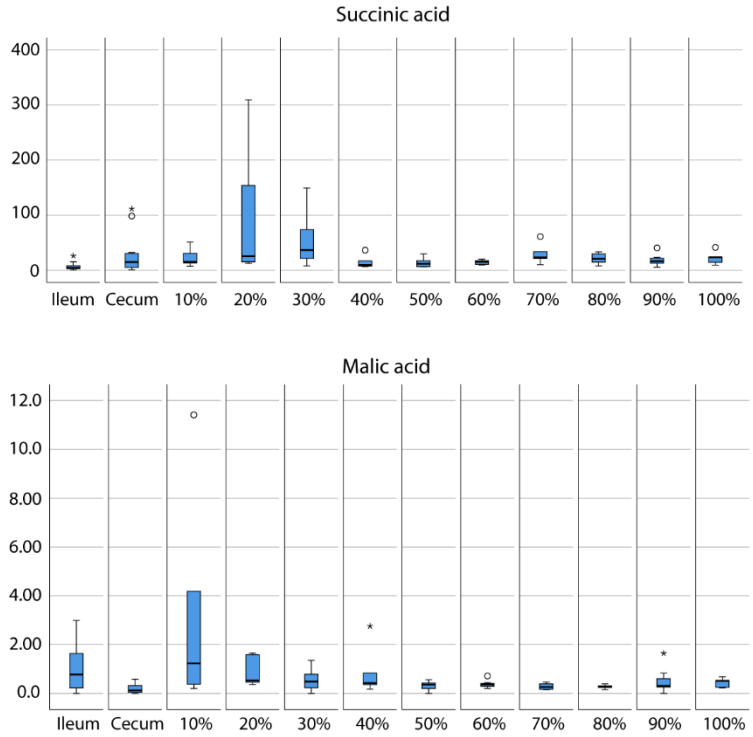

Figure 3.28. Box plots for succinic acid and malic acid values (ion intensity normalized to internal standard and mg dry stool) detected via GC-MS corresponding to locations of the colon including ileum, cecum, proximal (10-30 %), mid (40-60%) and distal colon (70-100%).

Succinic acid and malic acid appear to be correlated in figure 3.28, but in this case is better observed in the proximal colon rather than the ileum and cecum. In the first 10% levels of malic acid are relatively high and decrease in the 20% range, which is where an increase in succinic acid occurs. Shortly after, at 40% the concentrations of both have neared 0.

Other carboxylic acids observed by NMR include acetoin and aceotacetate. Acetoin is produced by bacteria from pyruvate during the process of formation of carbon dioxide (CO_2), and its formation is believed to help regulate pH due to the loss of SCFAs.[58, 59] Acetoin appears to increase in concentration in the mid colon (Figure 3.27), before perhaps being converted to CO_2 in the distal colon.

Acetoacetate's concentration differs from acetoin with concentrations reaching their peak in the distal colon. Acetoacetate is a ketone body that colonocytes can utilize and produce them from acetyl-CoA or SCFAs. It was reported that colonic epithelial cells utilize respiratory fuels in the preferred order of butyrate > acetoacetate > glucose, with acetoacetate being a more favored carbon source than glucose.[60] It could be hypothesized that we observe a higher concentration of acetoacetate in the distal colon because here levels of butyrate are quite low and the colonocyte may choose to convert acetyl-CoA to acetoacetate. Alternatively, acetoacetate may be produced at a similar rate throughout the colon, but when it reaches the distal colon transport may become more difficult as a result of the much lower water content producing a buildup of this metabolite.

3.3.9 Miscellaneous metabolites

During analysis, several metabolites were measured that did not fit into the classes chosen for discussion in this chapter, with the results obtained summarized in the heat map shown in Figure 3.29. These metabolites are low in abundance and do not contribute significantly to sample segregation in the multivariate analysis. Nevertheless, their presence should be discussed. ^{1}H-NMR was able to detect both ethanol and methanol in stool extracts with the highest average concentrations being detected in the ileum, cecum, and proximal colon followed by a decrease in concentration throughout the mid and distal colon. This trend may be explained by the formation of both ethanol and methanol during digestion, and its rapid absorption into the bloodstream to be cleaned by the liver and excreted in urine. It is interesting to note that low levels of ethanol and methanol are naturally found in the gastrointestinal tract, but high levels of alcohol mainly from consumption can permeate the epithelium producing damage known as "Leaky Gut Syndrome".[61-63]

Another well-known metabolite, taurine, is found at above average concentrations in the ileum, cecum, and proximal colon. Taurine is a major constituent of bile that aids in the digestion of lipids in the small intestine. This explains the presence of taurine in the beginning of the colon. Like many other metabolites, taurine is metabolized by the gut bacteria.[64, 65] Not all metabolites provide clear trends along the length of the colon that can be easily explained. This is true of two similar compounds detected, N-acetylneuraminic acid, and N-glycolyneuraminic acid.

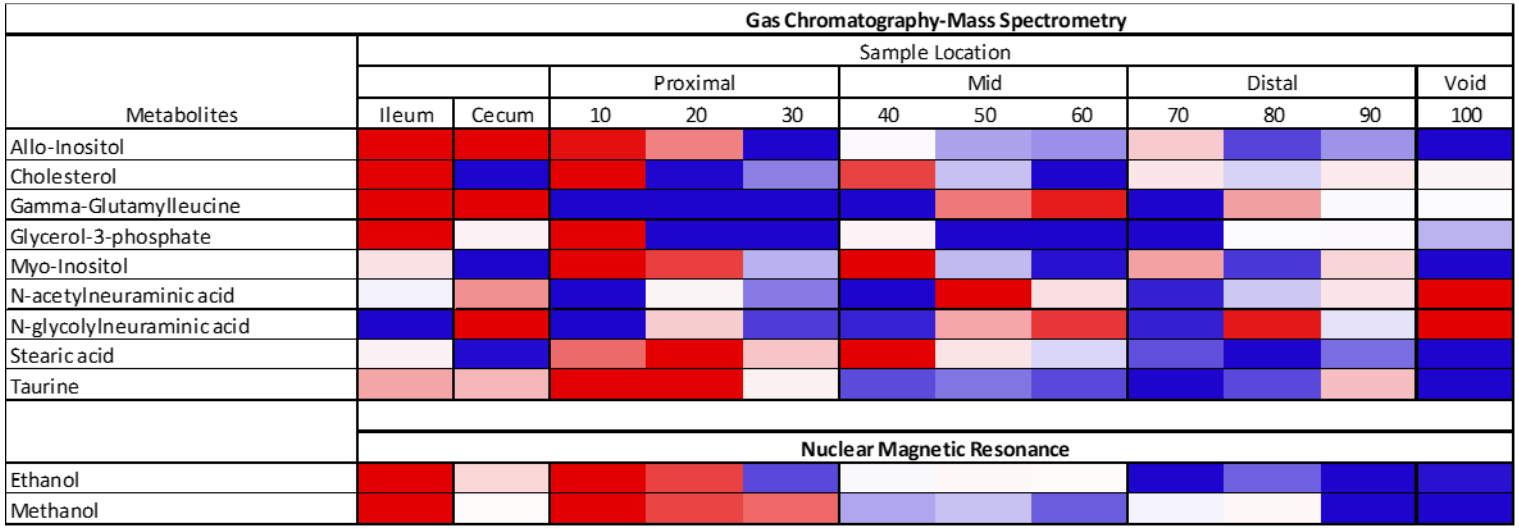

Figure 3.29. Heat map of miscellaneous compound concentrations along the length of the colon displayed in the form of averages for each segment, color coded to display change in averages for each metabolite as presented as percentiles.

These metabolites are found on mucins and glycoproteins at the cell membrane in the mucous that lines the eipithelial tissue of the colon. This mucous is important in intestinal motility, and acts as a barrier against cellular damage due to the toxic waste produced within the colon.[66] Both of these metabolites can serve as bacterial nutrients, providing both carbon and nitrogen sources.[67] Only N-acetylneuraminic acid exists in humans, with N-glycolylneuraminic only found in non-human mammals. These compounds do not appear to follow a clear trend, (Figure 3.29) with concentrations seeming sporadic. Their presence in the stool extracts is most likely due to the presence of mucous in stool.

3.4 Conclusions

In this study, the use of IC, NMR, and GC-MS provided information pertaining to the metabolic profiles of over 100 metabolites found in the luminal metabolome of the rat. Each instrumental method produces complementary data providing results for a different set of metabolites. Figure 3.30 depicts the coverage of metabolites between methods, with minimal overlap observed. IC provided data on 7 inorganic ions that could not be detected in the other methods, and only 2 organic acids could be measured in both IC and NMR. NMR provided results for small molecules such as alcohols, and SCFAs that were not detectable with the other methods.

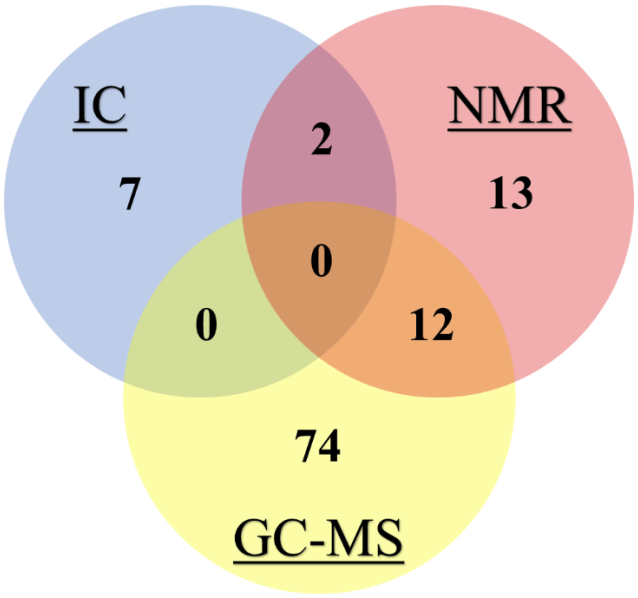

Figure 3.30. Venn diagram of metabolite coverage across IC, NMR, and GC-MS. IC analysis included 9 metabolites with 7 exclusively IC, and 3 shared with NMR. NMR also shared 12 metabolites with GC-MS, but detected 13 metabolites exclusively for a total of 27. GC-MS provided the largest dataset with 73 metabolites analyzed exclusively.

Overlaps in coverage by NMR and GC-MS due to their ability to detect amino acids, and various nitrogen or carboxylic containing metabolites increases confidence in the trends observed. Using GC-MS, we were able to measure an additional 74 metabolites not determined by IC or NMR, greatly increasing the coverage of the luminal metabolome.

The metabolite profiles detected along the length of the colon provide evidence for the existence of segmental stratification, highlighting the fact that the complex processes of digestion alter the luminal metabolome significantly from beginning to end. The evidence provided in this chapter suggests that microbial metabolites have a major influence on host physiology, fueling the need for identification of the metabolites involved in epithelial transport.[32] The experiments performed in this study identified over 100 metabolites afforded access to epithelial transport including inorganic ions, SCFAs, amino acids, sugars, and nitrogen containing and aromatic compounds. Quantitative data was obtained, profiling the fate of these metabolites along the length of the colon. These results not only indicate where the metabolites are digested, but also identifies many metabolites generated by the gut microbiome which can be a key to assessing gut health.

Unfortunately, from the data obtained we can only hypothesized which metabolites are transported across the epithelium based on the metabolic profiles obtained, but we have determined which metabolites are afforded access to the epithelium in different segments of the colon laying the groundwork for future experiments. Chapter 4 discusses experimental methods and collected data that is a continuation of this work in the study of active transport across the epithelium of the rat cecum.

3.5 References

1. Brown, D. G.; Rao, S.; Weir, T. L.; O'Malia, J.; Bazan, M.; Brown, R. J.; Ryan, E. P., Metabolomics and metabolic pathway networks from human colorectal cancers, adjacent mucosa, and stool. *Cancer & Metabolism* **2016,** *4*.

2. Zhao, Y.; Wu, J.; Li, J. V.; Zhou, N.-Y.; Tang, H.; Wang, Y., Gut Microbiota Composition Modifies Fecal Metabolic Profiles in Mice. *Journal of Proteome Research* **2013,** *12* (6), 2987-2999.

3. Lamichhane, S.; Yde, C. C.; Schmedes, M. S.; Jensen, H. M.; Meier, S.; Bertram, H. C., Strategy for Nuclear-Magnetic-Resonance-Based Metabolomics of Human Feces. *Analytical Chemistry* **2015,** *87* (12), 5930-5937.

4. Koh, A.; De Vadder, F.; Kovatcheva-Datchary, P.; Backhed, F., From Dietary Fiber to Host Physiology: Short-Chain Fatty Acids as Key Bacterial Metabolites. *Cell* **2016,** *165* (6), 1332-1345.

5. Guinane, C. M.; Cotter, P. D., Role of the gut microbiota in health and chronic gastrointestinal disease: understanding a hidden metabolic organ. In *Therap Adv Gastroenterol*, 2013; Vol. 6, pp 295-308.

6. Jacobs, D. M.; Deltimple, N.; van Velzen, E.; van Dorsten, F. A.; Bingham, M.; Vaughan, E. E.; van Duynhoven, J., H-1 NMR metabolite profiling of feces as a tool to assess the impact of nutrition on the human microbiome. *Nmr in Biomedicine* **2008,** *21* (6), 615-626.

7. Sjögren, Y. M.; Department of Immunology, T. W. G. I., Stockholm University, Stockholm, Sweden,; Jenmalm, M. C.; Division of Paediatrics, T. D. o. C. a. E. M., Faculty of Health Sciences, Linköping University, Linköping, Sweden and; Böttcher, M. F.; Division of Paediatrics, T. D. o. C. a. E. M., Faculty of Health Sciences, Linköping University, Linköping, Sweden and; Björkstén, B.; Institute of Environmental Medicine, K. I., Stockholm, Sweden; Sverremark-Ekström, E.; Department of Immunology, T. W. G. I., Stockholm University, Stockholm, Sweden,, Altered early infant gut microbiota in children developing allergy up to 5 years of age. *Clinical & Experimental Allergy* **2016,** *39* (4), 518-526.

8. de Theije, C. G.; Wopereis, H.; Ramadan, M.; van Eijndthoven, T.; Lambert, J.; Knol, J.; Garssen, J.; Kraneveld, A. D.; Oozeer, R., Altered gut microbiota and activity in a murine model of autism spectrum disorders. *Brain Behav Immun* **2014,** *37*, 197-206.

9. Cryan, J. F.; Dinan, T. G., Mind-altering microorganisms: the impact of the gut microbiota on brain and behaviour. *Nature Reviews Neuroscience* **2012,** *13* (10), 701-712.

10. Yu, Y.-N.; Fang, J.-Y., Gut Microbiota and Colorectal Cancer. *Gastrointestinal Tumors* **2016,** *2* (1), 26-32.

11. Yamamoto, M.; Matsumoto, S., Gut microbiota and colorectal cancer. *Genes and environment : the official journal of the Japanese Environmental Mutagen Society* **2016,** *38*, 11-11.

12. Jansson, J.; Willing, B.; Lucio, M.; Fekete, A.; Dicksved, J.; Halfvarson, J.; Tysk, C.; Schmitt-Kopplin, P., Metabolomics Reveals Metabolic Biomarkers of Crohn's Disease. *Plos One* **2009,** *4* (7), 10.

13. Le Gall, G.; Noor, S. O.; Ridgway, K.; Scovell, L.; Jamieson, C.; Johnson, I. T.; Colquhoun, I. J.; Kemsley, E. K.; Narbad, A., Metabolomics of Fecal Extracts Detects Altered Metabolic Activity of Gut Microbiota in Ulcerative Colitis and Irritable Bowel Syndrome. *Journal of Proteome Research* **2011,** *10* (9), 4208-4218.

14. Qin, J.; Li, Y.; Cai, Z.; Li, S.; Zhu, J.; Zhang, F.; Liang, S.; Zhang, W.; Guan, Y.; Shen, D.; Peng, Y.; Zhang, D.; Jie, Z.; Wu, W.; Qin, Y.; Xue, W.; Li, J.; Han, L.; Lu, D.; Wu, P.; Dai, Y.; Sun, X.; Li, Z.; Tang, A.; Zhong, S.; Li, X.; Chen, W.; Xu, R.; Wang, M.; Feng, Q.; Gong, M.; Yu, J.; Zhang, Y.; Zhang, M.; Hansen, T.; Sanchez, G.; Raes, J.; Falony, G.; Okuda, S.; Almeida, M.; LeChatelier, E.; Renault, P.; Pons, N.; Batto, J.-M.; Zhang, Z.; Chen, H.; Yang, R.; Zheng, W.; Li, S.; Yang, H.; Wang, J.; Ehrlich, S. D.; Nielsen, R.; Pedersen, O.; Kristiansen, K.; Wang, J., A metagenome-wide association study of gut microbiota in type 2 diabetes. *Nature* **2012,** *490*, 55-60.

15. Musso, G.; Gambino, R.; Cassader, M., Interactions Between Gut Microbiota and Host Metabolism Predisposing to Obesity and Diabetes. *http://dx.doi.org/10.1146/annurev-med-012510-175505* **2011**.

16. Backhed, F.; Ding, H.; Wang, T.; Hooper, L. V.; Koh, G. Y.; Nagy, A.; Semenkovich, C. F.; Gordon, J. I., The gut microbiota as an environmental factor that regulates fat storage. *Proc Natl Acad Sci U S A* **2004,** *101* (44), 15718-23.

17. Frizzell, R. A.; Hanrahan, J. W., Physiology of Epithelial Chloride and Fluid Secretion. *Cold Spring Harbor Perspectives in Medicine* **2012,** *2* (6).

18. Vernay, M., COLONIC ABSORPTION OF INORGANIC-IONS AND VOLATILE FATTY-ACIDS IN THE RABBIT. *Comparative Biochemistry and Physiology a-Physiology* **1986,** *83* (4), 775-784.

19. Rechkemmer, G., REGULATION OF ELECTROLYTE ABSORPTION AND SECRETION IN THE LARGE-INTESTINE. *Journal of Animal Physiology and Animal Nutrition-Zeitschrift Fur Tierphysiologie Tierernahrung Und Futtermittelkunde* **1991**, 101-110.

20. Trygg, J.; Wold, S., Orthogonal projections to latent structures (O-PLS). *Journal of Chemometrics* **2002,** *16* (3), 119-128.

21. Talbot, C.; Lytle, C., Segregation of Na/H exchanger-3 and Cl/HCO3 exchanger SLC26A3 (DRA) in rodent cecum and colon. **2010**.

22. den Besten, G.; van Eunen, K.; Groen, A. K.; Venema, K.; Reijngoud, D. J.; Bakker, B. M., The role of short-chain fatty acids in the interplay between diet, gut microbiota, and host energy metabolism. In *J Lipid Res*, 2013; Vol. 54, pp 2325-40.

23. Donohoe, D. R.; Garge, N.; Zhang, X. X.; Sun, W.; O'Connell, T. M.; Bunger, M. K.; Bultman, S. J., The Microbiome and Butyrate Regulate Energy Metabolism and Autophagy in the Mammalian Colon. *Cell Metabolism* **2011,** *13* (5), 517-526.

24. Canfora, E. E.; Jocken, J. W.; Blaak, E. E., Short-chain fatty acids in control of body weight and insulin sensitivity. *Nature Reviews Endocrinology* **2015,** *11* (10), 577-591.

25. Bloemen, J. G.; Venema, K.; de Poll, M. C. V.; Damink, S. W. O.; Buurman, W. A.; Dejong, C. H., Short chain fatty acids exchange across the gut and liver in humans measured at surgery. *Clinical Nutrition* **2009,** *28* (6), 657-661.

26. Topping, D. L.; Clifton, P. M., Short-chain fatty acids and human colonic function: Roles of resistant starch and nonstarch polysaccharides. *Physiological Reviews* **2001,** *81* (3), 1031-1064.

27. Ruppin, H.; Barmeir, S.; Soergel, K. H.; Wood, C. M.; Schmitt, M. G., ABSORPTION OF SHORT-CHAIN FATTY-ACIDS BY THE COLON. *Gastroenterology* **1980,** *78* (6), 1500-1507.

28. Mo, H. P.; Harwood, J. S.; Raftery, D., Receiver gain function: the actual NMR receiver gain. *Magnetic Resonance in Chemistry* **2010,** *48* (3), 235-238.

29. Wishart, D. S.; Jewison, T.; Guo, A. C.; Wilson, M.; Knox, C.; Liu, Y.; Djoumbou, Y.; Mandal, R.; Aziat, F.; Dong, E.; Bouatra, S.; Sinelnikov, I.; Arndt, D.; Xia, J.; Liu, P.; Yallou, F.; Bjorndahl, T.; Perez-Pineiro, R.; Eisner, R.; Allen, F.; Neveu, V.; Greiner, R.; Scalbert, A., HMDB 3.0--The Human Metabolome Database in 2013. *Nucleic Acids Res* **2013,** *41* (Database issue), D801-7.

30. Wishart, D. S.; Tzur, D.; Knox, C.; Eisner, R.; Guo, A. C.; Young, N.; Cheng, D.; Jewell, K.; Arndt, D.; Sawhney, S.; Fung, C.; Nikolai, L.; Lewis, M.; Coutouly, M. A.; Forsythe, I.; Tang, P.; Shrivastava, S.; Jeroncic, K.; Stothard, P.; Amegbey, G.; Block, D.; Hau, D. D.; Wagner, J.; Miniaci, J.; Clements, M.; Gebremedhin, M.; Guo, N.; Zhang, Y.; Duggan, G. E.; Macinnis, G. D.; Weljie, A. M.; Dowlatabadi, R.; Bamforth, F.; Clive, D.; Greiner, R.; Li, L.; Marrie, T.; Sykes, B. D.; Vogel, H. J.; Querengesser, L., HMDB: the Human Metabolome Database. *Nucleic Acids Res* **2007,** *35* (Database issue), D521-6.

31. Farup, P. G.; Rudi, K.; Hestad, K., Faecal short-chain fatty acids - a diagnostic biomarker for irritable bowel syndrome? *Bmc Gastroenterology* **2016,** *16*.

32. Rios-Covian, D.; Ruas-Madiedo, P.; Margolles, A.; Gueimonde, M.; de los Reyes-Gavilan, C. G.; Salazar, N., Intestinal Short Chain Fatty Acids and their Link with Diet and Human Health. *Frontiers in Microbiology* **2016,** *7*.

33. Hoverstad, T.; Fausa, O.; Bjorneklett, A.; Bohmer, T., SHORT-CHAIN FATTY-ACIDS IN THE NORMAL HUMAN FECES. *Scandinavian Journal of Gastroenterology* **1984,** *19* (3), 375-381.

34. Miyamoto, J.; Kasubuchi, M.; Nakajima, A.; Irie, J.; Itoh, H.; Kimura, I., The role of short-chain fatty acid on blood pressure regulation. *Current Opinion in Nephrology and Hypertension* **2016,** *25* (5), 379-383.

35. Pomare, E. W.; Branch, W. J.; Cummings, J. H., CARBOHYDRATE FERMENTATION IN THE HUMAN-COLON AND ITS RELATION TO ACETATE CONCENTRATIONS IN VENOUS-BLOOD. *Journal of Clinical Investigation* **1985,** *75* (5), 1448-1454.

36. Byrne, C. S.; Chambers, E. S.; Morrison, D. J.; Frost, G., The role of short chain fatty acids in appetite regulation and energy homeostasis. *International Journal of Obesity* **2015,** *39* (9), 1331-1338.

37. Cummings, J. H.; Pomare, E. W.; Branch, W. J.; Naylor, C. P.; Macfarlane, G. T., Short chain fatty acids in human large intestine, portal, hepatic and venous blood. *Gut* **1987,** *28* (10), 1221-7.

38. Tedelind, S.; Westberg, F.; Kjerrulf, M.; Vidal, A., Anti-inflammatory properties of the short-chain fatty acids acetate and propionate: A study with relevance to inflammatory bowel disease. *World Journal of Gastroenterology* **2007,** *13* (20), 2826-2832.

39. Hareland, W. A.; Crawford, R. L.; Chapman, P. J.; Dagley, S., METABOLIC FUNCTION AND PROPERTIES OF 4-HYDROXYPHENYLACETIC ACID 1-HYDROXYLASE FROM PSEUDOMONAS-ACIDOVORANS. *Journal of Bacteriology* **1975,** *121* (1), 272-285.

40. Curtius, H. C.; Mettler, M., Study of the intestinal tyrosine metabolism using stable isotopes and gas chromatography-mass spectrometry. Journal of Chromatography A: 1976; Vol. 126, pp 569-580.

41. Smith, E. A.; Macfarlane, G. T., Enumeration of human colonic bacteria producing phenolic and indolic compounds: Effects of pH, carbohydrate availability and retention time on dissimilatory aromatic amino acid metabolism. *Journal of Applied Bacteriology* **1996,** *81* (3), 288-302.

42. Wikoff, W. R.; Anfora, A. T.; Liu, J.; Schultz, P. G.; Lesley, S. A.; Peters, E. C.; Siuzdak, G., Metabolomics analysis reveals large effects of gut microflora on mammalian blood metabolites. *Proceedings of the National Academy of Sciences of the United States of America* **2009,** *106* (10), 3698-3703.

43. Loh, H. H.; Berg, C. P., CONVERSION OF D-TRYPTOPHAN TO NICOTINIC ACID IN RAT. *Journal of Nutrition* **1971,** *101* (12), 1601-&.

44. Snyderman, S. E.; Ketron, K. C.; Carretero, R.; Holt, L. E., SITE OF CONVERSION OF TRYPTOPHAN INTO NICOTINIC ACID IN MAN. *Proceedings of the Society for Experimental Biology and Medicine* **1949,** *70* (4), 569-571.

45. Lee, W. J.; Hase, K., Gut microbiota-generated metabolites in animal health and disease. *Nature Chemical Biology* **2014,** *10* (6), 416-424.

46. Holguin, S.; Martinez, J.; Chow, C.; Wurtman, R., Dietary uridine enhances the improvement in learning and memory produced by administering DHA to gerbils. *Faseb Journal* **2008,** *22* (11), 3938-3946.

47. Jeengar, M. K.; Thummuri, D.; Magnusson, M.; Naidu, V. G. M.; Uppugunduri, S., Uridine Ameliorates Dextran Sulfate Sodium (DSS)-Induced Colitis in Mice. *Scientific Reports* **2017,** *7*.

48. Ma, W. W.; Saif, W. M.; El-Rayes, B. F.; Fakih, M.; Cartwright, T. H.; Posey, J.; von Borstel, R.; Bamat, M. K., Clinical trial experience with uridine triacetate for 5-fluorouracil toxicity. *Journal of Clinical Oncology* **2016,** *34* (4).

49. Abraham, J., Uridine triacetate provides antidote for 5-fluorouracil overdose and toxicity. *Journal of Community and Supportive Oncology* **2016,** *14* (8), 332-333.

50. Pizzorno, G.; Cao, D. L.; Leffert, J. J.; Russell, R. L.; Zhang, D. K.; Handschumacher, R. E., Homeostatic control of uridine and the role of uridine phosphorylase: a biological and clinical update. *Biochimica Et Biophysica Acta-Molecular Basis of Disease* **2002,** *1587* (2-3), 133-144.

51. Onodera, R.; Kandatsu, M., LYSINE AND PIPECOLIC ACID METABOLISM IN RUMEN .4. CATABOLISM OF LYSINE BY MIXED RUMEN BACTERIA. *Agricultural and Biological Chemistry* **1975,** *39* (6), 1239-1246.

52. Hyland, N. P.; Cryan, J. F., A gut feeling about GABA: focus on GABA(B) receptors. *Frontiers in Pharmacology* **2010,** *1*.

53. Stein, E. D.; Diamond, J. M., DO DIETARY LEVELS OF PANTOTHENIC-ACID REGULATE ITS INTESTINAL UPTAKE IN MICE. *Journal of Nutrition* **1989,** *119* (12), 1973-1983.

54. Vadlapudi, A. D.; Vadlapatla, R. K.; Mitra, A. K., Sodium Dependent Multivitamin Transporter (SMVT): A Potential Target for Drug Delivery. *Current Drug Targets* **2012,** *13* (7), 994-1003.

55. Blachier, F.; Boutry, C.; Bos, C.; Tome, D., Metabolism and functions of L-glutamate in the epithelial cells of the small and large intestines. *American Journal of Clinical Nutrition* **2009,** *90* (3), 814S-821S.

56. Asano, T.; Yuasa, K.; Kunugita, K.; Teraji, T.; Mitsuoka, T., EFFECTS OF GLUCONIC ACID ON HUMAN FECAL BACTERIA. *Microbial Ecology in Health and Disease* **1994,** *7* (5), 247-256.

57. Biagi, G.; Piva, A.; Moschini, M.; Vezzali, E.; Roth, F. X., Effect of gluconic acid on piglet growth performance, intestinal microflora, and intestinal wall morphology. *Journal of Animal Science* **2006,** *84* (2), 370-378.

58. Xiao, Z. J.; Xu, P., Acetoin metabolism in bacteria. *Critical Reviews in Microbiology* **2007,** *33* (2), 127-140.

59. Juni, E., MECHANISMS OF FORMATION OF ACETOIN BY BACTERIA. *Journal of Biological Chemistry* **1952,** *195* (2), 715-726.

60. Roediger, W. E. W., UTILIZATION OF NUTRIENTS BY ISOLATED EPITHELIAL-CELLS OF THE RAT COLON. *Gastroenterology* **1982,** *83* (2), 424-429.

61. Ferrier, L.; Berard, F.; Debrauwer, L.; Chabo, C.; Langella, P.; Bueno, L.; Fioramonti, J., Impairment of the intestinal barrier by ethanol involves enteric microflora and mast cell activation in rodents. *American Journal of Pathology* **2006,** *168* (4), 1148-1154.

62. Qin, X. F.; Deitch, E. A., Dissolution of lipids from mucus: A possible mechanism for prompt disruption of gut barrier function by alcohol. *Toxicology Letters* **2015,** *232* (2), 356-362.

63. Leclercq, S.; Matamoros, S.; Cani, P. D.; Neyrinck, A. M.; Jamar, F.; Starkel, P.; Windey, K.; Tremaroli, V.; Backhed, F.; Verbeke, K.; de Timary, P.; Delzenne, N. M., Intestinal permeability, gut-bacterial dysbiosis, and behavioral markers of alcohol-dependence severity. *Proceedings of the National Academy of Sciences of the United States of America* **2014,** *111* (42), E4485-E4493.

64. Ridlon, J. M.; Kang, D. J.; Hylemon, P. B.; Bajaj, J. S., Bile acids and the gut microbiome. *Current Opinion in Gastroenterology* **2014,** *30* (3), 332-338.

65. Long, S. L.; Gahan, C. G. M.; Joyce, S. A., Interactions between gut bacteria and bile in health and disease. *Molecular Aspects of Medicine* **2017,** *56*, 54-65.

66. Johansson, M. E. V.; Ambort, D.; Pelaseyed, T.; Schutte, A.; Gustafsson, J. K.; Ermund, A.; Subramani, D. B.; Holmen-Larsson, J. M.; Thomsson, K. A.; Bergstrom, J. H.; van der Post, S.; Rodriguez-Pineiro, A. M.; Sjovall, H.; Backstrom, M.; Hansson, G. C., Composition and functional role of the mucus layers in the intestine. *Cellular and Molecular Life Sciences* **2011,** *68* (22), 3635-3641.

67. Matsuo, K.; Ota, H.; Akamatsu, T.; Sugiyama, A.; Katsuyama, T., Histochemistry of the surface mucous gel layer of the human colon. *Gut* **1997,** *40* (6), 782-789.

CHAPTER FOUR

^{1}H-NMR based identification of metabolites involved in colonic epithelial transport by Ussing chamber experiments

Abstract: The large intestine, also known as the colon, has recently been recognized as an astonishingly complex biochemical factory of vital importance to human health. It plays a major role in digestion and absorption by salvaging nutrients from indigestible complex carbohydrates (mainly fiber) and proteins via fermentation initiated by the bacteria that make up our gut microbiome. The subsequent residual fermentation products undergo various methods of transport and absorptive processes as the stool travels along the length of the colon, causing changes in the composition. This work demonstrates the detection of metabolite transport across the epithelial tissue that lines the large intestine by ^{1}H NMR analysis in Ussing chamber experiments in which colon tissue is situated vertically between two chambers representing both the mucosal (lumen or apical) and serosal (blood-circulation or basolateral) sides of the tissue. Metabolites involved in transport processes will appear in the opposing chamber and can be measured simultaneously by a universal detector of organic compounds, ^{1}H NMR, alleviating the need for fluorescent or radiolabeled compounds.

4.1 Introduction

The colon is vitally important to human health. Also referred to as the "gut microbiome", the colon contains ~1000 species of bacteria that help harvest energy, synthesize vitamins, metabolize toxins, and shape the immune system.[1, 2] It has been observed that changes in metabolite composition may happen throughout the host, but we must begin to shift the focus of determining "who is there", to "what is happening". This is accomplished by obtaining greater understanding of the colon's transport mechanisms and metabolism.[3]

While the colon is a considered a single organ, the proximal and distal colon have different embryological origins derived from the mid and hindgut, respectively, with the proximal colon acting as a reservoir and the distal more like a conduit.[4] The data gathered from voided stool samples represent the end products of digestion and lack information on the transport and transformation of stool along the length of the colon, obscuring changes that occur due to segmental stratification.

In an effort to better understand the functionality of a particular region of the colon we utilize Ussing chamber experiments, which allow the in vitro study of metabolite transport across the colonic epithelial tissue by mounting a 1 cm^2 segment of tissue between two chambers that represent the mucosal (lumen or apical) and serosal (blood-circulation or basolateral) membranes of the intestine.[5]

Ussing chamber studies have been previously used in the study of colonic transport with a variety of approaches employed for the detection of transported metabolites including fluorescence labeling,[6] enzyme-linked immunosorbent assay (ELISA),[7] radioisotope tracers,[8, 9] and high performance liquid chromatography (HPLC) with ultraviolet (UV),[10, 11] diode array detection (DAD),[12] and MS/MS[13]. Each of these analytical methods has limitations. Adding a fluorescent tag changes the structure of a compound, and has the potential to greatly affect the rate of transport. The high cost and limited availability of radio-labeled compounds poses problems, especially when the aim is to monitor the transport properties of multiple metabolic species. An added downfall of using labeled compounds is that these methods reduce the ability to study the simultaneous transport of multiple metabolites. Similarly, though ELISA offers good sensitivity, because it relies on antibodies, it is highly specific only to targeted analytes.

The separation provided by HPLC-UV or -DAD methods allows for the simultaneous detection of metabolites, but these compounds must contain a chromophore. HPLC-UV or -DAD methods also require that the identity of a metabolite is known, and that standards are available to obtain calibration plots for quantitation. HPLC-MS/MS, commonly referred to as LC-MS/MS offers advantages of increased sensitivity, and a mass analyzer to aid in identification. However, as discussed in Chapter 1.2.3, LC-MS/MS is better suited for targeted analysis, due to the required optimization of sample preparation and separation methods. This advantage in targeted analysis is why LC-MS/MS is often used in conjunction with the Ussing chamber in studies of drug absorption and metabolism.[14, 15]

Applications of ^{1}H-NMR in metabolomics research continue to grow due to its ability to analyze a wide variety of compounds in a single acquisition and without destruction of sample.[16, 17] ^{1}H-NMR presents a comprehensive overview of the sample components facilitating both identification of unknown metabolites based on chemical structure information, and quantification of compounds in a single acquisition relative to an internal standard.[18] Based on the need to identify and quantify a wide variety of unknown metabolites involved in epithelial transport in a restricted sample volume, ^{1}H-NMR was chosen as the analysis platform for our Ussing chamber experiments.[19]

4.2 Materials and methods

The studies described in this chapter focus on the epithelial tissue obtained from the cecum of the rat. The cecum is the main site of carbohydrate fermentation processes within the colon.[20] For Ussing chamber analysis, the tissue undergoes what is called a seromuscular strip to separate the mucosal and submucosal layers from the submusculature layer containing circular and longitudinal muscle as well as the serosa. The mucosal/submucosal layer is used for metabolite transport analysis.

4.2.1 Tissue isolation and mounting

Female Sprague Dawley rats (190-250 g) were purchased from Taconic Biosciences and housed at 23±1°C on a 12:12-h light-dark cycle and allowed free access to water with a standard rodent diet. All animal protocols were approved by the University of California Riverside Institutional Animal Care and Use Committee.

Solute flux, electrical resistance (RT) and short-circuit current (Isc) across isolated segments of rat intestine were measured using a conventional Ussing chamber technique.[5] Our studies focused on the cecum, a predominant site of microbial fermentation along the distal intestine. Paired segments (2 cm) of the cecum (extending 0-4 cm from the cecocolonic junction) were isolated from rats immediately after CO_2 euthanasia and rinsed in Parson's solution comprised of: 110 mM NaCl, 25 mM $NaHCO_3$, 4 mM KCl, 2 mM Na_2HPO_4, 1.25 mM $CaCl_2$, 1 mM $MgSO_4$, and 12 mM glucose saturated with 5%CO_2/95% O_2. This solution was adjusted to an osmolality of 305 mOsm (matching that of native fecal fluid) by the addition of NaCl or water.

The intestinal wall was cut open along the mesentery and partially stripped of serosal and muscle layers to obtain a mucosa-submucosa preparation.[5] Tissues were mounted on small pins across an oblong aperture (5 x 22 mm with an exposed tissue area of 1.0 cm^2, Physiologic Instruments P2252) and incubated in an Ussing chamber (Physiologic Instruments EM-CSYS-2). Chambers were maintained at 37°C by heated water jackets and continuously mixed by gas lift (100% O_2 on the mucosal side, 5%CO_2/95% O_2 on the serosal side).

Indomethacin (3 μM) was added to the serosal bath (from a 64 mM stock solution in deuterated DMSO) to suppress prostanoid and neural influences. The transmucosal potential difference (VT) was measured through 170 mM KCl agar bridges connected to a pair of calomel electrodes and monitored with a voltage clamp amplifier (Physiological Instruments VCC-MC2). The mucosa was maintained in an "open circuit" mode except during periodic (every 5 min) measurements of transmucosal conductance (GT) to monitor tissue integrity. To measure GT, VT was briefly (10 s) clamped at 0 mV by applying a current (Isc) through a pair of Ag/AgCl electrodes kept in contact with the mucosal and serosal solutions via 170 mM KCl agar bridges. GT was calculated using Ohm's law from the change in Isc evoked by a 2 mV bipolar pulse.

Tissues were pre-incubated with bilateral Parson's solution for 30 min to establish a basal steady-state condition. The luminal bath was then replaced with 2 mL of either undiluted bacteria-free fecal fluid or Parson's solution of matching osmolality. To measure the rates at which luminal solutes accumulate in the serosal bath, the whole volume of serosal solution (2 mL) was harvested after 45 min and 90 min and replaced with fresh Parson's solution; care was taken to remove and replace solutions in both hemi-chambers at the same rate to avoid hydrostatic pressure gradients across the tissue. Samples of the luminal and serosal solutions were analyzed by ^{1}H NMR and/or GC-MS, as described below, and the relationship between the serosal concentration of a given solute and time (0, 45, 90 min) was fit by linear regression to obtain an estimate of absorptive flux rate (μmol/h•cm^2).

4.2.2 Evaluation of tissue viability

At the end of the flux measurement, forskolin (10 μM) was added to the serosal bath to evoke electrogenic Cl^- secretion; the peak secretory Isc response was recorded after 10 min. Tissues exhibiting signs of functional impairment, i.e., low electrical resistance ($\leq$ 50 Ohm•cm^2), weak secretory Isc response ($\leq$ 50 μA/cm^2), or significant differences in the rate of absorptive flux between the first (45°) and second (90°) flux interval, were excluded from analyses.

4.2.3 Artificial cecal stool fluid (cecal flush)

A synthetic solution resembling rat cecal stool fluid was formulated to contain 107 mM Na^+, 48 mM K^+, 20 mM Mg^{2+}, 2.5 mM Ca^{2+}, 67 mM Cl^-, 3 mM SO_4^{2-}, 63 mM acetate, 43 mM butyrate, and 18 mM propionate at pH 6.5 and 305 mOsm.

4.2.4 Stool Fluid

Undiluted fecal fluid was isolated from the cecum. Stool from this segment is most abundant and has the highest fluid content and microbial fermentative capacity (Talbot and Lytle, 2010). Solid material was removed by 4 successive cycles of centrifugation (15,500xg, 7 min), followed by filtration (0.45 μm) to remove microbes and residual particulates. The pH of this fluid was 5.70 ± 0.21 (n = 13 rats).

4.2.5 ^{13}C-labeled butyrate stool fluid

Similarly to the artificial cecal flush solution described in section 4.2.3, a synthetic solution resembling rat cecal stool fluid was prepared to contain 107 mM Na^+, 48 mM K^+, 20 mM Mg^{2+}, 2.5 mM Ca^{2+}, 67 mM Cl^-, 3 mM SO_4^{2-}, and 17 mM uniformly ^{13}C-labeled butyrate at pH 6.5 and 305 mOsm.

4.2.6 ^{1}H-NMR spectroscopic analysis

For sample preparation for Ussing chamber sample analysis, refer to section 2.3.1.2. Data acquisition parameters can be found in section 2.3.2.3, as well as processing parameters in section 2.3.4.

4.2.7 Quantitative data analysis

Quantitative analysis methods including T_1 calculations and adjustments, can be found in section 2.3.5.

4.3 Results and discussion

The Ussing chamber has been widely used in the study of transport of charged or labeled species across epithelial tissue, including the short chain fatty acids (SCFAs) including acetate, propionate, and butyrate.[21-24] Many previous reports were limited in their ability to study multiple metabolites simultaneously because of the analytical platforms used. To better understand the transport behavior of the tissue, we must be able to compare how composition or metabolite availability affects transport. ^{1}H-NMR potentially provides the ability to study both the transport and transformation fate of metabolites within stool as it passes through the colon.

In this study, we investigate the use of ^{1}H-NMR to follow transport of metabolites across the epithelium of the rat cecum in Ussing chamber experiments. Figure 4.1 provides a schematic view of the Ussing chamber, which is comprised of two buffer chambers separated by tissue mounted to a slide containing a window that allows the tissue to be in contact with both chambers. The chamber on the left of Figure 4.1 represents the lumen (mucosal) side of the tissue that in the rat is exposed to stool. The chamber on the right is the serosal side of the tissue which is the side in contact with the circulatory system. The Ussing chamber allows experimental control over what is loaded into the mucosal chamber to act as stool, and determination of those compounds transported across the tissue into the serosal chamber.

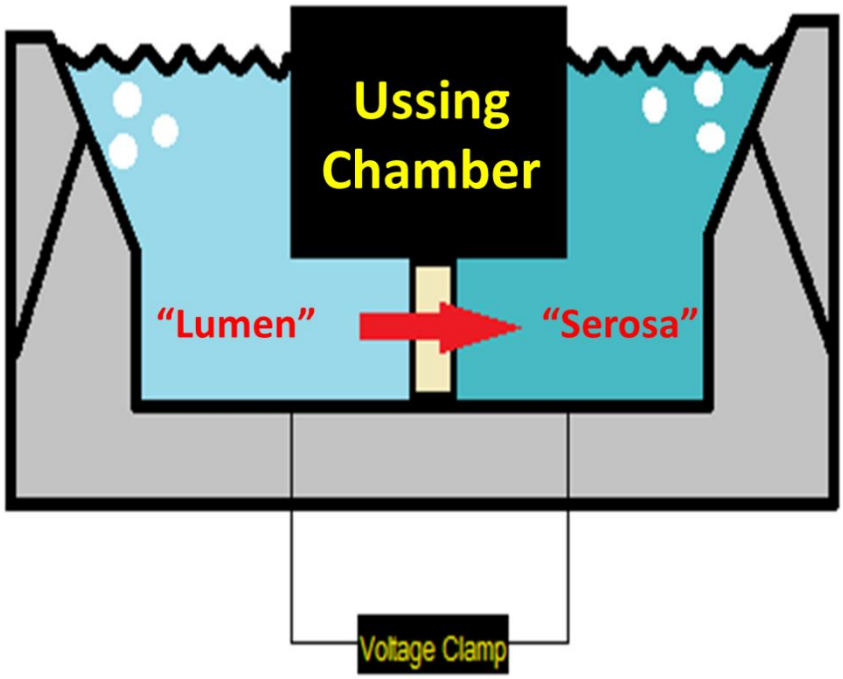

Figure 4.1. Diagram of the Ussing chamber used to monitor metabolite transfer across excised rat epithelium.

The use of ^{1}H-NMR as the detection method provides unique advantages beyond the simultaneous detection of metabolites involved in transport without the use of labels, including the ability to use a single internal standard for quantification. The power of NMR for untargeted analyses also facilitates the detection of new compounds in the serosal bath that may have been transformed by the tissue during transport.

In NMR, the response factor for a given resonance is simply equal to the number of protons that give rise to that resonance making it possible to quantify without authentic standards or the need for calibration plots.[25] Relative rates of metabolite transport across the endothelial tissue can be easily determined upon quick examination of the NMR spectrum. For example, in our initial studies we found that the rate of transport for SCFA's remains stable over the time course of the experiment allowing us to ensure that the tissue remained viable during the study. (Figure 4.2)

A variety of metabolite sources with a range of complexities can be examined in Ussing chamber experiments. For example, Figure 4.3A shows the ^{1}H NMR spectrum measured for the complex cecal stool fluid loaded into the mucosal bath of the Ussing chamber. The cecal stool fluid is a 2 mL solution containing stool fluid removed from the cecum of the rat colon. This fluid is composed of the metabolites available for transport through the cecal epithelium under native conditions. The spectrum shown in Figure 4.3B was measured for an aliquot extracted from the Ussing chamber serosal bath after 45 min and contains the resonances of metabolites that were transported across the colonic epithelial tissue.

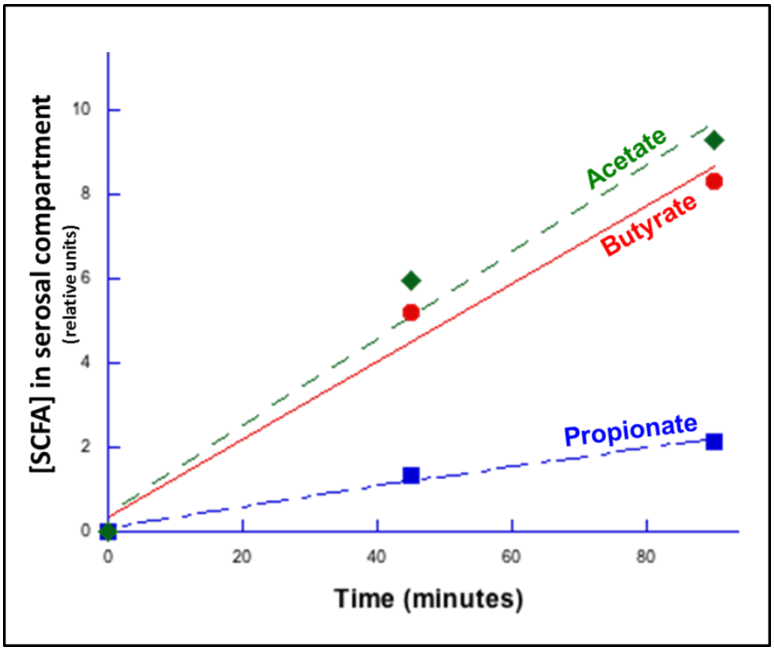

Figure 4.2. Transport rates for butyrate (red), propionate (blue), and acetate (green) across the excised rat cecum epithelium indicating that the tissue remained viable over the length of the experiment.

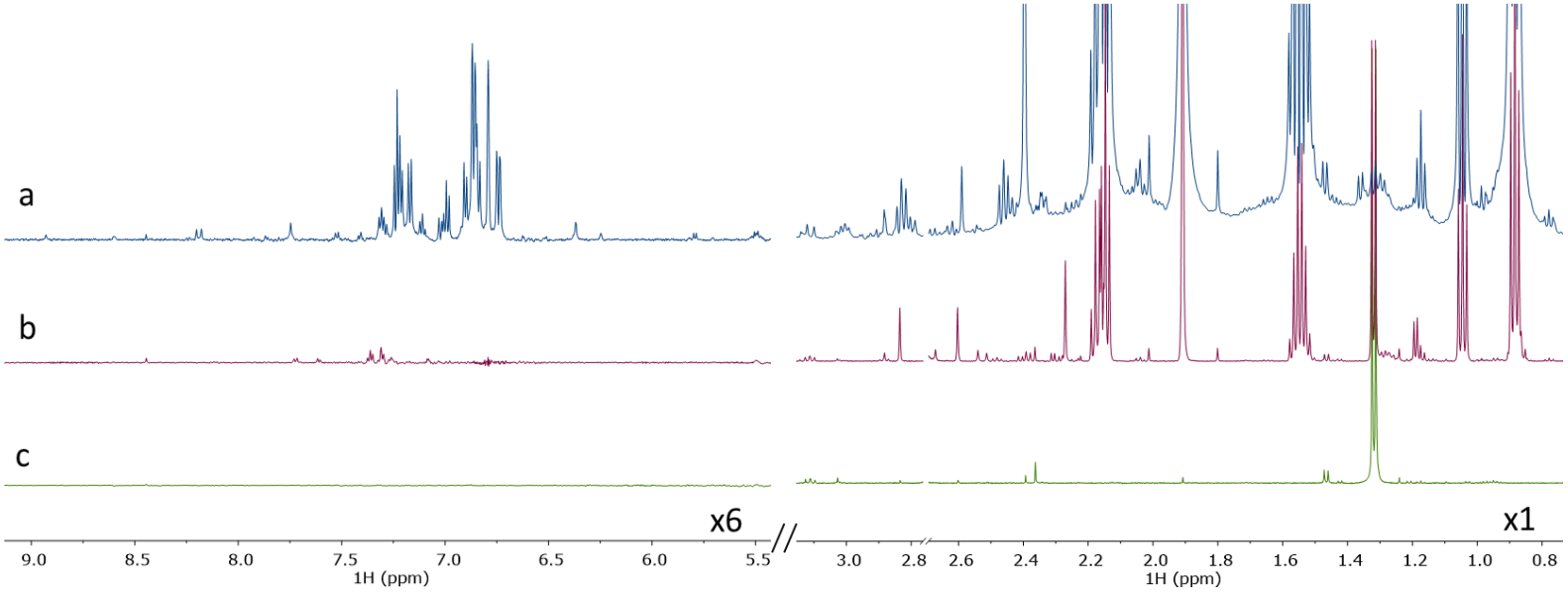

Figure 4.3. ^{1}H NMR spectra of (a) cecal fluid, (b) Ussing chamber serosal bath sample resulting from cecal fluid in the mucosal bath, and (c) Ussing chamber bath sample resulting from Parson's solution in the two chambers with a carbon source of only glucose to serve as a blank, highlighting the ability to detect metabolites being transported across and produced by the epithelial tissue.

The resonances of the SCFAs acetate, butyrate, and propionate are intense in Figure 4.3B, consistent with their rapid transport across the epithelium. The resonances of several additional metabolites are also observed in Figure 4.3B including 3-hydroxybutyrate, acetoacetate, succinate, citrate, isoleucine, choline, phenylalanine, hydrocinnamate, formate, tyrosine, tyramine, pyruvate, oxaloacetate, lysine, and valine. Transport for most of these metabolites has been determined in studies pertaining to the small intestine, however, experimental data for transport of choline, phenylalanine, tyramine, and oxaloacetate in the large intestine (colon) could not be located in our detailed review of the literature.

Because the epithelial tissue used to study transport remains viable for the course of the experiment, we hypothesized that there are two possible sources of the metabolite resonances detected in Figure 4.3B: transport and active metabolism by the epithelial tissue. To test this hypothesis, we acquired a spectrum using a blank of Parson's solution loaded into both chambers of the Ussing apparatus with the only carbon source being glucose provided in the serosal bath. The spectrum shown in Figure 4.3C was obtained for an aliquot of the fluid from the serosal chamber after 45 min. The resonances observed in this spectrum result from metabolites produced endogenously by the tissue.

Table 4.1 reports the metabolites and corresponding chemical shifts identified in the cecal stool fluid loaded into the mucosal side of the Ussing chamber. Average concentrations are not reported for the cecal stool fluid because T_1 values depend on the sample matrix, and it was difficult to determine accurate T_1 values within the cecal stool fluid due to overlapping resonances and low analyte concentrations. Table 4.1 also reports metabolites detected in the 3 different sample types removed from the serosal chamber. The first type correlates to samples removed from the serosal chamber when cecal stool fluid is loaded on the mucosal side with concentrations reported in units of μM. We observe that when stool fluid is presented in the mucosal chamber 19 metabolites can be identified in the serosal chamber, 4 of which are not present in the stool fluid and are hypothesized to be generated by the metabolism of the epithelial tissue.

The next serosal sample correlates with loading artificial cecal flush in the mucosal chamber, with a composition reported in section 4.2.3. This artificial cecal flush lacks the complexity of the cecal stool fluid, and allows us to observe how the presence of other metabolites mediate transport by controlling what is added to the mixture. If we compare values for the SCFAs acetate, butyrate, and propionate it can be determined that in the absence of the entire luminal metabolome, the rates of SCFA transport are not affected, which may not be true for all metabolites. Still these rates provide evidence that the tissue is not suffering in the absence the full luminal metabolome.

Table 4.1. Metabolites are displayed below with corresponding chemical shifts. (X) denotes presence of the metabolite in the corresponding matrix, while (-) denotes absence of metabolite from that matrix, and (NQ) signifies metabolites detected in the serosal chamber, but below limit of quantitation. The four matrix types included from left to right are the stool fluid that is loaded into the mucosal chamber, and the resulting serosal chamber sample, the serosal chamber when cecal flush is loaded in the mucosal chamber, and the metabolites generated when Parson's solution is loaded into both chambers.

		Mucosal	Serosal		
Metabolites	^{1}H-NMR Chemical shift	Stool Fluid	Ussing chamber Stool fluid (µM)	Ussing chamber Cecal flush (µM)	Parson's & Parson's
1. 3-hydroxybutyrate	1.18 (d), 2.29 (m), 2.39 (m), 4.13 (m)	—	X	X	—
2. Acetate	1.91 (s)	X	X	X	—
3. Acetoacetate	2.27 (s), 3.34 (s)	X	X	X	—
4. Acetoin	1.37 (d), 2.22 (s), 4.42 (q)	X	—	—	—
5. Alanine	1.47 (d), 3.78 (q)	X	—	—	X
6. Allantoin	5.38 (s)	X	—	—	—
7. Arabinose	5.05 (dd), 3.66 (m), 3.81 (dd), 3.89 (m), 3.93 (m), 4.02 (m), 4.51 (d), 5.23 (d)	X	—	—	—
8. Arginine	1.68 (m), 1.91 (m), 3.23 (t), 3.75 (t)	X	—	—	—
9. Asparagine	2.84 (dd), 2.94 (dd), 3.99 (dd)	X	—	—	—
10. Aspartate	2.74 (m), 3.89 (dd)	X	—	—	—
11. Benzoate	7.48 (dd), 7.55 (t), 7.88 (d)	X	—	—	—
12. Butyrate	0.88 (t), 1.55 (m), 2.15 (t)	X	X	X	—
13. Citrate	2.66(d), 2.76 (d)	—	—	X	—
14. Choline	3.21 (s), 3.52 (m), 4.07 (m)	X	X	X	X
15. Dimethylamine	2.52 (s)	X	—	—	—
16. Ethanol	1.17 (t), 3.64 (q)	X	—	—	—
17. Formate	8.44 (s)	X	X	X	—
18. Glutamate	2.05 (m), 2.12 (m), 2.34 (m), 3.74 (q)	X	—	—	—
19. Glycine	4.77 (s)	X	—	—	—
20. Histidine	3.13 (dd), 3.23 (dd), 3.97 (dd), 7.06 (s), 7.80 (s)	X	—	—	—
21. Hydroxycinnamate	2.48 (t), 2.88 (t), 7.31 (m)	X	X	—	—
22. Isoleucine	0.93 (t), 1.00 (d), 1.25 (m), 1.46 (m), 1.97 (m), 3.66 (d)	X	X	X	—
23. Isobutyrate	1.13 (d), 2.57 (m)	X	—	—	—
24. Lactate	1.32 (d), 4.10 (q)	X	X	X	X
25. Leucine	0.95 (t), 1.71 (m), 3.72 (m)	X	—	—	—
26. Lysine	1.47 (m), 1.72 (m). 1.90 (m), 3.20 (t), 3.74 (t)	X	X	X	—
27. Malonate	3.11 (s)	**	—	—	—
28. Methanol	3.34 (s)	X	—	—	—
29. Methionine	2.13 (m), 2.63 (t), 3.85 (dd)	X	—	—	—
30. Methylamine	2.61 (s)	**	—	—	—
31. Nicotinate	7.51 (dd), 8.24 (m), 8.60 (dd), 8.93 (d)	X	NQ	—	—
32. Nicotinurate	4.28 (s), 8.25 (t), 9.00 (m), 9.25 (s)	X	—	—	—
33. Oxaloacetate	2.37 (s)	—	X	X	—
34. Phenylalanine	3.20 (m), 3.98 (dd), 7.32 (d), 7.36 (m), 7.42 (m)	X	X	X	—
35. Propionate	1.05 (t), 2.17 (m)	X	X	X	—
36. Pyruvate	2.35 (s)	—	X	X	X
37. Serine	3.83 (dd), 3.95 (m)	X	—	—	—
38. Stachyose	3.52 (t), 3.56 (dd), 3.79 (m), 3.99 (m), 4.05 (m), 4.14 (dd), 4.22 (d), 4.00 (m), 5.42 (d)	X	—	—	—
39. Succinate	2.40 (s)	X	X	X	X
40. Taurine	3.27 (t), 3.43 (t)	X	—	—	—
41. Threonine	1.32 (d), 3.57 (d), 4.24 (m)	X	—	—	—
42. Trehalose	3.44 (t), 3.64 (dd), 3.76 (m), 3.81 (m), 5.18 (d)	X	—	—	—
43. Trimethylamine	2.89 (s)	**	—	—	—
44. Tyramine	2.82 (t), 3.12 (t), 6.75 (d), 7.12 (d)	X	X	—	—
45. Tyrosine	3.05 (dd), 3.19 (dd), 3.93 (dd), 6.89 (m), 7.18 (m)	X	X	X	—
46. Uracil	5.79 (d), 7.52 (d)	X	—	—	—
47. Valine	0.98 (d), 1.03 (d), 2.26 (m), 3.82 (d)	X	X	X	—
48. τ-methylhistidine	3.24 (m), 3.71 (s), 3.93 (dd), 7.05 (s), 7.92 (s)	X	NQ	—	—

It is interesting that the cecal flush solution contains only glucose, acetate, butyrate, and propionate, but 15 of the same metabolites appear in the serosal chamber as when cecal stool fluid is present in the mucosal chamber. The last sample reported in table 4.1 is removed from the serosal side of the Ussing chamber with Parson's solution loaded into both sides. Concentrations are not reported due to the limit of quantitation for these low-level metabolites.

Though the metabolically rich cecal stool fluid provides a number of possible carbon sources, when cecal flush is introduced into the mucosal chamber the tissue has only glucose as a carbon source. The metabolites observed in the serosal bath include lactate, alanine, and pyruvate and may be explained by the metabolism of glucose. However, choline is also produced by the epithelium when no nitrogen source was provided suggesting active metabolism by the tissue and possible transformation of metabolites in addition to transport.

To conclude that the observed metabolism is due to the epithelial tissue it is necessary to rule out any contribution from bacteria. As observed throughout Chapter 3, bacteria play a large role in metabolism along the length of the colon, and can rapidly alter the stool composition. The initial seromuscular strip to remove the mucosa and submucosa layers should remove any bacteria, but to validate this assumption a set of Ussing chamber experiments was conducted using tissue treated with antibacterial compounds. The tissue was mounted in the Ussing chamber and then soaked for 45 minutes in a Parson's solution containing 50 μg/mL metronidazole and 100 μg/mL streptomycin at 37°C.

After the 45 min, the solution was removed and the chambers were rinsed with fresh Parson's solution before loading cecal stool fluid into the mucosal chamber and Parson's solution into the serosal chamber. At this point, experimental procedures proceeded as usual.

The samples from the antibacterial treated tissue were compared to those without the pretreatment to determine if any of the observed metabolites were generated by bacteria (Figure 4.4). The only observable changes in the entire spectrum were 2 singlets that appeared at 2.50 ppm, and 8.05 ppm that match the resonances of metronidazole. The concentration of the metronidazole present in the serosal samples was estimated to be about 1.7 μg/mL, indicating that some residual metronidazole remained after rinsing. This confirms that the transformation products observed with cecal flush in the mucosal chamber are not produced by bacterial metabolism, but by the metabolism of the epithelium.

Figure 4.5 compares the concentrations of the detected metabolites in the serosal samples by ^{1}H-NMR. The red bar represents the rates determined from the serosal bath after 45 min when pure cecal stool fluid is initially loaded in the mucosal chamber. In contrast, the blue bar represents rate of metabolite transport when cecal flush solution is loaded into the mucosal bath. For most metabolites including propionate, butyrate, lactate, phenylalanine, formate, succinate, oxaloacetate, choline, and valine, the transport rates for both sample types are in good agreement, providing evidence that rate of transport and transformation is not measurably affected by the metabolic composition of stool in the lumen. However, this is not true for all metabolites.

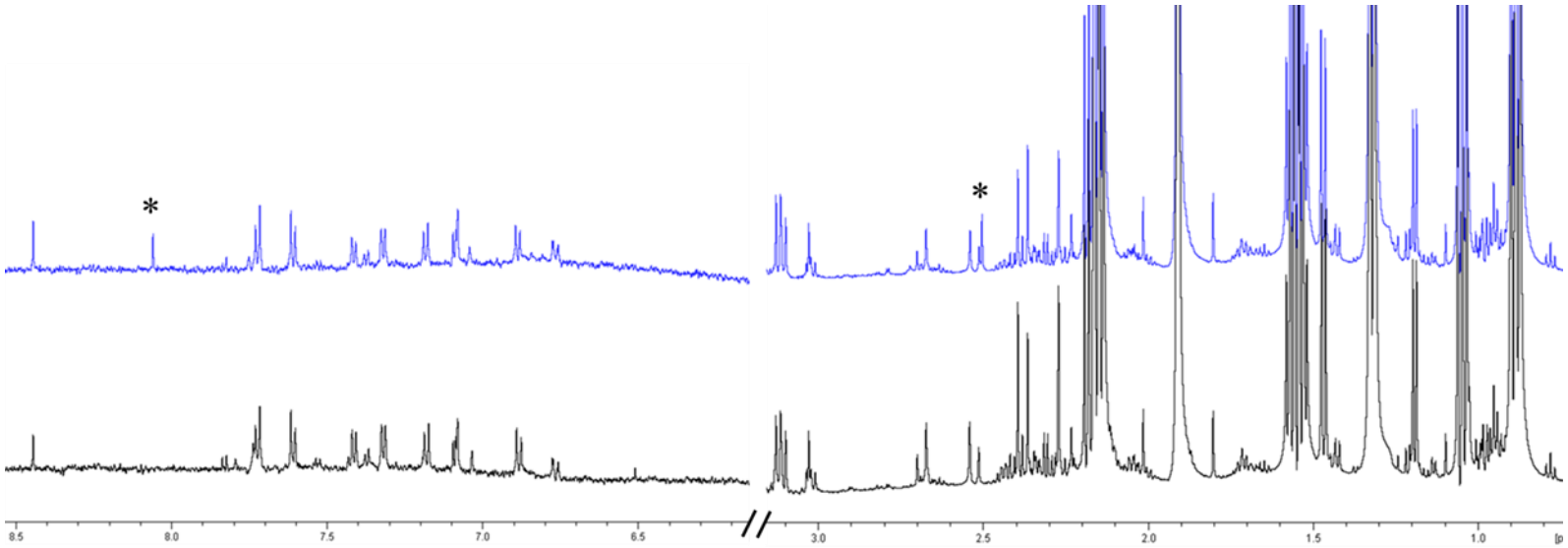

Figure 4.4. ^{1}H-NMR spectra of samples removed from the serosal chamber with the presence of stool fluid in the luminal chamber. The top (blue) spectrum represents experiments in which the tissue was pretreated with antibiotics, metronidazole (50 µg/mL) and streptomycin (100 µg/mL) for 45 minutes prior to loading the stool fluid into the luminal chamber. The bottom (black) spectrum is not pretreated with antibacterial compounds prior to Ussing chamber experimentation.

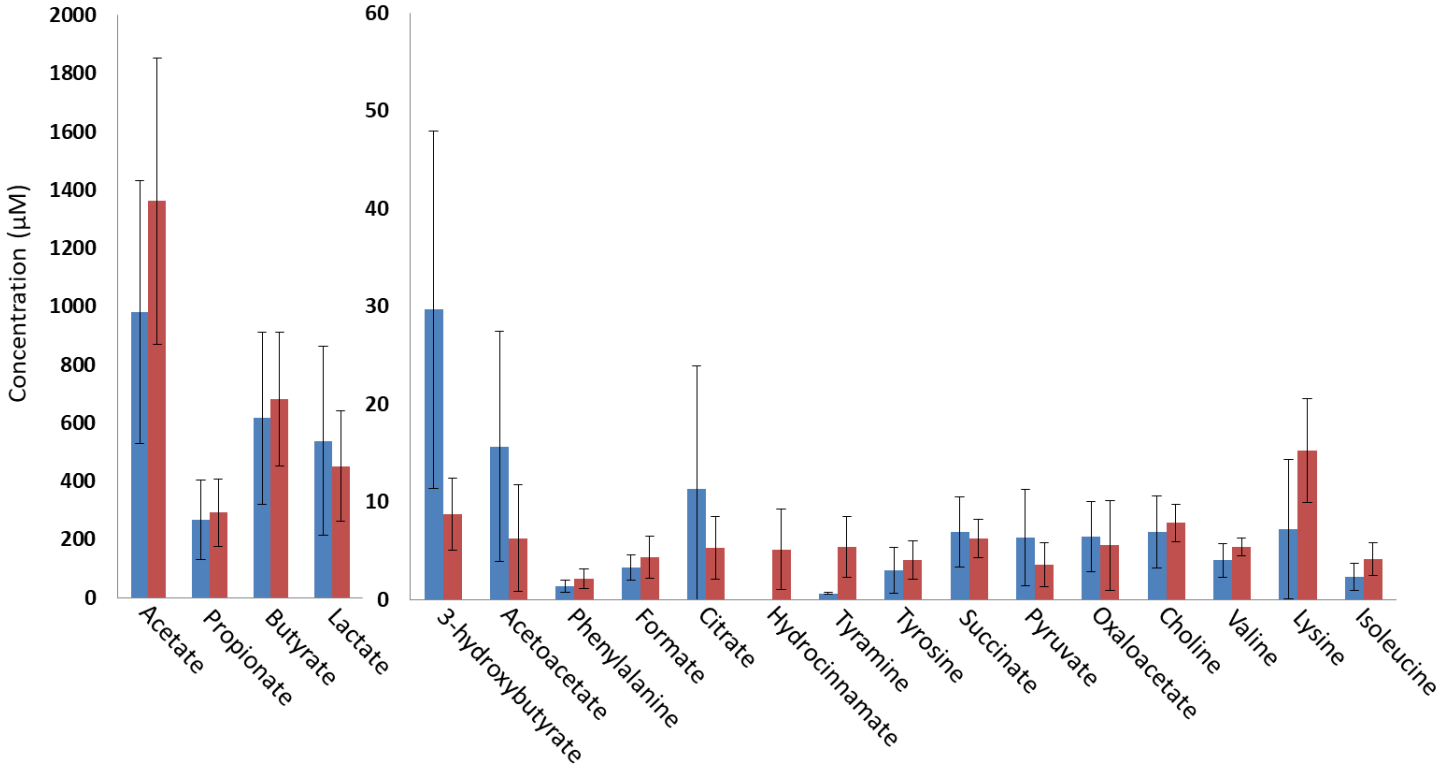

Figure 4.5 Bar graph showing metabolite concentration (µM) for acetate, butyrate, propionate, lactate, acetoacetate, phenylalanine, 3-hydroxybutyrate, choline, formate, citrate, hydrocinnamate, tyramine, tyrosine, succinate, pyruvate, oxaloacetate, valine, lysine, and isoleucine taken at 45 minute intervals to represent the rate of transport across cecal epithelial tissue. Blue (n=6) and red (n=8) represent samples in which cecal stool fluid and cecal flush solution, respectively, are loaded in the lumen chamber.

There is a large increase in the apparent rate of appearance of 3-hydroxybutyrate, acetoacetate, and citrate in the serosal samples from cecal flush solution compared to the cecal stool fluid. Acetoacetate and 3-hydroxybutyrate are often associated with ketosis and can be produced via butyrate metabolism, as it is well established that within the colonocyte that butyrate undergoes a β-oxidation to produce acetylCoA and subsequently CO_2 and ketone bodies.[26]

Citrate is involved in the Krebb's cycle, and comes from the conversion of acetylCoA. One possibility is that increased β-oxidation of butyrate in the cecal flush experiments leads to increased production of acetylCoA to fuel the Krebb's cycle pathways. Subtle differences can also be observed in among amino acids, in which levels are higher for the cecal stool fluid than that of the cecal flush solution. This may be explained by the availability of the metabolites to be afforded transport. Amino acids are not provided in the cecal flush solution; therefore we expect a much lower rate of appearance in the serosal bath, if any at all.

Some analyses were limited based on sensitivity of the NMR. With increased sensitivity we should be able to detect and quantify additional metabolites. A small subset of metabolites including nicotinate (niacin) and τ-methylhistidine were identifiable by ^{1}H-NMR in the serosal chamber, but lacked a sufficient signal-to-noise ratio to be quantified. This limitation could potentially be overcome with the use of a higher field magnet, such as a 700 or 800 MHz equipped with a cryoprobe.

Methods to increase concentration were attempted, including lyophilization. Challenges occurred when trying to reconstitute the freeze dried sample in a smaller volume due to the high salt concentrations of the Parson's buffer solution. Due to the interest in studying small molecules such as acetate and formate, a "de-salting" or clean-up step was not an option due to the risk of signifcant losses for these metabolites.

^{1}H-NMR, as performed herein, lacks a separation step and can often suffer from overlapping resonances for metabolites of interest. The area of the spectrum that includes glucose resonances is very crowded, and challenged our ability to quantify compounds such as glycine and ethanolamine. This could be improved with additional sample preparation steps prior to analysis, such as solid-phase extraction. However, this would increase the analysis time and complicate quantitative analysis due to variations in recovery. As discussed in Chapter 2, mass spectrometry (MS) methods such as gas-chromatography (GC-MS) and liquid chromatography (LC-MS) would increase the resolution and sensitivity of some metabolites they also require additional sample preparation steps which can introduce loss of some analytes and reduce precision. In contrast to NMR, GC-MS and LC-MS also require the use of standards and calibration plots or isotopically labeled compounds for quantitation of each metabolite due to the different response factors for each compound.

4.4 Isotope labeling to explore metabolic flux

To examine the transformation of metabolites in the Ussing chamber experiments, the use of isotope labeled compounds was explored. Data obtained from the cecal flush solution suggested that metabolites were being generated from one of the few compounds added to the solution such as acetate, butyrate, propionate, and glucose. Knowing that butyrate is the preferred energy source for the colonocytes, Ussing chamber experiments were performed using uniformly labeled ^{13}C-butyrate in the cecal flush solution in place of the SCFAs.

The ^{1}H-NMR spectrum in Figure 4.6 for isotope labelled butyrate initially appears different due to the intensity of the ^{13}C-satellites of butyrate, and subsequent absence of the resonances for protons bonded to a ^{12}C atom. From analysis of the ^{1}H NMR spectrum, the percentage of label incorporation from butyrate into downstream metabolites can potentially be calculated using the ratio of ^{12}C and ^{13}C resonances for a particular proton signal. Unfortunately, many of these resonances are plagued by substantial overlap with interfering resonances. In these types of experiment where only a few percent of the label may be incorporated into other metabolites during the relatively short incubation time (e.g. 45 min), it is difficult to determine the extent of label incorporation with the necessary precision.

To overcome the limited resolution in the ^{1}H-NMR experiments, 2D-NMR ^{1}H-^{13}C heteronuclear single quantum correlation spectroscopy (HSQC) was used to examine the ^{13}C-labeled butyrate samples (Figure 4.7). The region selected for closer examination matches that presented in Figure 4.6 to show how the second dimension, ^{13}C shift, complements the ^{1}H data. The enhance resolution of the HSQC allows peaks that were once overlapped to be distinguished, for example ethanol and 3-hydroxybutyrate. Previous results indicated that 3-hydroxybutyrate was being metabolized, most likely from butyrate. In the ^{1}H-NMR spectrum the resonance of 3-hydroxybutyrate and it's ^{13}C-satellites are obscured by the large amount of ethanol present, and incorporation of ^{13}C cannot be observed. However, the HSQC in figure 7 allows us to distinguish the 3-hydroxybutyrate from ethanol. While the HSQC spectrum is optimal for identification, and based on relative peak intensities can tentatively confirm that 3-hydroxybutyrate is produced by metabolism of butyrate; it is challenging to quantify the amount of ^{13}C being introduced into 3-hydroxybutyrate from the HSQC spectrum. An alternative approach for future experiments could be the use of a mass spectrometry platform, such as GC-MS, to monitor isotope incorporation, however, this will require method development specific to metabolic flux analyses, and will be discussed in greater detail in Chapter 5.

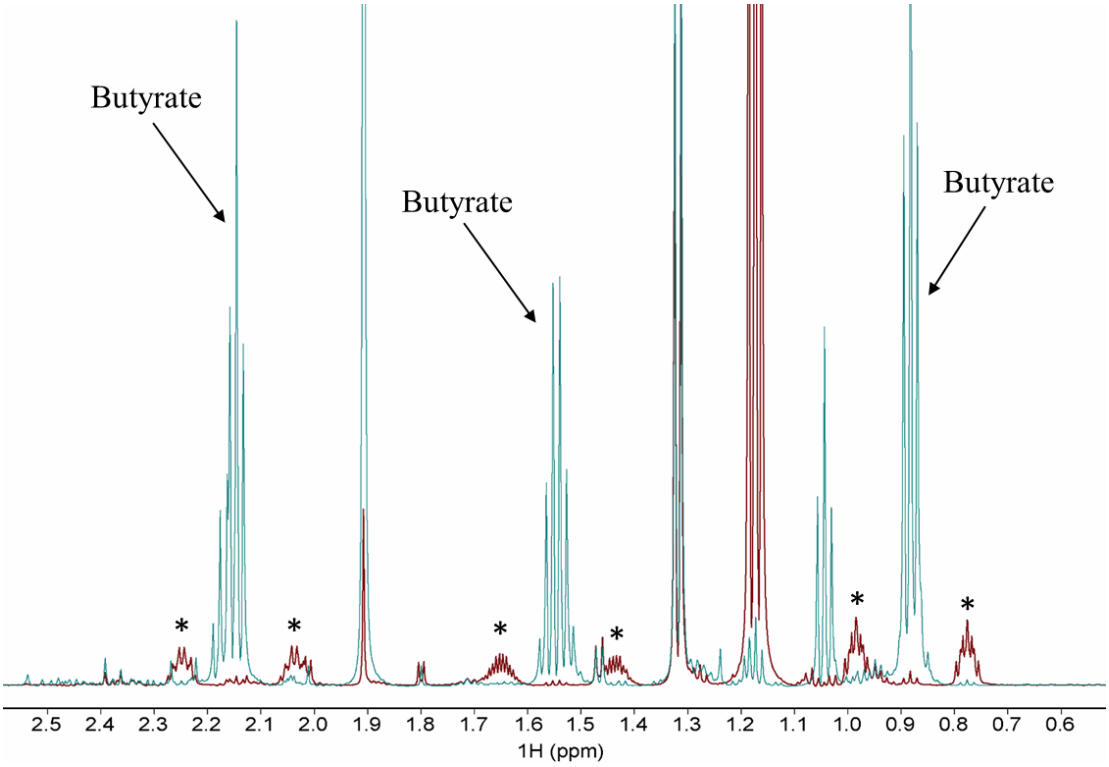

Figure 4.6. ^{1}H-NMR spectrum of serosal chamber samples after 45 min incubation with cecal flush solution loaded in the luminal chamber (blue) or cecal flush solution containing uniformly labeled ^{13}C-butyrate (red). Butyrate resonances are labeled with (*) denoting the butyrate ^{13}C-satellite peaks.

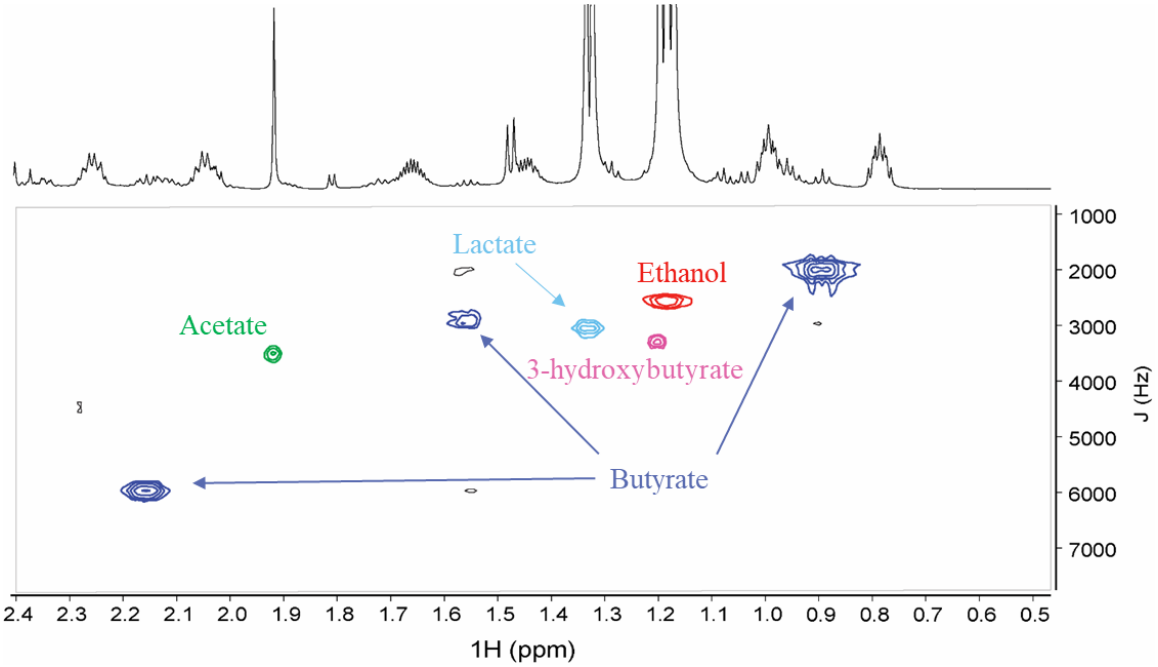

Figure 4.7. 2D [^{1}H-^{13}C] HSQC spectrum of serosal chamber samples after a 45 min incubation with cecal flush solution containing uniformly labeled ^{13}C-butyrate. Metabolites observed in this region include butyrate, acetate, lactate, ethanol, and 3-hydroxybutyrate.

4.5 Conclusions

The use of ^{1}H-NMR to detect transported metabolites from Ussing chamber experiments allows the simultaneous identification and quantification of multiple metabolites. Quantitative data was obtained for 19 metabolites involved in colonic epithelial transport processes, including a few metabolites (choline, phenylalanine, tyramine, and oxaloacetate) for which, to the best of our knowledge, transport rates across colonic epithelial tissue have not been reported. To the best of our knowledge, this is also the first experimental setup using the Ussing chamber in conjunction with metabolite detection using NMR.

The use of NMR as a method for detection allows us to study multiple metabolites simultaneously without the use of labeled compounds. This allows for the comparison of how the metabolite composition in the lumen may impact the transport rates of the epithelial tissue. Results determined that transport remained consistent across both the cecal stool extract and the artificial cecal flush, with only an observed elevation of the metabolites affected by the β-oxidation pathway within the colonocyte; acetoacetate and 3-hydroxybutyrate.

The method described herein was able to not only detect metabolites involved in transport, but provided evidence for the presence of metabolites in the serosal chamber produced by the metabolism of the epithelial tissue. The active metabolism of compounds as they are transported across the tissue could provide important new knowledge associated with the overall health and function of the tissue.

Future experiments should aim to identify the transformation of metabolites using ^{13}C-labeled compounds, as well as employing Ussing chamber experiments to detect differences in transport and transformation using excised tissue from other regions of the colon or animals suffering from inflammation.

4.5 References

1. Guinane, C. M.; Cotter, P. D., Role of the gut microbiota in health and chronic gastrointestinal disease: understanding a hidden metabolic organ. In *Therap Adv Gastroenterol*, 2013; Vol. 6, pp 295-308.

2. Jacobs, D. M.; Deltimple, N.; van Velzen, E.; van Dorsten, F. A.; Bingham, M.; Vaughan, E. E.; van Duynhoven, J., H-1 NMR metabolite profiling of feces as a tool to assess the impact of nutrition on the human microbiome. *Nmr in Biomedicine* **2008,** *21* (6), 615-626.

3. Ursell, L. K.; Haiser, H. J.; Van Treuren, W.; Garg, N.; Reddivari, L.; Vanamala, J.; Dorrestein, P. C.; Turnbaugh, P. J.; Knight, R., The Intestinal Metabolome: An Intersection Between Microbiota and Host. *Gastroenterology* **2014,** *146* (6), 1470-1476.

4. Szmulowicz, U. M.; Hull, T. L., Colonic Physiology. *Ascrs Textbook of Colon and Rectal Surgery, Second Edition* **2011**, 23-39.

5. Clarke, L. L., A guide to Ussing chamber studies of mouse intestine. *American Journal of Physiology-Gastrointestinal and Liver Physiology* **2009,** *296* (6), G1151-G1166.

6. Hubbard, D.; Ghandehari, H.; Brayden, D. J., Transepithelial Transport of PAMAM Dendrimers across Isolated Rat Jejunal Mucosae in Ussing Chambers. **2014**.

7. Song, D. R.; Guo, J.; Han, F.; Zhang, W.; Wang, Y. N.; Wang, Y. H., Establishment of an in Vitro Model of the Human Placental Barrier by Placenta Slice Culture and Ussing Chamber. *Bioscience Biotechnology and Biochemistry* **2013,** *77* (5), 1030-1034.

8. Cehak, A.; Schroder, B.; Feige, K.; Breves, G., In vitro studies on intestinal peptide transport in horses. *Journal of Animal Science* **2013,** *91* (11), 5220-5228.

9. Rozehnal, V.; Nakai, D.; Hoepner, U.; Fischer, T.; Kamiyama, E.; Takahashi, M.; Yasuda, S.; Mueller, J., Human small intestinal and colonic tissue mounted in the Ussing chamber as a tool for characterizing the intestinal absorption of drugs. *European Journal of Pharmaceutical Sciences* **2012,** *46* (5), 367-373.

10. Ungell, A. L.; Nylander, S.; Bergstrand, S.; Sjoberg, A.; Lennernas, H., Membrane transport of drugs in different regions of the intestinal tract of the rat. *Journal of Pharmaceutical Sciences* **1998,** *87* (3), 360-366.

11. Fortuna, A.; Alves, G.; Falcao, A.; Soares-da-Silva, P., Evaluation of the permeability and P-glycoprotein efflux of carbamazepine and several derivatives across mouse small intestine by the Ussing chamber technique. *Epilepsia* **2012,** *53* (3), 529-538.

12. Bergmann, H.; Rogoll, D.; Scheppach, W.; Melcher, R.; Richling, E., The Ussing type chamber model to study the intestinal transport and modulation of specific tight-junction genes using a colonic cell line. *Molecular Nutrition & Food Research* **2009,** *53* (10), 1211-1225.

13. Scherbl, D.; Muentnich, S.; Richling, E., In vitro absorption studies of chlorogenic acids from coffee using the Ussing chamber model. *Food Research International* **2014,** *63*, 456-463.

14. van de Kerkhof, E. G.; Ungell, A. L. B.; Sjoberg, A. K.; de Jager, M. H.; Hilgendorf, C.; de Graaf, I. A. M.; Groothuis, G. M. M., Innovative methods to study human intestinal drug metabolism in vitro: Precision-cut slices compared with Ussing chamber preparations. *Drug Metabolism and Disposition* **2006,** *34* (11), 1893-1902.

15. Miyake, M.; Koga, T.; Kondo, S.; Yoda, N.; Emoto, C.; Mukai, T.; Toguchi, H., Prediction of drug intestinal absorption in human using the Ussing chamber system: A comparison of intestinal tissues from animals and humans. *European Journal of Pharmaceutical Sciences* **2017,** *96*, 373-380.

16. Lindon, J. C.; Nicholson, J. K., Spectroscopic and Statistical Techniques for Information Recovery in Metabonomics and Metabolomics. *http://dx.doi.org/10.1146/annurev.anchem.1.031207.113026* **2008**.

17. Nicholson, J. K.; Lindon, J. C., Systems biology: Metabonomics. *Nature* **2008,** *455* (7216), 1054-1056.

18. Barding, G. A., Jr.; Salditos, R.; Larive, C. K., Quantitative NMR for bioanalysis and metabolomics. *Analytical and Bioanalytical Chemistry* **2012,** *404* (4), 1165-1179.

19. Larive, C. K.; Barding, G. A.; Dinges, M. M., NMR Spectroscopy for Metabolomics and Metabolic Profiling. *Analytical Chemistry* **2015,** *87* (1), 133-146.

20. Remesy, C.; Behr, S. R.; Levrat, M. A.; Demigne, C., FIBER FERMENTABILITY IN THE RAT CECUM AND ITS PHYSIOLOGICAL CONSEQUENCES. *Nutrition Research* **1992,** *12* (10), 1235-1244.

21. Sehested, J.; Diernaes, L.; Moller, P. D.; Skadhauge, E., Ruminal transport and metabolism of short-chain fatty acids (SCFA) in vitro: effect of SCFA chain length and pH. *Comparative Biochemistry and Physiology a-Molecular and Integrative Physiology* **1999,** *123* (4), 359-368.

22. Suzuki, T.; Yoshida, S.; Hara, H., Physiological concentrations of short-chain fatty acids immediately suppress colonic epithelial permeability. *British Journal of Nutrition* **2008,** *100* (2), 297-305.

23. Kramer, T.; Michelberger, T.; Gurtler, H.; Gabel, G., Absorption of short-chain fatty acids across ruminal epithelium of sheep. *Journal of Comparative Physiology B-Biochemical Systemic and Environmental Physiology* **1996,** *166* (4), 262-269.

24. Dengler, F.; Rackwitz, R.; Benesch, F.; Pfannkuche, H.; Gabel, G., Bicarbonate-dependent transport of acetate and butyrate across the basolateral membrane of sheep rumen epithelium. *Acta Physiologica* **2014,** *210* (2), 403-414.

25. Ouyang, S. Q.; Beecher, C. N.; Wang, K.; Larive, C. K.; Borkovich, K. A., Metabolic Impacts of Using Nitrogen and Copper-Regulated Promoters to Regulate Gene Expression in Neurospora crassa. *G3-Genes Genomes Genetics* **2015,** *5* (9), 1899-1908.

26. Moreau, N. M.; Champ, M. M.; Goupry, S. M.; Bizec, B. J. L.; Krempf, M.; Nguyen, P. G.; Dumon, H. J.; Martin, L. J., Resistant Starch Modulates In Vivo Colonic Butyrate Uptake and Its Oxidation in Rats with Dextran Sulfate Sodium-Induced Colitis. *The Journal of Nutrition* **2004**.

CHAPTER FIVE

Conclusions and future directions

5.1 Conclusions

The work presented herein identifies and quantifies over 100 metabolites including inorganic ions, short chain fatty acids (SCFAs), sugars, amino acids, aromatic compounds, as well as other carboxylic acids and amine containing molecules in the luminal metabolome. Significantly, this work is the first to map the changes in the composition of the luminal metabolome along the length of the colon. The luminal metabolome holds a wealth of knowledge about the overall health of the colon. By profiling metabolites in stool water extract samples using the complementary analytical techniques of ion chromatography (IC), nuclear magnetic resonance (NMR), and gas chromatography-mass spectrometry (GC-MS), significant new knowledge has been gained about the luminal metabolome and how it changes over the different segments of the colon.

The greatest statistical difference in the metabolite composition of stool water extracts is observed between the ileum and the cecum. As discussed in Chapter 3, the ileum is the last part of the small intestine that feeds waste and nutrients into the cecum of the large intestine. The cecum acts as a fermenting pouch, breaking down complex sugars and starchy fiber into smaller molecules, primarily the short chain fatty acids (SCFAs) including acetate, butyrate, and propionate that act as the primary energy source for the colonocytes.

Samples removed from the ileum show the presence of stachyose, a tetrasaccharide found in the diet of vivarium housed rats. In the cecum the stachyose concentration drops below the limits of detection, and new metabolites appear including glucose and the SCFAs. It was interesting to notice that while formate and isobutyrate are technically SCFAs, their trends along the length of the colon differ from acetate, propionate, and butyrate.

As a group, the amino acids have similar trends in concentration along the length of the colon starting at high concentrations in the ileum and the first 10% of the proximal colon. Amino acids decrease in concentration through the rest of the proximal and mid colon until finally reaching low or undetectable levels at the end of the distal colon, similar to the levels found in voided stool. As the levels of amino acids decreased, the apparent products of their metabolism appeared. Many of the aromatic compounds detected come from the breakdown of tyrosine, phenylalanine, and tryptophan including hydrocinnamic acid and nicotinic acid that appear in Chapter 4 as metabolites that are transported across the epithelium.

It is important to distinguish the changes in composition due to the impact of the complex gut microbiome and those due to transport function of colonic tissue. The Ussing chamber experiments described in Chapter 4 provide the ability to conduct *in vitro* experiments to study metabolite transport. Reasonably, the presence of certain metabolites could mediate or inhibit the transport of others, and thus to mimic transport in a living host we must consider the luminal contents in their entirety. Because of the dynamic processes involved, metabolites can be transformed prior, during, or after transport across the epithelial tissue.

The use of NMR for detection in the Ussing chamber experiments enables the study of the transport of multiple metabolites simultaneously. In these experiments we have control over what metabolites are present in the luminal chamber and are afforded access to the transport mechanisms of the colonic epithelial tissue.

The Ussing chamber experiments in Chapter 4 identified 19 metabolites in the serosal chamber including acetate, butyrate, and propionate that are known to be transported across the epithelial tissue. Other metabolites like choline, phenylalanine, tyramine, and oxaloacetate for which transport rates have not been previously reported also appeared in the serosal chamber. The results of our experiments confirmed that some of the compounds detected in the serosal samples were due to the metabolism of transported compounds. This metabolism was confirmed to occur in the cecal tissue with contamination by bacterial metabolism ruled out. These results indicated that the colonocytes take up and metabolize various compounds during transport to the serosal bath. Products of metabolism include 3-hydroxybutyrate, acetoacetate, choline, pyruvate, succinate, and lactate.

The presence of some of these serosal metabolites coincides with the type of sample loaded in the lumen chamber. When SCFAs are present, 3-hydroxybutyrate and acetoacetate can be observed, but in the case where only glucose is the provided as a carbon source in the mucosal chamber, they are no longer detected but instead alanine is observed.

Interestingly, both alanine and choline are detected in the serosal bath even though no nitrogen containing metabolite was provided to the tissue during experimentation. This means that the tissue is generating endogenous metabolites from its own metabolic stores. This generation of metabolites continues at the same rate after the 45 min sample and replace, which poses about the epithelial uptake of metabolites and their subsequent metabolism.

It is important to address the issue that variability can be quite large between animals, and while laboratory rats allow us to control many of the factors that could exacerbate this issue, significant variability between animals remains. Variability is also present within samples from the same animal. Two different and distinct sections of the same rat cecum can exhibit different transport behavior in Ussing chamber experiments. This may have a biological basis because the cecum is not a perfectly round homogeneous sack with transporters uniformly distributed throughout the tissue. The colon is in fact quite complex with different transporters occurring in different segments that relate to the metabolites present in these specific locales. Based on data obtained in Chapter 3, we can conclude that the composition of stool as it enters the cecum from the ileum is much different than the output from the cecum into the proximal colon.

Based on this data, in conjunction with the observation of large variance within the collected cecal samples, it could be hypothesized that the locations of transporters and overall transport behavior varies across the cecum. Regardless of biological variance, significant differences were observed for a large subset of metabolites along the length of the colon including but not limited to sodium, chloride, formate, acetate, stachyose, glucose, tyrosine, hydrocaffeic acid, phenylalanine, acetoin, and taurine.

The results presented in this dissertation support the concept that the colon exhibits complex segmental stratification and transport behaviors that vary not only due to the presence of the gut microbiome, but because of the colonic tissue itself. The colon contains a complex network of strategically placed transporters that enable the overall function of the colon.

5.2 Future directions

5.2.1 Comparison of healthy colonic function versus induced inflammation

With more than 1.6 million Americans affected by inflammatory bowel diseases (IBD) including Crohn's disease and ulcerative colitis, it is important to understand how inflammation affects the function of the colon. The current recommended procedure for diagnosing IBD is ileocolonoscopy with biopsies,[1] but this procedure is expensive and not advisable for younger patients with IBS symptoms.[2, 3] Colonoscopies could be avoided if reliable non-invasive tests were available.

It will be important in future experiments to investigate the effects of colonic inflammation on the metabolic processes of the colon by providing insight into the transport mechanisms affected by inflammation. It would be optimal to use the rat model to allow for comparative analyses with the data already collected. One way to induce inflammation is to supplement the rat diet with dextran sodium sulfate.[4, 5] Unfortunately, the inflammation would not be limited to the colon, causing one to question whether the metabolite composition that enters the colon was being compromised due to inflammation within the stomach and small intestine. Instead a mouse model could be employed due to the availability to obtain mice with induced colitis. The methods of analytical and statistical analyses of IC, NMR, and GC-MS results presented in Chapter 3, could be applied to healthy mice and animals with induced colitis so that direct comparisons could be made along the length of the colon.

Another option could be to use dextran sodium sulfate to induce inflammation in tissue excised from the rat colon for Ussing chamber analysis. Ussing chamber experiments would be conducted using the same methods as described in Chapter 4, potentially providing new insights into if and how inflammation affects metabolite transport and transformation. Though simpler in concept than moving to an animal inflammation model, a concern about this approach is that dextran sodium sulfate induced inflammation requires an induction period that may not be compatible with the time frame in which the tissue remains viable following excision.

5.2.2 Ussing chamber metabolic transport studies comparing colonic segments

To confirm the apparent differences in transport rates suggested by the work summarized in Chapter 3, Ussing chamber studies could be conducted with colonic epithelial tissue excised from different locations of the colon including the proximal, mid, and distal colon. Standard test solutions with a known composition of 10-20 metabolites would be loaded into the luminal chamber (as described in Chapter 4), and samples analyzed with NMR and LC-MS. NMR provides a robust quantitative view that is easily compared between samples and makes analysis straightforward. It is predicted that upon comparison of the serosal solutions, differences in metabolites present would be detectable and quantifiable indicating levels of absorptive transport are segmentally stratified.

As discussed in Chapter 1, LC-MS is an advantageous analytical technique for targeted metabolomics studies due to the enhanced sensitivity and resolution of this method. By limiting the metabolites afforded access to the epithelial tissue in the Ussing chamber apparatus to a subset of known compounds, targeted analyses can be pursued to determine transport rates. The added sensitivity of LC-MS should facilitate detection of lower level metabolites that are transported at a slower rate or metabolic products transformed by the tissue that were missed by NMR. These experiments would allow us to build a library of compounds found in the luminal metabolome with the corresponding rates of transport throughout the different segments of colon. This is necessary to fully understand the function of the colon and how it relates to overall health.

5.2.3 Ussing chamber experiments using isotopically labeled compounds for the study of colonic epithelium metabolism

Our Ussing chamber results obtained from samples using cecal flush solution, considered as a "blank", showed evidence of ongoing colonic cell metabolism when only glucose is provided as an available carbon source. As mentioned in section 5.2.2, we also observe the apparent transformation of metabolites during their transport across the epithelial tissue. Though this seems like a sensible outcome in retrospect, based on prior literature reports using labeled compounds, we were initially surprised by this result and feel that it that requires further study.

In future studies, Ussing chamber experiments would be conducted with one ^{13}C-labeled compound at a time added to mixture of non-labeled compounds loaded into the luminal chamber. After ample time, samples from both the luminal and serosal chamber would be removed an analyzed using NMR and GC-MS to look for evidence of ^{13}C incorporation in metabolites such as 3-hydroxybutyrate, acetoacetate, pyruvate, succinate, lactate, choline, and alanine that were being generated by the epithelium. The NMR experiments for ^{13}C analysis would involve more 2D-experiments like the HSQC and acquisition of ^{13}C-edited one-dimensional spectra which may offer better quantitation. These experiments would be performed on the 700 MHz NMR equipped with a cryoprobe recently added to the UCR NMR facility, providing increased resolution and sensitivity.

Importantly, the GC-MS derivatization methods described in section 2.4.2 are not optimized for isotope tracing because fragmentation of the trimethylsilane (TMS) derivative typically does not produce an observable molecular ion. To overcome this limitation, in our future experiments we will derivatize using a tert-butyldimethylsilyl ether (TBDMS) group that is larger, and fragments such that the molecular ion can be observed, facilitating quantification of total ^{13}C incorporation.

Unfortunately, with a different derivatization technique, we lose the ability to use databases such as the Golm database for identification of unknown metabolites. Considerable time will be required to produce a library of standards with the new derivatization method to match metabolite retention times and masses for future analyses.

5.2.3.1 NMR experiments with isotopically labeled tags

For complex biological samples, most regions of the ^{1}H-NMR spectrum contain overlapped resonances making identification and quantitation difficult. Increases in magnetic field can improve spectral resolution, but come at a high cost and are often insufficient to resolve the peaks in crowded regions of the spectrum. As described above, one option to improve the spectral resolution is through 2D experiments such as HSQC which correlates ^{1}H resonances with directly coupled ^{13}C or ^{15}N nuclei capitalizing on the greater chemical shift dispersion of the heteroatom.

To overcome the limitations associated with the low natural abundance of ^{13}C and ^{15}N, chemical derivatization methods have been developed to target specific functional groups and increase the signal from low level molecules normally not detectable by HSQC. Using selective ^{13}C and/or ^{15}N labeled tags can increase the coverage of metabolic profiling experiments, providing data for metabolites that might otherwise be undetectable, or lost in crowded regions of the NMR spectra.[6-8]

In Chapter 3, the aliphatic region of the NMR spectra from 0.90-2.50 ppm presented a challenge due to significant resonance overlap with the SCFAs which were at high concentration in many samples. The intense resonances of acetate, butyrate, and propionate occur in spectral regions known to contain amino acid and other small carboxylic acid resonances. By adding an isotopically labeled tag to these metabolites, their signal will be better resolved in the HSQC spectrum, and quantitative analysis could be performed using the resonance produced by the tag, which is expected to have fairly uniform relaxation properties in different molecules and sample matrices.

5.3 References

1. Annese, V.; Daperno, M.; Rutter, M. D.; Amiot, A.; Bossuyt, P.; East, J.; Ferrante, M.; Gotz, M.; Katsanos, K. H.; Kiesslich, R.; Ordas, I.; Repici, A.; Rosa, B.; Sebastian, S.; Kucharzik, T.; Eliakim, R.; Ecco, European evidence based consensus for endoscopy in inflammatory bowel disease. *Journal of Crohns & Colitis* **2013,** *7* (12), 982-1018.

2. Loktionov, A.; Chhaya, V.; Bandaletova, T.; Poullis, A., Inflammatory bowel disease detection and monitoring by measuring biomarkers in non-invasively collected colorectal mucus. *Journal of Gastroenterology and Hepatology* **2017,** *32* (5), 992-1002.

3. Chey, W. D.; Nojkov, B.; Rubenstein, J. H.; Dobhan, R. R.; Greenson, J. K.; Cash, B. D., The Yield of Colonoscopy in Patients With Non-Constipated Irritable Bowel Syndrome: Results From a Prospective, Controlled US Trial. *American Journal of Gastroenterology* **2010,** *105* (4), 859-865.

4. Melgar, S.; Karlsson, A.; Michaelsson, E. M., Acute colitis induced by dextran sulfate sodium progresses to chronicity in C57BL/6 but not in BALB/c mice: correlation between symptoms and inflammation. *American Journal of Physiology-Gastrointestinal and Liver Physiology* **2005,** *288* (6), G1328-G1338.

5. Tanaka, T.; Kohno, H.; Suzuki, R.; Yamada, Y.; Sugie, S.; Mori, H., A novel inflammation-related mouse colon carcinogenesis model induced by azoxymethane and dextran sodium sulfate. *Cancer Science* **2003,** *94* (11), 965-973.

6. Ye, T.; Mo, H.; Shanaiah, N.; Gowda, G. A. N.; Zhang, S.; Raftery, D., Chemoselective N-15 Tag for Sensitive and High-Resolution Nuclear Magnetic Resonance Profiling of the Carboxyl-Containing Metabolome. *Analytical Chemistry* **2009,** *81* (12), 4882-4888.

7. Shanaiah, N.; Desilva, M. A.; Gowda, G. A. N.; Raftery, M. A.; Hainline, B. E.; Raftery, D., Class selection of amino acid metabolites in body Fluids using chemical derivatization and their enhanced C-13 NMR. *Proceedings of the National Academy of Sciences of the United States of America* **2007,** *104* (28), 11540-11544.

8. Larive, C. K.; Barding, G. A.; Dinges, M. M., NMR Spectroscopy for Metabolomics and Metabolic Profiling. *Analytical Chemistry* **2015,** *87* (1), 133-146.